

DUAL PORT MICROSTRIP PATCH ANTENNAS AND CIRCUITS
WITH HIGH INTERPORT ISOLATION FOR IN-BAND FULL DUPLEX
(IBFD) WIRELESS APPLICATIONS

By

HAQ NAWAZ

Submitted to the Graduate School of Engineering and Natural Sciences
in partial fulfillment of
the requirements for the degree of
Doctor of Philosophy

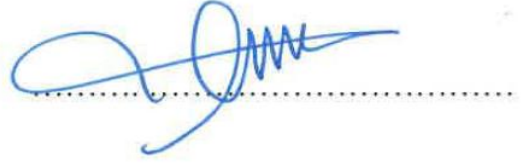
Sabancı University

January 2017

DUAL PORT MICROSTRIP PATCH ANTENNAS AND CIRCUITS WITH
HIGH INTERPORT ISOLATION FOR IN-BAND FULL DUPLEX (IBFD)
WIRELESS APPLICATIONS

APPROVED BY:

Professor Dr. Ibrahim Tekin
(Dissertation Supervisor)




Associate Professor Dr. Ayhan Bozkurt



Associate Professor Dr. Hüsnu Yenigün



Professor Dr. İrşadi Aksun



Associate Professor Dr. Vakur B. Erturk



DATE OF APPROVAL: 06.01.2017

© Haq Nawaz 2017

All Rights Reserved

ABSTRACT

DUAL PORT MICROSTRIP PATCH ANTENNAS AND CIRCUITS WITH HIGH INTERPORT ISOLATION FOR IN-BAND FULL DUPLEX (IBFD) WIRELESS APPLICATIONS

HAQ NAWAZ

Ph.D. Dissertation, January 2017

Supervisor: Prof. Dr. Ibrahim Tekin

Keywords: Full duplex antenna, high isolation, microstrip antenna, self interference cancellation, differential antenna, co-polarization, cross polarization

In-Band Full Duplex (IBFD) is one effective way to increase the spectral efficiency and the throughput of wireless communication systems by transmitting and receiving simultaneously on the same frequency band but the coupling (called Self Interference or SI) of transmit signal to its receiver is one major problem. IBFD operation can be realized successfully by suppressing this coupling or Self Interference (SI).

The required amount of SI cancellation depends on the power and bandwidth of transmitted signal. Generally, the SI should be suppressed to RF transceiver noise floor. To achieve this amount of SI suppression, SI suppression mechanism is normally implemented at three stages across the IBFD transceiver and they are known as antenna cancellation, RF/analog cancellation and digital base-band cancellation. Most of the SI suppression is achieved at antenna stage to relax the required amount of SI cancellation at the rest of two stages. Thus, a dual port microstrip patch antenna with very high port to port RF isolation is required in addition to digital self interference cancellation techniques to enable simultaneous transmit and receive wireless operation at same carrier frequency using single antenna for full duplex radio transceivers.

The objective of my research work presented in this dissertation is to design, implement and measure dual port microstrip patch antennas which deploy different feeding techniques along with Self Interference Cancellation (SIC) circuits to get high interport isolation to enable such antennas for realization of IBFD wireless operation using single/shared antenna architecture. The goal is to achieve high interport isolation for dual port antenna with minimum effect on radiation performance of antennas.

ÖZET

IBFD Kablosuz Uygulamaları İçin Portlar Arası İzolasyonu Yüksek, Çift Portlu Mikro Şerit Yama Antenlerin ve Devreleri

HAQ NAWAZ

Doktora Tezi , Ocak 2017

Tez Danışmanı : Prof. Dr. İbrahim Tekin

Anahtar Kelimeler : Tam çift yönlü anten, mikro-şerit anten, öz-girişim baskılama, diferansiyel anten, ko-polarizasyon, çapraz polarizasyon.

IBFD, kablosuz sistemlerin aynı anda ve aynı frekans bandında alım ve gönderim yapmasına olanak sağladığı için, spektral verimliliği ve toplam sistem kapasitesini artırmakta etkili bir yöntemdir, fakat gönderilen sinyalin alıcısındaki sinyale karışması (öz girişim) en büyük problemlerden birisini oluşturmaktadır. IBFD operasyonu öz girişimin baskılanıp azaltılması ile başarılı bir şekilde gerçekleştirilebilir.

Baskılanması gereken öz girişim miktarı gönderilen sinyal gücünün bant genişliğine ve gücüne bağlıdır. Genelde, öz girişim radyolarda gürültü seviyesine kadar düşürülmesi gerekmektedir. Bu kadar baskılamayı gerçekleştirebilmek için öz-girişim mekanizması bir IBFD radyoda normalde üç farklı adımda gerçekleştirilir ve bunlar anten baskılama, RF/analog baskılama ve dijital baz-bantta baskılama şeklindedir. Bu baskılamanın büyük bir kısmı anten düzeyinde gerçekleştirilip, geri kalan öz-girişim sinyali diğer adımlarda azaltılmaya çalışılır. Bu sebepten ötürü, aynı anda aynı frekans bandı üzerinden tek bir anten kullanarak kablosuz alım ve gönderim yapabilmek için portları arasında yüksek izolasyona sahip çift portlu bir mikro şerit yama anten tasarımı gereklidir.

Bu tezde sunulan araştırmamın amacı, IBFD operasyonun gerçekleştirebilmesi için gerekli olan portlar arası izolasyonu yüksek, tek/paylaşımlı anten mimarisine sahip, farklı besleme teknikleri ile öz-girişim baskılama devreleri kullanarak çift portlu mikro şerit yama antenlerin dizayn, uygulama ve ölçümlerinin oluşturulmasıdır. Hedef, çift port antenler için anten radyasyon performansı üzerinde minimum etkisi olan, portlar arası yüksek izolasyon gerçekleştirmektir.

Acknowledgements

First of all, I express sincere appreciation to my dissertation advisor ***Prof. Dr. Ibrahim Tekin*** for his kind and valuable guidance and very active support at every stage of my PhD studies which enabled me to carry out this research work to conclude my PhD in Electronics engineering. I am really impressed by his excellent research profile and his versatile personality. It was a great honour for me to work under his research supervision. I am also really thankful to my dissertation progress committee members, ***Associate Professor Dr. Ayhan Bozkurt*** and ***Associate Professor Dr. Husnu Yenigun*** for their valuable time to monitor my dissertation progress. I really appreciate all jury members including my dissertation supervisor, dissertation progress committee members and both external jury members ***Professor Dr. İrsadi Aksun (Koç University)*** and ***Associate Professor Dr. Vakur B. Erturk (Bilkent University)*** who honored me with their attendance and valuable time to judge my PhD dissertation.

I would like to acknowledge Mr. Ali Kasal (FENS PCB design Lab) for his patience and very supportive role for my antennas fabrication using LPKF PCB prototype machine.

I would like to say bundles of thanks to my father, mother, both brothers and specially my sister for their encouragement, motivation and moral support during my PhD studies. Special thanks go to my wife for her love, support and care to keep me motivated and healthy during our whole stay in Turkey for my PhD studies. Many thanks to parents of my wife for their unconditional support and motivation for my PhD studies abroad.

And most of all, I thank Allah, my Lord and Savior who gave me strength and blessed me with good health to complete my PhD studies.

Table of Content

	Page
IN BAND FULL DUPLEX (IBFD) WIRELESS COMMUNICATION.....	1
1.1 Motivation.....	1
1.2 Issues and Challenges in Realization of IBFD operation.....	2
1.3 Problem statement.....	5
1.4 Research Objectives and Contributions of this research work.....	6
1.5 Organization of Dissertation	8
IBFD ANTENNA INTERFACING AND LITERATURE REVIEW	10
2.1 IBFD Transceiver Architecture.....	10
2.1.1 Separate antenna architecture	10
2.1.2 Single/shared antenna architecture	12
2.2 Review of some implemented IBFD antenna systems	13
2.3 Applications of dual port, dual polarized antennas in IBFD Wireless Systems	16
2.3.1 Continuous Wave (CW) Radars	16
2.3.2 Retrodirective communication systems	17
2.3.3 Full Duplex Relaying(FDR) systems	17
2.3.4 Applications in other wireless Systems	18
DESIGN DETAILS AND SIMULATION RESULTS FOR PROPOSED IBFD MICROSTRIP ANTENNAS.....	19
3.1 Design and Simulation of Proposed IBFD Antennas.....	19
3.1.1 Dual port ,dual polarized Antenna fed with quarter wave Microstrip feeds	20
3.1.2 Dual port ,dual polarized Antenna fed with microstrip-T feeds	23
3.1.3 Dual port Orthogonal Polarized Antenna with feed forward loop.....	26
3.1.4 Dual Port Linearly Co-Polarized Patch Antenna with High Inter-Port Isolation using External SIC Circuit	31
3.1.5 Dual port ,dual Polarized Antenna with quarter wave microstrip (MS) feeds using single SIC Circuit for high Inter-Port isolation	35
3.1.6 Dual port ,dual Polarized Antenna with microstrip-T (MS-T) feeds using single SIC Circuit for high Inter-Port isolation	38
3.1.7 Dual port, dual Polarized microstrip patch antenna with quarter wave feeds and using two SIC circuits	41
3.1.8 Dual port ,dual Polarized Antenna array with quarter wave microstrip (MS) feeds using single SIC Circuit for high Inter-Port isolation	44
3.1.9 Dual port ,orthogonal Polarized Slot Coupled Microstrip Patch Antenna	46
3.1.10 Dual port ,orthogonal Polarized Slot Coupled Microstrip Patch Antenna	50

3.1.11 Three ports microstrip patch antenna with dual linear and linear co-polarization characteristics	54
IMPLEMENTATION DETAILS & PERFORMANCE EVALUATION OF IMPLEMENTED ANTENNAS	60
4.1 Dual port ,dual polarized Antenna fed with quarter wave Microstrip feeds	61
4.2 Dual port ,dual polarized Antenna fed with both microstrip-T feeds	62
4.3 Dual port Orthogonal Polarized antenna with feed forward mechanism	65
4.4 Dual Port dual Polarized Patch Antenna with high Inter-Port isolation using feeding from same edge	71
4.5 Dual port ,dual Polarized Antenna with quarter wave microstrip (MS) feeds using single SIC Circuit for high Inter-Port isolation	78
4.6 Dual port ,dual Polarized Antenna with microstrip-T (MS-T) feeds using single SIC Circuit for high Inter-Port isolation	79
4.7 Dual port ,dual Polarized Antenna with quarter wave feeds (MS) using two SIC Circuits for high Inter-Port isolation	81
4.8 Dual port ,dual Polarized Antenna array with quarter wave microstrip (MS) feeds using single SIC Circuit for high Inter-Port isolation	82
4.9 Dual port ,orthogonal polarized Slot Coupled Antenna	84
4.10 Dual port ,orthogonal Polarized Slot Coupled Antenna with SIC Circuit	85
4.11 Three ports microstrip patch antenna with dual linear and linear co-polarization characteristics	87
4.12 Compact Dual Port, Single Element Planar Circular Disc Monopole Antenna for Wide-Band MIMO Based Wireless Applications	90
4.13 Interport RF isolation versus impedance bandwidth of dual port, dual polarized microstrip patch antennas	104
CONCLUSION AND FUTURE WORK	110
REFERENCES	112

LIST OF FIGURES

	Page
Figure 1.1: SI Phenomenon in IBFD transceiver which uses single antenna for transmit and receive.....	3
Figure 1.2: SI Phenomenon in IBFD transceiver which uses separate antenna for transmit and receive.....	4
Figure 1.3: Various components of self interference which are required to be suppressed for successful realization of IBFD wireless operation	5
Figure 1.4: Self Interference Cancellation(SIC) using combination of antenna stage and digital SIC techniques across radio transceiver.....	7
Figure 2.1: Passive SIC Cancellation techniques for IBFD transceiver with separate antenna architecture	11
Figure 2.2: IBFD transceiver with shared antenna architecture	12
Figure 2.3: Self Interference Cancellation across analog, digital and antenna stages for IBFD Transceiver with shared orthogonal-polarized antenna architecture ...	13
Figure 3.1: Geometry of dual port microstrip patch antenna with both quarter wave microstrip feeds	20
Figure 3.2: Interport isolation vs feeding location from respective antenna edge	21
Figure 3.3: Simulated and measured S11, S22 and S12 for dual polarized microstrip antenna with both quarter wave microstrip feeds	21
Figure 3.4: Simulated gains and surface currents of dual polarized antenna with $\lambda/4$ microstrip feeds for each port excitation	22
Figure 3.5: HFSS simulated co-polarization and cross polarization gain patterns for dual polarized antenna with $\lambda/4$ microstrip feeds	23
Figure 3.6: Geometry of dual port microstrip antenna with both microstrip-T coupled ports	24
Figure 3.7: Simulated S11, S22 and S12 for dual polarized microstrip antenna with both microstrip-T feeds.....	24
Figure 3.8: Geometry of dual port microstrip patch antenna with one $\lambda/4$ microstrip feed and one microstrip-T feed	25
Figure 3.9: Simulated S11, S22 and S12 for dual polarized microstrip antenna with one $\lambda/4$ microstrip feed and one microstrip-T feed	26
Figure 3.10: Simulated S11, S22 and S12 parameters for dual port patch antenna	27
Figure 3.11: Simulation results for Interport isolation variations vs port 2 feeding positions	28
Figure 3.12: ADS schematic and simulation setup for dual port patch antenna with feed forward loop	29
Figure 3.13: Simulated S11, S22 ,S12 for dual port patch antenna with feed forward loop.....	30
Figure 3.14: Complete PCB layout for antenna with feed forward loop.....	30
Figure 3.15: (a) ADS Momentum Models of antenna and Hybrid coupler, (b) Simulated S-Parameters Results for antenna (c),(d) Simulated S-Parameters Results for Ring Hybrid coupler	32
Figure 3.16: Simulated gain patterns and current distribution of three port antenna for each port excitation.....	33
Figure 3.17: (a) ADS Schematic and simulation set up (b) PCB layout for compact Design	34

Figure 3.18: Simulated S11, S22 ,S12 for dual port linear co-polarized patch antenna using SIC circuit	35
Figure 3.19: EM Model for three port dual polarized antenna with quarter wave microstrip feeds	36
Figure 3.20: (a) ADS schematic and simulation setup (b) PCB layout for compact antenna	36
Figure 3.21: Simulated S-Parameters for three port dual polarized patch antenna with quarter wave microstrip feeds and differentially excited by hybrid coupler ..	37
Figure 3.22: HFSS simulated co-polarization and cross polarization gain patterns for dual polarized differential fed antenna with $\lambda/4$ microstrip feeds	38
Figure 3.23: EM Model for three port dual polarized antenna with microstrip-T feeds ..	39
Figure 3.24: Simulated S-Parameters for three port dual polarized patch antenna with microstrip-T feeds and differentially excited by ring hybrid coupler	39
Figure 3.25: PCB layout for compact antenna structure with MS-T feeds and SIC circuit	40
Figure 3.26: (a) Four ports Antenna's EM Model (b) ADS Simulation Results	41
Figure 3.27: ADS schematic and simulation setup for four ports patch antenna with two SIC Circuits	42
Figure 3.28: Simulation results for dual polarized patch with two SIC Circuits.....	43
Figure 3.29: HFSS simulated co-polarization and cross polarization gain patterns for dual polarized differential fed antenna with $\lambda/4$ microstrip feeds	43
Figure 3.30: EM Model for dual polarized differential fed patch antenna array.....	44
Figure 3.31: ADS schematic and simulation setup for antenna array with SIC Circuit.....	45
Figure 3.32: Simulation results for patch antenna array with SIC Circuit	46
Figure 3.33: Geometry of dual port microstrip antenna with one microstrip fed port and other port is slot coupled	47
Figure 3.34: (a) EM Model of proposed antenna (b) Simulation Results	48
Figure 3.35: Simulated Radiation characteristics of slot coupled microstrip patch antenna for each port excitation	49
Figure 3.36: HFSS simulated co-polarization and cross polarization gain patterns for dual polarized slot coupled patch antenna	49
Figure 3.37: Simulated 2D gain pattern for dual polarized slot coupled microstrip antenna at 2.4GHz	50
Figure 3.38: (a) EM Model for three port antenna (b) Simulation results	51
Figure 3.39: ADS schematic and simulation setup for proposed slot coupled antenna ...	51
Figure 3.40: Simulation results for dual port dual polarized antenna with SIC Circuit	52
Figure 3.41: PCB layout for compact differential fed slot coupled patch antenna	53
Figure 3.42: HFSS simulated co-polarization and cross polarization gain patterns for dual polarized differential fed slot coupled patch antenna	53
Figure 3.43: Three ports 2.4GHz proximity coupled microstrip patch antenna.....	54
Figure 3.44: (a) EM Model for three port antenna (b) EM model for compact structure .	55
Figure 3.45: Linear co-polarized radiation characteristics of proposed proximity coupled antenna with port 1 and port 2 excitations.....	56
Figure 3.46: Linear dual polarized radiation characteristics of proposed proximity coupled antenna with port 1 and port 2 excitations.....	57
Figure 3.47: (a) Simulated S-parameters results for linear co-polarized antenna configuration as compared with direct fed linear co-polarized antenna.....	58
Figure 3.48: Simulated S-parameters results for linear dual polarized antenna configuration as compared with direct fed linear dual polarized antenna.....	59
Figure 4.1: Dual polarized 2.4GHz patch antenna implemented on 1.6mm thick FR-4 substrate	61

Figure 4.2: Simulated and measured S11, S22 and S12 for dual polarized microstrip fed microstrip patch antenna.....	62
Figure 4.3: Implemented Dual polarized 2.4GHz patch antenna with both EM coupled ports	63
Figure 4.4: Simulated and measured S11, S22 and S12 parameters for dual polarized microstrip patch antenna with both EM coupled ports.....	63
Figure 4.5: Implemented Dual polarized 2.4GHz antenna with one MS-T and one $\lambda/4$ feed	64
Figure 4.6: Simulated and measured S11, S22 and S12 parameters for dual polarized microstrip patch antenna with one EM coupled port and one microstrip fed port.....	64
Figure 4.7: Implemented 2.4GHz dual port patch antenna on RT5880 substrate	65
Figure 4.8: Simulated and measured S11 and S12 for a dual port orthogonal polarized patch antenna	66
Figure 4.9: E-plane radiation pattern at 2.4GHz for a dual port orthogonal polarized antenna.....	66
Figure 4.10: Measured co-polarization and cross polarization gain patterns for dual polarized antenna with $\lambda/4$ microstrip feeds and fabricated on 0.787mm thick RT5880	67
Figure 4.11: Implemented two port ,dual polarized 2.4GHz antenna with feed forward loop.....	68
Figure 4.12: Simulated vs Measured S11, S22 and S12 parameters for antenna with feedforward loop	69
Figure 4.13: Measured interport isolation (S12) with peak isolation at lower cutoff and upper cutoff operating frequencies adjusted through loop tuning	70
Figure 4.14: Measured S-Parameters for three port linear co-polarized antenna	71
Figure 4.15: Simulated vs measured 2D gain patterns at 2.5GHz for three port antenna ..	72
Figure 4.16: Test and measurement of three port antenna with SIC Circuit	72
Figure 4.17: Simulated and measured S11, S22 and S12 parameters for linear co-polarized Microstrip patch antenna interfaced with SIC Circuit through RF cables.....	73
Figure 4.18: (a) Implemented compact dual polarized microstrip patch antenna (b) Simulated and measured S11, S22 and S12 for dual polarized patch antenna	74
Figure 4.19: 2D Gain Pattern of compact dual port Microstrip patch antenna at 2.5GHz (a) for Port 1 excitation (b) for Port 2 excitation	75
Figure 4.20: 2D Gain Pattern of compact dual port Microstrip patch antenna at 2.5GHz (a) for vertical polarization(pol2) (b) for horizontal polarization(pol1)	77
Figure 4.21: (a) Implemented compact dual (b) Simulated and measured S11, S22 and S12 for polarized antenna with SIC dual polarized antenna with SIC	78
Figure 4.22: Measured co-polarization and cross polarization gain patterns for dual polarized differential fed antenna with $\lambda/4$ microstrip feeds	79
Figure 4.23: (a) Implemented compact dual (b) Simulated and measured S11, S22 and S12 polarized antenna with SIC for dual polarized antenna with SIC	80
Figure 4.24: Implemented Dual polarized antenna with two Self Interference Circuits(SICs)	81
Figure 4.25: Simulated and measured S11, S22 and S12 parameters for four port Microstrip patch antenna two with SIC Circuits	82
Figure 4.26: Implemented compact dual polarized antenna array using differential feeding	83

Figure 4.27: S-parameters measurement results for compact polarized antenna array with differential feeding	83
Figure 4.28: Constructed dual port, dual polarized slot coupled patch antenna	84
Figure 4.29: Simulated and measured S11, S22 and S12 parameters for dual polarized slot coupled antenna.....	85
Figure 4.30: Constructed dual port, dual polarized differential fed slot coupled patch antenna	86
Figure 4.31: Simulated and measured S11, S22 and S12 parameters for dual polarized differential fed slot coupled antenna	86
Figure 4.32: Measured co-polarization and cross polarization gain patterns for dual polarized differential fed slot coupled antenna	87
Figure 4.33: Implemented 2.4GHz compact proximity coupled patch antenna	88
Figure 4.34: Measured input matching (S11, S22) and interport isolation (S12) results for implemented linear co-polarized patch antenna	89
Figure 4.35: Measured input matching (S11, S33) and port isolation (S13) characteristics of implemented linear dual polarized patch antenna	89
Figure 4.36: Single port circular disc monopole antenna with rectangular groove in partial ground plane.....	94
Figure 4.37: Simulated S11 variations with different values of circular disc radius (r)	95
Figure 4.38: Simulated S11 for different values of ground plane width (Lg)	96
Figure 4.39: Simulated vs. measured S11 for implemented single port circular monopole antenna	96
Figure 4.40: HFSS simulated peak realized gain for single port circular monopole antenna	97
Figure 4.41: Dual port monopole antenna based on single circular disc element with circular cut of radius Rc in ground plan.....	98
Figure 4.42: Current distributions for proposed dual port circular disc antenna at 6GHz with port 1 excitation (a) without circular cut (b)with Rc=14mm circular cut in ground plane.....	98
Figure 4.43: HFSS simulation results for (a) S11, S22 with different radius(Rc) of circular cut in ground plane (b) S12 with different radius(Rc) of circular cut in ground plane	100
Figure 4.44: HFSS simulated peak realized gain for dual port single element circular monopole antenna	100
Figure 4.45: Simulated vs. measured S-Parameters for dual port monopole antenna printed on RT5880.....	101
Figure 4.46: Simulated (dotted lines) vs. measured(solid lines) E-Plane (red lines) and Hplane(blue lines) gain patterns of dual port antenna at 3GHz, 4GHz,5GHz and 6GHz for port 1 excitation	102
Figure 4.47: Simulated and measured correlation coefficient for dual port single element monopole antenna.....	103
Figure 4.48: Single layer, dual polarized 2.4GHz microstrip patch antenna	105
Figure 4.49: Peak isolation frequency variations vs. port 2 feeding location	106
Figure 4.50: Simulated and measured S- parameters for dual polarized 1GHz microstrip patch antenna	107
Figure 4.51: Simulated and measured S11, S22 and S12 parameters for dual polarized 2.4GHz microstrip patch antenna	108
Figure 4.52: Simulated S11, S22 and S12 for dual polarized 5.1GHz antenna	109
Figure 4.53: Measured input matching (S11, S22) and port isolation (S12) for implemented dual polarized 2.4GHz proximity coupled patch antenna	110

ABBREVIATIONS

Abbreviation	Description
IBFD	In Band Full Duplex
SI	Self Interference
MIMO	Multi Input Multi Output
QoS	Quality-of-Service
FD:	Full Duplex
SIC	Self Interference Cancellation
LTE	Long Term Evolution
RF	Radio Frequency
MHz	Mega Hertz
GHz	Giga Hertz
EM	Electromagnetic
PCB	Printed Circuit Board
Tx/Rx	Transmitter/Receiver
FDR	Full Duplex Relaying
OFDM	Orthogonal Frequency Division Multiplexing
DFN	Differential Feeding Network

CPW	Coplanar Waveguide
CW	Continuous Wave
FD	Full Duplex
ADC	Analog to Digital Converter
DAC	Digital to Analog Converter
HDR	Half Duplex Relaying
CR	Cognitive Radio
WLAN	Wireless Local Area Networks

CHAPTER 1

IN-BAND FULL DUPLEX (IBFD) WIRELESS COMMUNICATION

1.1 Motivation

The electromagnetic radio spectrum is a very precious natural resource and has very fundamental role in wireless networks. These days so many multimedia rich services are being introduced and offered and there is huge demand for wireless networks which are capable to carry high data rates. This also requires the effective and efficient utilization of already available radio resources. The main challenge for future wireless networks is high data traffic management using limited spectrum [1]. Consequently, new wireless technologies are being introduced such as Long Term Evolution (LTE) and LTE-Advanced which have capabilities of providing high speed, large capacity, and guaranteed quality-of-service (QoS) mobile services. For the case of wireless networks, the new technologies should have capability of using frequency spectrum in more effective and efficient way. However, the existing wireless communication systems achieve the full-duplex wireless operation by deploying two separate, half duplex channels with different frequencies or time slots for transmission and reception of radio signal to avoid the Self-Interference (SI) that is caused by simultaneous transmission and reception with same uplink and downlink frequencies [1],[3],[4-5]. Such wireless systems cause spectral loss [1].

In-Band Full Duplex (IBFD) is one attractive solution to increase the spectral efficiency and the throughput of wireless communication systems by transmitting and receiving simultaneously on the same frequency band but IBFD operation has a number of challenges including antenna and circuit design for IBFD transceivers. One of the major problem for IBFD wireless operation is the coupling (called Self Interference or SI) of transmit signal to its receiver when IBFD transceiver tends to transmit and receive simultaneously at the same carrier frequency [1]. IBFD operation can be realized successfully by suppressing this coupling of transmitter to its own receiver. Recently, a significant research

work has been carried out to investigate and implement Self-Interference (SI) cancellation techniques to enable Full Duplex (FD) operation at same frequency for the next generation cellular networks [6-11].

Successful realization of IBFD transceivers can reduce the spectrum needs of wireless networks to half as compared to traditional duplexing techniques as In Band Full Duplex (IBFD) transceiver is able to transmit and receive simultaneously at the same radio frequency. For example, LTE system which uses two separate uplink and downlink channels with equal bandwidth for full duplex operation, IBFD operation can provide comparable performance by using only single channel. Thus, In Band Full Duplex (IBFD) wireless is one emerging technology for next generation wireless networks and currently being investigated for 5G networks as it has potential to double the data throughput of wireless communication systems. IBFD systems are not only spectral efficient but also they are low cost as they can readily use the current MIMO transceivers for full duplex operation [1]. In Band Full Duplex not only has the capability to double the spectral efficiency but it can also help to resolve some critical issues in existing wireless communication networks, such as hidden terminals, drop in throughput caused by congestion and large end to end network delays [11].

1.2 Issues and Challenges in Realization of IBFD operation

Although IBFD mechanism increases the throughput, IBFD operation has a number of challenges including antenna and circuit design for IBFD terminals/transceivers. The main problem for IBFD wireless operation is the coupling of transmit signal to its receiver when IBFD terminal tends to transmit and receive simultaneously at the same carrier frequency [1], [3]. In-Band Full Duplex (IBFD) wireless communication operation can be realized by suppressing this Self Interference (SI) at the receiver that is caused by coupling from its own transmitter. Such coupling from transmit to receive chain is caused from both antenna circuitry, environmental reflections and also contributed by non-linear behaviour of RF components in transmit chain. This so called self interference is complex combination of linear and nonlinear RF leakage to receiver from its own radio transmitter. Linear SI components are linear combination of direct RF leakage from transceiver own transmitter to receiver and any reflections from environment [12].

For IBFD transceiver which shares single antenna to transmit and receive RF signals, the linear component of SI is contributed by direct coupling between antenna ports (also termed as interport coupling) and environmental reflections as shown in Fig.1.1. The interport coupling can be reduced to some extent using circulator between transmit and receive ports of antenna but more amount of SI suppression is required in order to realize IBFD operation.

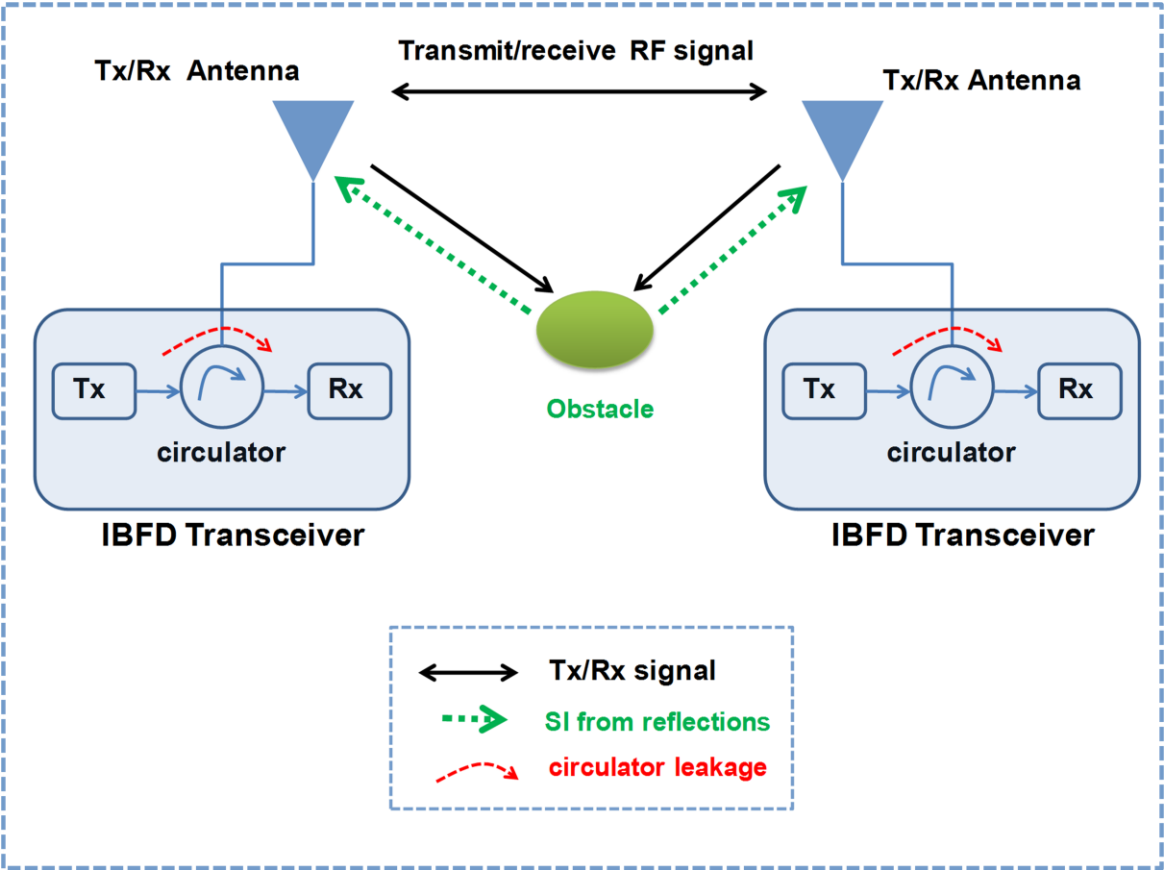


Figure 1.1: SI phenomenon in IBFD transceiver which uses single antenna for transmit and receive

On the other hand, IBFD transceivers with separate transmit and receive antennas; the linear component of SI is contributed by EM coupling between transmit and receive antenna and reflections from environment as indicated in Fig.1.2. EM coupling between transmit and receive antenna can be partially suppressed by electromagnetic isolation of both antennas.

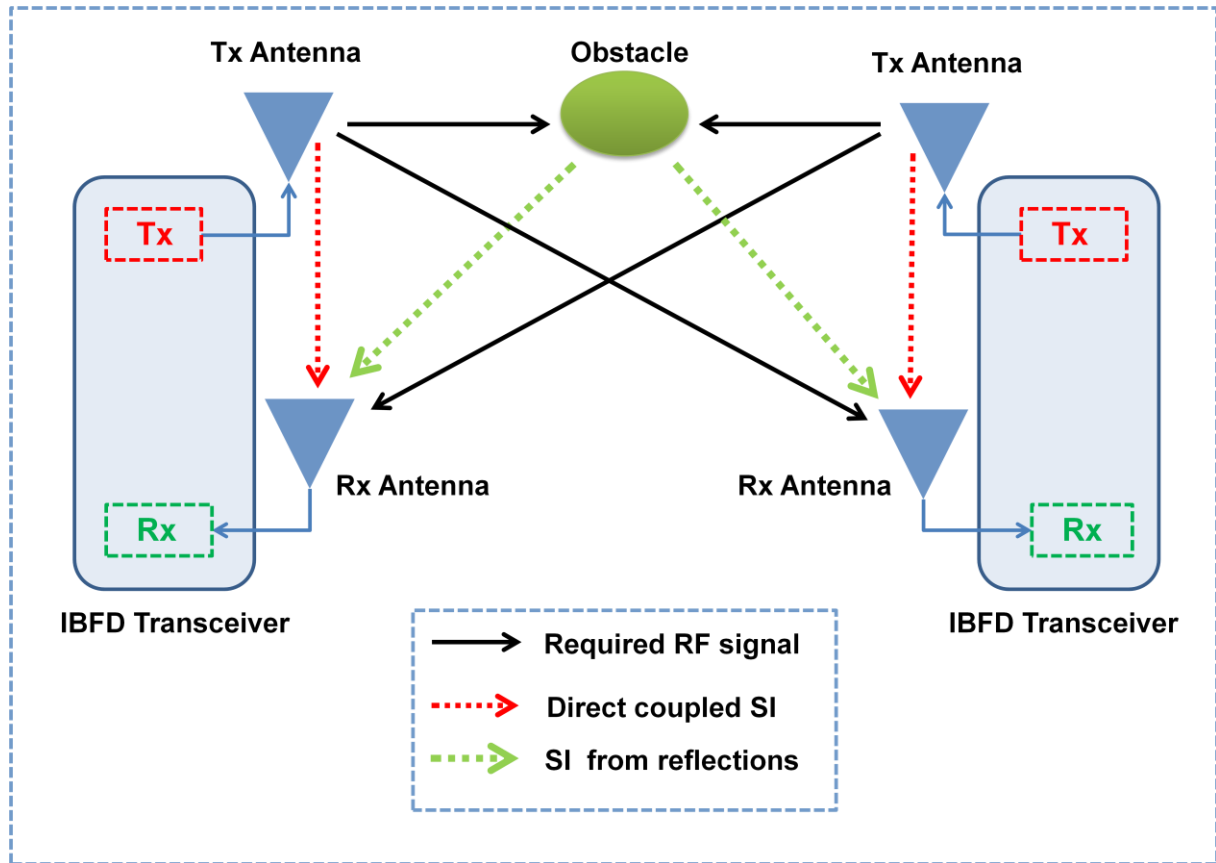


Figure 1.2: SI Phenomenon in IBFD transceiver which uses separate antenna for transmit and receive

The actual transmitted signal differs significantly from that we expect to be transmitted as it contains non-linear components along with transmitter noise. The various components used in transmitter section of radio transceiver produce linear and non-linear distortion and contribute significant amount of noise power so the transmitted signal is a complex function of ideal transmitted RF signal along with noise contributed by transmit chain [12]. The non-linear components of SI (which are generated by RF circuits and their frequencies fall within or very close to band of transmitted signal) are also required to be suppressed significantly for IBFD transceivers. In addition, the transmitter noise or broadband noise [13] should also be suppressed which is generated from high power amplifiers. The transmitter noise or broadband noise power is additional noise -90dBm which is inherently generated by RF transmitter [14] and causes a general increase in base signal level as depicted in Fig.1.3. In fact, a complex interplay exists between different components in the RF chain including antenna which affects spectral-efficiency gains achievable through IBFD [15]. For example,

the phase noise of oscillator directly affects the performance of analog domain SIC techniques [16] and performance of IBFD transceivers. This phase noise generated by local oscillators is merged with main signal.

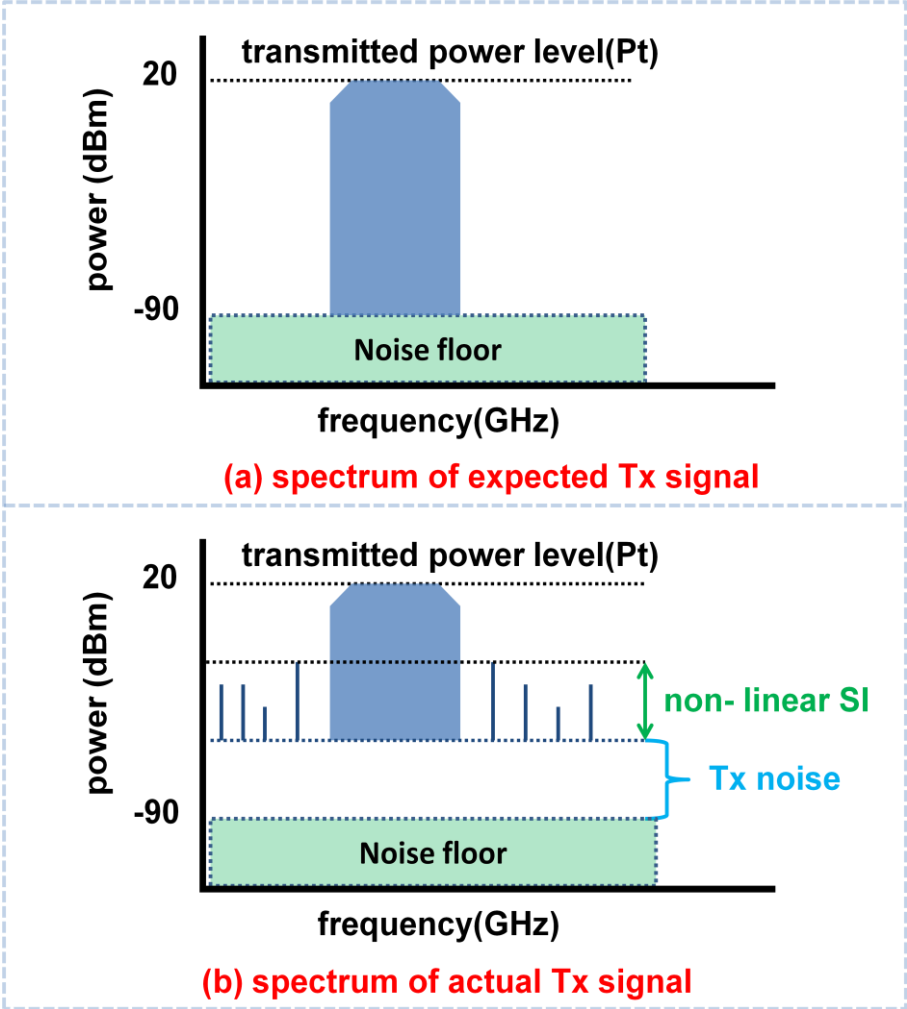


Figure 1.3: Various components of self interference which are required to be suppressed for successful realization of IBFD wireless operation

1.3 Problem Statement

For IBFD transceivers, most of the SI should be suppressed or cancelled at antenna stage to relax the required amount of SI cancellation across other stages. Antenna stage SI suppression techniques should accomplish this task without significant degradation in antenna performance.

1.4 Research Objectives and Contributions of this research work

In order to accomplish full duplex wireless operation with its full gains, IBFD transceiver should suppress the self interference (which is caused by its own transmitted signal to received RF signal) to the receiver's noise floor. Normally, the amount of suppressed SI is considered as figure of merit for IBFD radio transceiver design [12]. The residual self interference (the amount of remaining SI after suppression) which acts as a noise degrades the signal to noise(SNR) ratio which results in degradation to achievable throughput of IBFD wireless operation and in some cases the resultant throughput is even worse than that achieved by half duplex radio transceiver [12]. The required amount of SI cancellation also depends on the power and bandwidth of transmitted signal. For example, as depicted in Fig.1.4, the transmitted power (P_t) for a radio transceiver is 20dBm and the noise floor is -90dBm, then the required amount of SI suppression should be $20\text{dBm} - (-90\text{dBm}) = 110\text{dB}$ for IBFD operation so that received signal is not disturbed by RF leakage from its own transmitter and SNR is not degraded. This amount of SI suppression is required to suppress the linear components of self interference or interference caused from main transmit signal. In addition, the self interference caused from harmonics (non-linear component of SI) and transmitter noise should also be suppressed to accomplish IBFD wireless operation.

To achieve this amount of suppression for various components of SI, the SI suppression mechanism is normally implemented at multiple stages across the IBFD transceiver and they are known as antenna cancellation, RF/analog cancellation and digital base-band cancellation. Normally, most of SI amount is suppressed by antenna stage cancellation mechanisms and residual SI components which also include non-linear SI and transmitter noise are suppressed using digital cancellation techniques/algorithm and analog noise cancellation techniques respectively [12]. The transmitter noise is random in nature and can be suppressed below noise floor only by analog noise cancellation using replica of generated noise.

A large amount of SI suppression is required at antenna stage to prevent the radio receiver to become saturate due to excessive self interference [12]. Thus, an antenna with very high interport isolation is required in addition to the analog and digital SI suppression stages to realize IBFD communication using single antenna for transmit and receive operation.

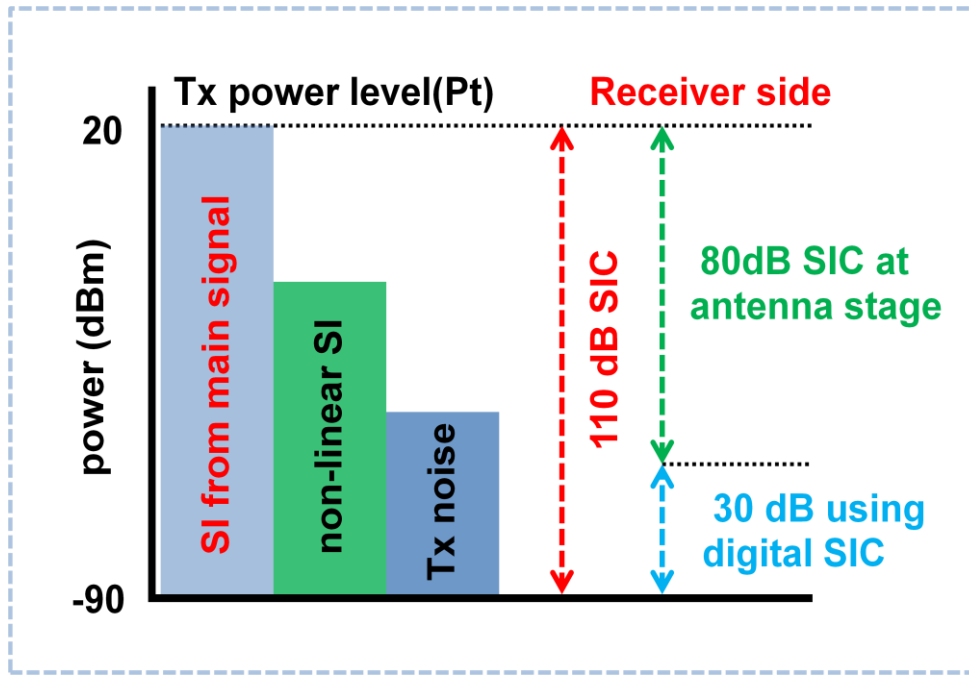


Figure 1.4: Self Interference Cancellation(SIC) using combination of antenna stage and digital SIC techniques across radio transceiver

As depicted in Fig.1.4 ,the aim of this research work is to achieve around 80dB SI suppression at antenna stage.This amount of SI suppression at antenna along with 30dB SI cancellation using digital base-band techniques achieves 110dB SI suppression to enable full duplex operation at the same transmit and receive carrier frequency. Our antenna stage SI suppression techniques will also suppress transmitter noise and residual SI is cancelled by using digital SI cancellation algorithms.

The objective of the research work presented in this dissertation is to design, implement and measure dual port microstrip patch antennas which deploy different feeding techniques and utilize Self Interference Cancellation (SIC) circuits to get high interport RF isolation to enable such antennas for realization of IBFD wireless operation using single/shared antenna architecture. In this dissertation, dual polarized microstrip patch antenna with different feeding mechanism along with SIC circuits have been implemented to achieve high interport RF isolation without antenna performance degradation. Around 70dB interport isolation for 50MHz bandwidth has been obtained for single layer three ports antenna with external SIC circuit. Almost same amount performance has been achieved by single layer antenna with microstrip-T feeds and external SIC circuit. This antenna also provides DC isolation between

transmit and receive ports which is required for active antenna applications. Three ports slot coupled antenna with external SIC circuit provides more than 80dB isolation at centre frequency and around 75dB port to port isolation for antenna's 10dB impedance bandwidth of 50MHz. This antenna provides almost 80dB interport isolation for 20MHz impedance bandwidth. This antenna configuration also achieves DC interport isolation due to one aperture coupled port. Implemented dual port circular disc MIMO antenna for wide band applications provides 15dB interport isolation for antenna's 10dB impedance bandwidth of 2-6GHz .

1.5 Organization of Dissertation

The first chapter describes the In-Band Full Duplex (IBFD) wireless communication operation and discusses the main problems related to realization of IBFD wireless communication for both shared antenna (single antenna for both transmit and receive) and separate antenna (separate antenna for transmit and receive) architectures. It elaborates the Self Interference (SI) phenomenon which results from circuit level coupling and environment reflections of RF signal. The non-linear SI and transmitter noise are also discussed. Then the problem statement and objectives of research work carried out for my PhD dissertation are stated. The main contribution and achievements of my accomplished research work are briefly discussed.

The second chapter is devoted to antenna interfacing with transmit and receive chains of IBFD transceiver. It describes the shared antenna architecture where single antenna is used for both transmit and receive operation. Then separate antenna architecture is also discussed which deploys dedicated antennas for full duplex operation. The literature review for antenna stage cancellation techniques normally used for IBFD communication transceivers with shared antenna and separate antenna architectures has been presented. The chapter concludes with some examples of wireless communication systems which can utilize the proposed dual port microstrip patch antennas to realize IBFD operation.

The third chapter provides the details of proposed dual port microstrip patch antennas. The design and simulation details of various proposed microstrip antennas for shared antenna IBFD transceiver architecture are given. Different feeding techniques for microstrip antennas and utilization of Self Interference Cancellation (SI) circuits are discussed which are deployed

to achieve high interport isolation for full duplex communication using single antenna for both transmit and receive operation. The simulation results for S-parameters (input matching for each port and interport isolation), co-polarization and cross-polarization gain patterns are presented for all proposed microstrip patch antennas.

Implementation and test and measurement results for performance evaluation (antenna port matching, interport isolation, measured co-polarization and cross-polarization gain patterns etc) for fabricated antennas are presented and discussed in chapter 4. Design and implementation details of dual port wideband (2-6 GHz) single circular disc radiating element based monopole antenna with partial ground plane has also been discussed in this chapter. Finally the dissertation is concluded.

CHAPTER 2

IBFD ANTENNA INTERFACING AND LITERATURE REVIEW

The chapter firstly describes the antenna interfacing with transmit and receive chains. It describes the shared or single antenna and separate antenna architectures. As the antennas proposed and implemented in this research work are to be used for IBFD transceiver with shared/single antenna architecture so the shared/single antenna architecture with dual port, dual polarized antenna and dual port, linear co-polarized antenna are also discussed. The literature review discusses the performance of some implemented antenna systems along with brief overview of SI cancellation mechanism for these antennas. The chapter concludes with some examples of wireless communication systems which can utilize the proposed dual port microstrip patch antennas to realize IBFD operation.

2.1 IBFD Transceiver Architecture

The antenna can be interfaced with transmit and receive processing chains in two distinctive ways. One is called the separate-antenna architecture and the other is the shared antenna architecture.

2.1.1 Separate antenna architecture

In the separate-antenna architecture, each transmit chain uses a dedicated radiating antenna and each receive chain uses a dedicated sensing antenna [17-18]. Mostly, the EM isolation is achieved by increasing the path loss between transmit and receive antennas that can be accomplished either by increasing the inter-spacing or by placing EM shielding between Tx and Rx antennas [17], [19] Direct coupling or Self Interference (SI) for separate-antenna architecture transceiver can be minimized by following three passive SIC techniques as depicted in Fig.2.1:

- Adjusting the separation distance between transmit and receive antennas
- Placing the Tx and Rx antennas on opposite sides of wireless device
- Using directional antennas

The technique of Directional antenna deployment is specially used for Full Duplex Relaying (FDR). Full Duplex Relaying significantly improves the throughput and coverage of wireless networks [20-21].

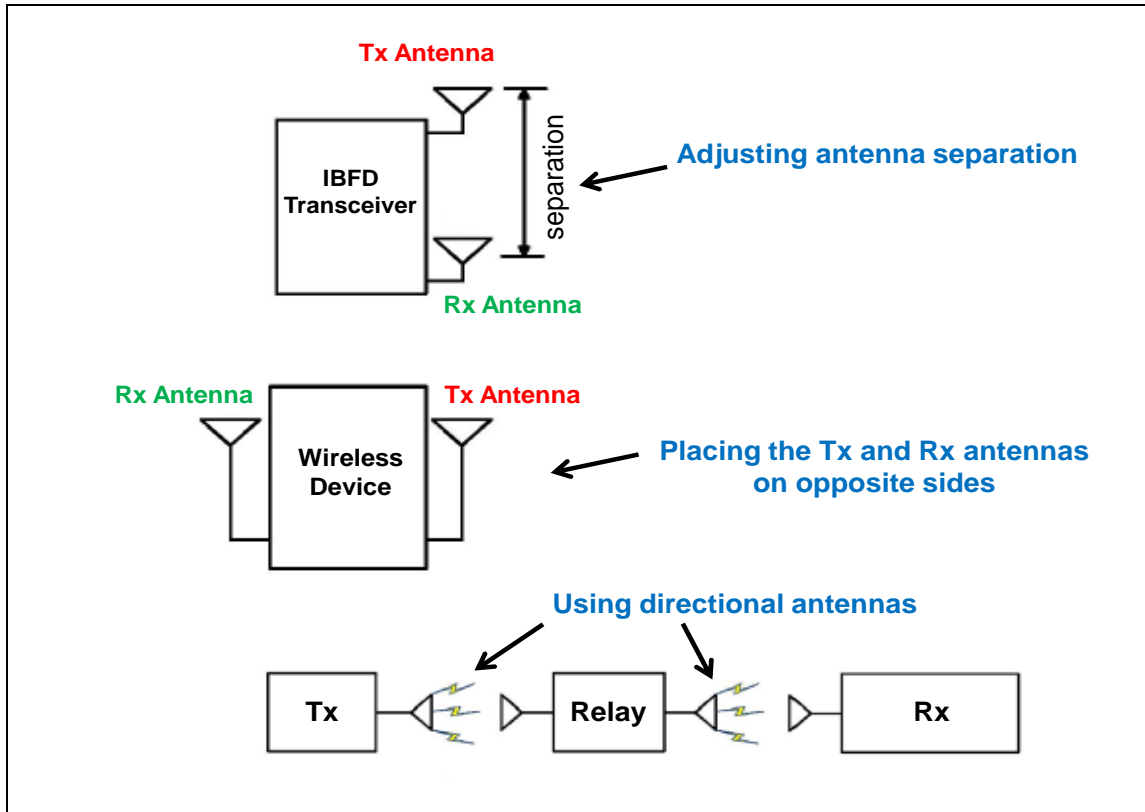


Figure 2.1: Passive SIC Cancellation techniques for IBFD transceiver with separate antenna architecture

The spacing between transmit and receive antennas can not be extended to very large extent as it prohibits the realization of compact radio transceivers. Some advanced techniques like the use of electromagnetic band gap (EBG) structures [22] which act as high impedance structures to minimize the surface waves, utilizing inductive loops [23], deploying wavetraps [24] and antennas with defected ground planes structures (DGS)[25] are also used to reduce mutual coupling between transmit and receive antennas. Some antennas also use neutralization techniques [26] and lumped elements [27] between transmit and receive ports to improve interport isolation.

2.1.2 Single/shared antenna architecture

In the shared-antenna architecture, transmit and receive-chains share a common antenna [28-29] as shown in Fig.2.2. Normally such antenna is cross polarized so that direct coupling between transmit and receive chain is reduced. Antenna stage SI suppression techniques target to minimize the inherent mutual coupling between transmit and receive ports of antenna by firstly employing cross polarization for transmit and receive operation and then use external circuitry to achieve additional isolation. For example, the reported antennas in [30-31] use orthogonally polarized single antennas with improved feeding methods to achieve high isolation between transmit and receive ports. Analog and digital domain SI cancellation stages are deployed to suppress the SI to enable IBFD operation using single antenna.

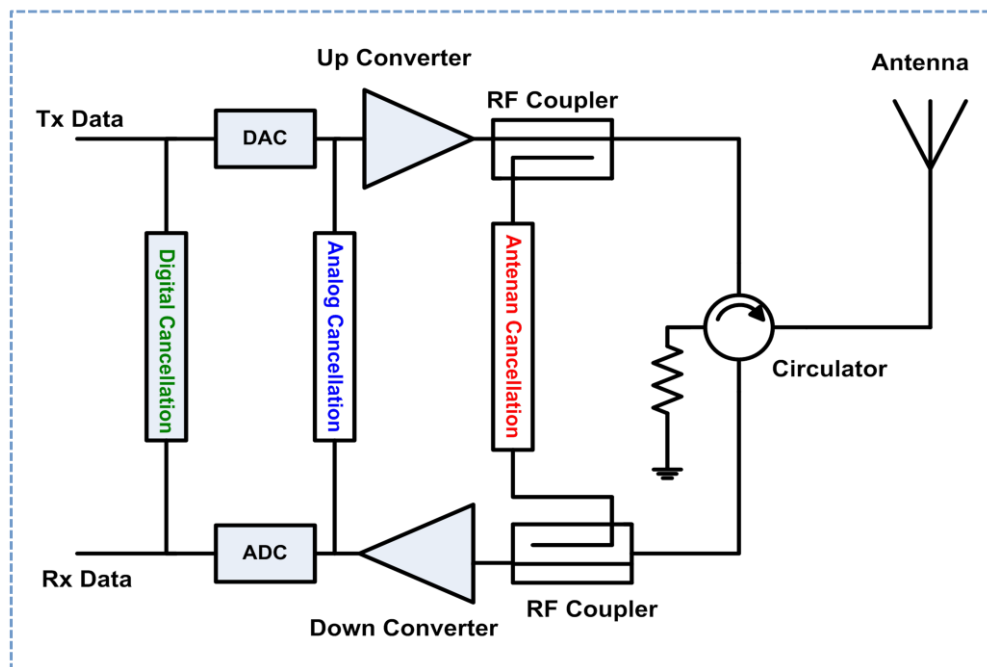


Figure 2.2: IBFD transceiver with shared antenna architecture

Cross polarized microstrip antenna electromagnetically isolates the IBFD transmit and receive signals. For example, IBFD terminal can transmit with horizontal polarization and receive with vertically polarization to avoid SI [32-34]. Fig.2.3 shows the interfacing of orthogonal polarized microstrip antenna with transmit and receive chains along with analog and digital SIC stages.

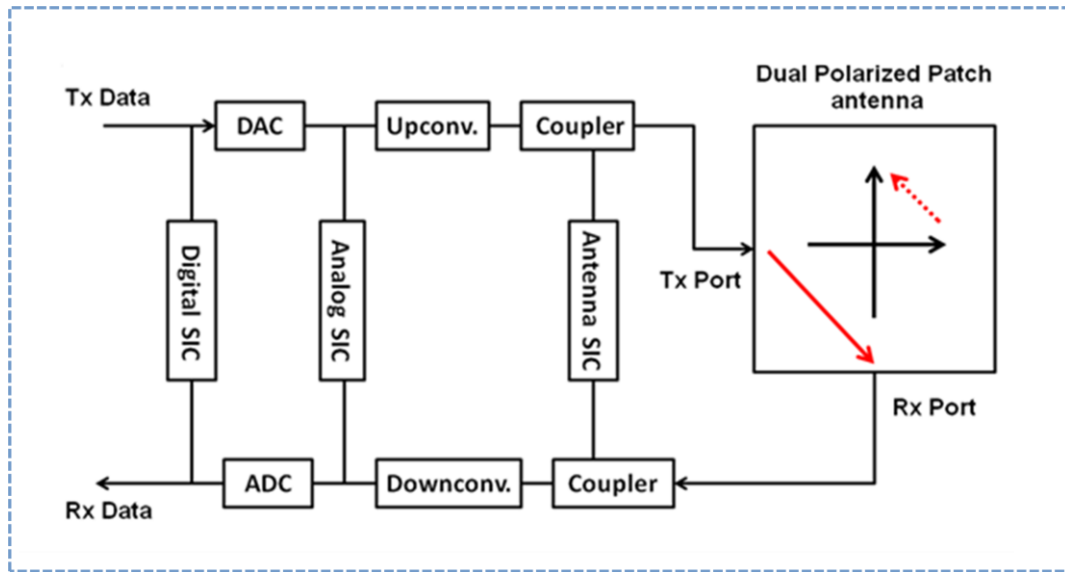


Figure 2.3: Self Interference Cancellation across analog, digital and antenna stages for IBFD Transceiver with shared orthogonal-polarized antenna architecture

2.2 Review of some implemented IBFD antenna systems

Self Interference (SI) can be partly suppressed using both passive and active cancellation techniques. The passive cancellation techniques use electromagnetically isolated transmit and receive antennas while active Self Interference Cancellation (SIC) techniques use transceiver own transmit signal to cancel the SI. Such SIC is performed by subtracting a sampled transmitted signal with the coupled signal to cancel SI. Active SIC can be accomplished over a transmission line [35] or over the air using extra antennas [4], [8].

Several full-duplex radio systems with separate antenna architecture have been implemented [4], [8], [36],[37] and most of the reported implementations require transceivers with more than one transmit and receive antennas to achieve sufficient isolation between transmit and receive chains. For example in [4], an antenna cancellation technique along with analog and digital cancellation techniques for SIC has been presented for single channel full duplex operation. The implemented antenna cancellation technique uses two transmit and one receive antennas. The two transmit antennas are placed at distances d and $d + \lambda/2$ from Rx antenna and two received signals at receiver are destructively added and cancel each other. Then noise cancellation and digital interference cancellation techniques are applied to remove the residual Interference. The presented antenna cancellation technique explores the option of SIC with multi antennas and describes how the Rx antenna placement effects the SIC

mechanism. The achieved SIC is dictated by $\lambda/2$ distance which corresponds to single frequency but wireless systems transmit in specific bandwidth (range of frequencies) so the impact of bandwidth on antenna cancellation is also investigated in this technique which concludes that this technique is sufficiently robust for narrowband systems. The implemented antenna cancellation is less effective for signals with more than 100MHz bandwidth.

In [8], a cancellation technique called BALUN (Balanced to Unbalanced transformer) cancellation has been presented which provides 40-45 dB signal cancellation over 10MHz bandwidth and 55 dB suppression at the center frequency. In this paper, two antennas (one transmit antenna and one receive antenna) scheme is deployed and a BALUN has been used as an analog SI canceller. The BALUN causes destructive interference of two signals by producing 180 degree phase shift. The BALUN is considered to have better frequency response over a wideband compared to that achieved by $\lambda/2$ apart asymmetrically placed antennas as discussed in [4]. The implemented Interference cancellation is very sensitive to performance of the active balun. The performance of this technique is also limited by variable attenuator and delay line which are inserted in loop to account for wireless linkage between transmit and receive antennas which complicates the tuning of loop elements to track the SI channel specially for wide band transmission channels.

In [36], signal inversion and adaptive cancellation has been used to design a full duplex transceiver. Signal inversion has been performed by a simple design based on BALUN (Balanced to Unbalanced transformer). This design supports wideband and high power systems regarding SI cancellation. Signal inversion technique alone provides 45dB signal cancellation across 40MHz bandwidth. In conjunction with digital domain SIC techniques, it provides 73dB signal suppression for a 10MHz OFDM signal.

The reported system in [37] focuses signal processing techniques that enable IBFD operation. The design uses combination of transmit and receiver SI cancellation techniques to achieve 45-50 dB interference suppression for the simultaneous transmit and receive link and achieve nearly 60 dB Interference signal suppression for Full Duplex Relaying (FDR).

For the shared antenna case, most of the reported antennas are cross polarized which provide interport isolation by polarization diversity and then improved feeding techniques are used to achieve additional isolation between transmit and receive ports[30-31]. A wideband

dual-polarised patch antenna with high isolation and a low cross-polarisation has been presented in [30]. Two orthogonal linearly-polarised modes are excited by the EM fed structure. One mode is excited by a pair of probes with 180 degree phase difference. The second mode is excited by a magnetic-coupled loop (metal loop and an open-ended transmission line). Two shorting pins have been introduced to enhance interport isolation more than 40 dB.

A broadband two port, dual-polarized microstrip antenna has been implemented in [31] which achieve low cross polarization and high interport isolation by using two different feeding methods for a single circular patch antenna. In first configuration, one port is probe fed and other port is H-shaped aperture coupled. In second configuration, one port is excited by Differential Feeding Network (DFN) which uses a pair of L-shaped probes with a 180 degree phase difference and the other port excitation is achieved by H-shaped aperture coupling. The implemented antenna achieves more than 40dB interport isolation. The reported design in [38] used balanced feed network to achieve high transmit to receive isolation for full duplex wireless system operating with a common RF carrier using single antenna. The measured isolation for this patch antenna with balanced feed network was reported as 40-45dB.

In [39], a two layers self duplexing stacked patch antenna has been proposed and it used one patch antenna on layer1 one and other patch antenna with two slits on layer 2. The slit in patch antenna on layer 2 has been used to excite the patch antenna on layer 1 by electromagnetic coupling. The proposed self duplexing antenna suppresses the mutual coupling less than -30dB.

The implemented antenna in [40] is single-layer wideband printed antenna for dual-polarized applications. Two orthogonal linear polarizations are achieved by hybrid feeding mechanisms. The horizontal polarization mode is excited by an aperture-coupled microstrip feed line while the vertical polarization mode is excited by Coplanar Waveguide (CPW) feed line. Interport Isolation better than 40 dB over the entire impedance bandwidth from 1.61GHz to 2.87 GHz with $SWR \leq 2$ has been achieved with good antenna radiation performance for each port.

2.3 Applications of dual port, dual polarized antennas in IBFD Wireless Systems

As the proposed antennas in this research work provide very high inter port isolation so they can be used for effective In-Band Full Duplex (IBFD) wireless communication operation using single antenna for many wireless applications. The goal of this section is to discuss some wireless communication systems where the proposed antennas can be deployed for IBFD operation by just using available hardware resources and without changing the transceiver architecture. Applications of proposed microstrip patch antennas for following IBFD wireless systems will be discussed:

- Continuous Wave (CW) Radars
- Retrodirective communication systems
- Full Duplex Relaying(FDR) systems
- Other wireless Systems

2.3.1 Continuous Wave (CW) Radars

Continuous Wave (CW) radar systems are required to carry out transmission and reception of RF signals at the same time. They can transmit and receive simultaneously either by using two separate antennas (bistatic mode or one shared antenna (monostatic mode) [41]. The self-interference or so called “transmitter leakage” in the radar literature [42] is one key challenge to realize CW radar operation. In the case of bistatic CW radars, the isolation between the transmitter and receiver is received through physical separation of Tx and Rx antennas while circulators with improved topologies [43-44] are deployed to improve interport isolation for monostatic CW Radars. Some digital SIC techniques have also been investigated for monostatic CW Radars [45].The amount of SIC for monostatic radars depend upon many factors including radar’s range and transmitted power. For low transmitted power, less SIC is required but the range of radar detection is also reduced. The microstrip patch antennas proposed here can be used effectively for 2.4GHz low power and low range monostatic CW Radar applications. Additionally, as the proposed antennas are small in size, compact CW radar systems can be implemented using these antennas.

2.3.2 Retrodirective communication systems

The retrodirective antenna arrays transmit the RF signal back in the same direction in which they receive without a prior knowledge of originating source location [46]. These systems are very useful and being used as collision avoidance systems and personal communication systems. For example, the proposed antennas can be used as an array element for 2.4GHz retrodirective transceiver similar to 1GHz system proposed in [47] which performs retrodirectivity by heterodyne mixing. Two such identical systems can be used to establish a bidirectional communication link for personal communication.

The proposed antennas can also be used for 2.4GHz Direction of Arrival (DOA)/Angle of Arrival (AOA) system. One such system is proposed in [48] which extracts angle of arrival informations using retrodirective Radar architecture. Although the proposed system in [48] is configured in bistatic Radar mode as it uses separate transmit and receive antennas but same system can be implemented in monostatic mode by using single antenna with high inter port isolation for both transmit and receive operation. Therefore the proposed antennas in our research work can be used for such applications.

2.3.3 Full Duplex Relaying(FDR) systems

One important application of IBFD operation in wireless communication is Full Duplex Relaying. IBFD repeater can simultaneously receive and re-transmit the amplified signals at the same frequency. Although the traditional IBFD relays use separate antenna architecture and SIC is performed using path loss techniques by increasing the physical separation between transmit and receive antennas [49-50] but many analog and digital SIC techniques have also been proposed for IBFD relaying systems [51-52]. Additional SI suppression is achieved by using directional antennas and antenna arrays for beam forming to nullify self interference [36], [53],[54]. In contrast to a Half Duplex Relay (HDR), a Full Duplex Relay (FDR) provides easy scheduling by decoupling the incoming and outgoing links. FDR can reduce the delay by instantaneous retransmission of incoming signal. A simple full duplex relay system can be realized by using RF transmit and receive components along with one of the proposed antennas with one antenna port for reception and other for retransmission of signals after amplification.

2.3.4 Applications in other wireless Systems

These antennas can also be used in Cognitive Radios (CR). Cognitive Radio is used to improve the efficiency of radio spectrum by exploiting the existence of idle band of frequencies which are not being utilized by primary user at a particular time. The cognitive radio suspends any transmission before sensing the spectrum. In a cognitive radio network, the interference to primary users can be reduced if secondary terminals have the capability to sense the spectrum without suspending the transmission activity. The secondary terminals with IBFD mechanism can accomplish this efficiently [55]. An IBFD transceiver with one of the proposed single antenna can work as secondary node as it will enable cognitive transmission and channel sensing simultaneously. One antenna port can be used for channel sensing while the other port for cognitive transmission.

As IBFD operation provides bidirectional link for wireless communication and reverse link can be used for several applications. The reverse link can provide real-time feedback link to wireless nodes including MIMO systems. Some such intended application using back channel of IBFD link has been discussed in [55]. In case of WLAN, by using this channel for data transmission wireless cut-through routing can be implemented, hidden terminal problems can be alleviated in addition to fairness in wireless LANs and real-time partial packet recovery [3] operation. Immediate collision notification and in-band channel status can be transmitted by using back channel for control traffic. Although the examples presented in [56] are investigated for IBFD transceiver which achieves required SIC from two Tx and one Rx antenna cancellation technique along with analog and digital SIC techniques, antenna stage cancellation can be replaced by using one of the antennas proposed in this research work.

Most of the reported research works are based on separate antenna architecture [7], [9] which use two antennas or even more [11] for IBFD transceivers. Some reported designs use single antenna, but the transmission and reception is carried out on two adjacent channels instead of simultaneous transmit and receive on same carrier frequency. Some hybrid SIC techniques are also implemented in order to suppress SI for realization of full duplex wireless communication. Another design which uses analog and digital SIC techniques to achieve 110dB SI suppression has been reported in [12]. This design uses delay lines with different lengths and variable attenuators to implement analog SIC circuit and achieves 60dB SI cancellation. The residual SI is suppressed by digital domain SIC techniques.

CHAPTER 3

DESIGN DETAILS AND SIMULATION RESULTS FOR PROPOSED IBFD MICROSTRIP ANTENNAS

This chapter provides design and simulation details about proposed dual port microstrip patch antennas which deploy different feeding techniques along with Self Interference Cancellation (SIC) circuits to get high interport isolation for single/shared antenna IBFD transceiver architecture. All the proposed antennas in this research work are orthogonal/cross polarized because such antenna systems firstly provide isolation through polarization diversity and then external SIC circuits are used to achieve additional interport isolation but one linear co-polarized antenna design has also been demonstrated here which uses same polarization for both transmit and receive mode. The feeding mechanism for this antenna is established in such a way that high interport isolation has been achieved by just using external SIC circuit with out polarization diversity. The target operating frequency is 2.4GHz for all designs.

3.1 Design and Simulation of Proposed IBFD Antennas

Following microstrip patch antennas have proposed for this research work:

- (i) Dual port ,dual polarized Antenna fed with quarter wave Microstrip feeds
- (ii) Dual port ,dual polarized Antenna fed with T-shaped microstrip feeds
- (iii) Dual port Orthogonal Polarized antenna with feed forward mechanism
- (iv) Dual Port dual Polarized Patch Antenna with high Inter-Port isolation using feeding from same edge
- (v) Dual port ,dual Polarized Antenna with quarter wave microstrip (MS) feeds using single SIC Circuit for high Inter-Port isolation
- (vi) Dual port ,dual Polarized Antenna with microstrip-T (MS-T) feeds using single SIC Circuit for high Inter-Port isolation
- (vii) Dual port ,dual Polarized Antenna with quarter wave feeds (MS) using two SIC Circuits for high Inter-Port isolation
- (viii) Dual port ,dual Polarized Antenna array with quarter wave microstrip (MS) feeds using single SIC Circuit for high Inter-Port isolation

- (ix) Dual port ,orthogonal Polarized Slot Coupled Antenna
- (x) Dual port ,orthogonal Polarized Slot Coupled Antenna with SIC Circuit
- (xi) Three ports microstrip patch antenna with dual linear and linear co-polarization characteristics

3.1.1 Dual port ,dual polarized Antenna fed with quarter wave Microstrip feeds

The geometry of dual polarized 2.4GHz square microstrip patch fed through two quarter wave microstrip feeds from two orthogonal edges is shown in Fig.3.1. The dimensions of antenna are kept identical in order to operate antenna at the same transmit and receive frequencies. The antenna was simulated using Keysight Advanced Design System (ADS) Momentum software.

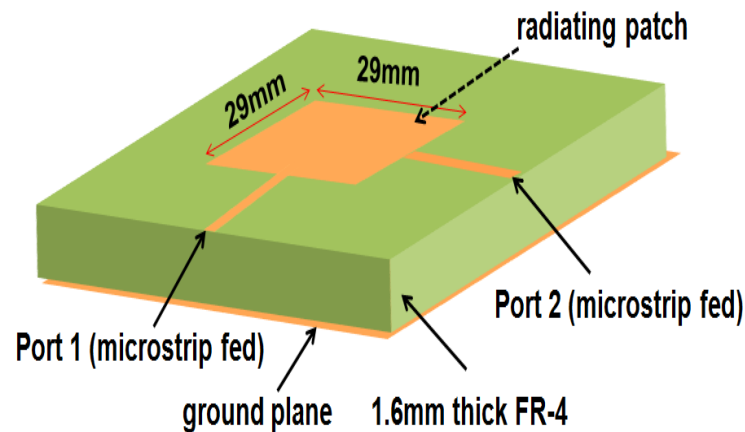


Figure 3.1: Geometry of dual port microstrip patch antenna with both quarter wave microstrip feeds

As reported in [57-58] and verified by simulation results in Fig.3.2, the maximum interport isolation for dual polarized microstrip patch antenna at required operating frequency is achieved when both perpendicular ports feed the antenna from the centre of respective edge. ADS Momentum simulation results in Fig.3.2 for different feeding locations of Port2 ($d=0.5\text{mm}$, 1mm and 1.5mm) on respective edge of antenna clearly demonstrate the effect of feeding point on interport isolation notch frequency. For example, with $d=1.5\text{mm}$ the interport isolation is 44dB as compared to 40dB for $d=0\text{mm}$; however, the interport isolation notch frequency is also shifted from 2.4GHz to 2.64GHz .

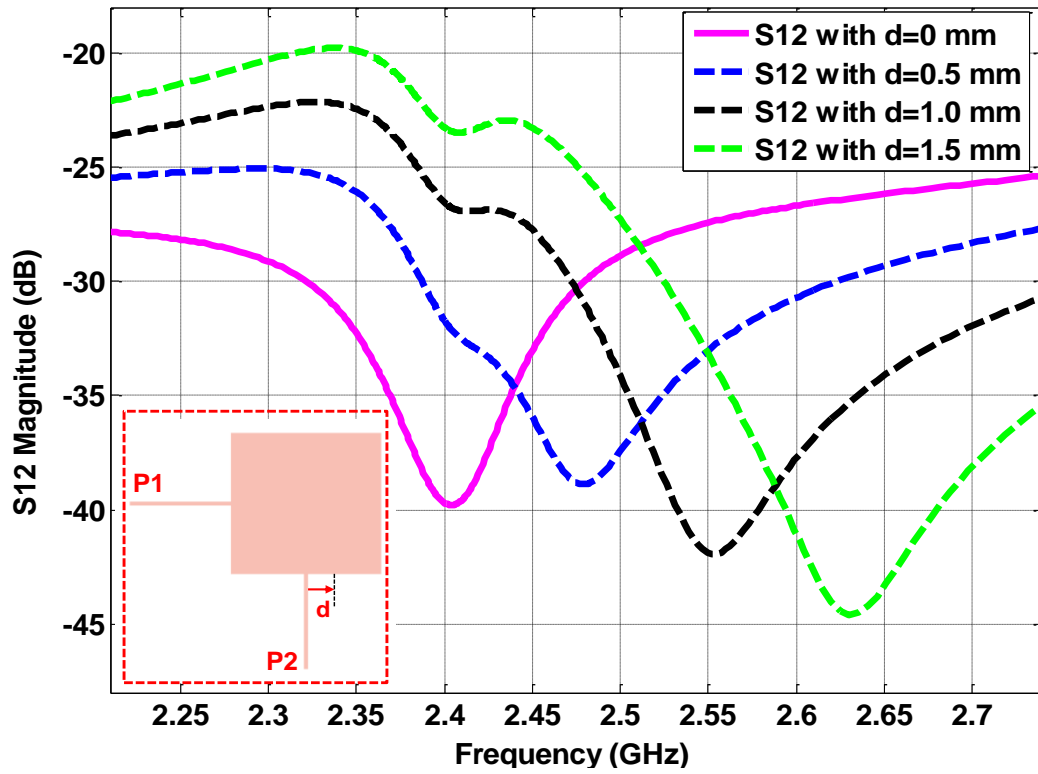


Figure 3.2: Interport isolation vs. feeding location from respective antenna edge

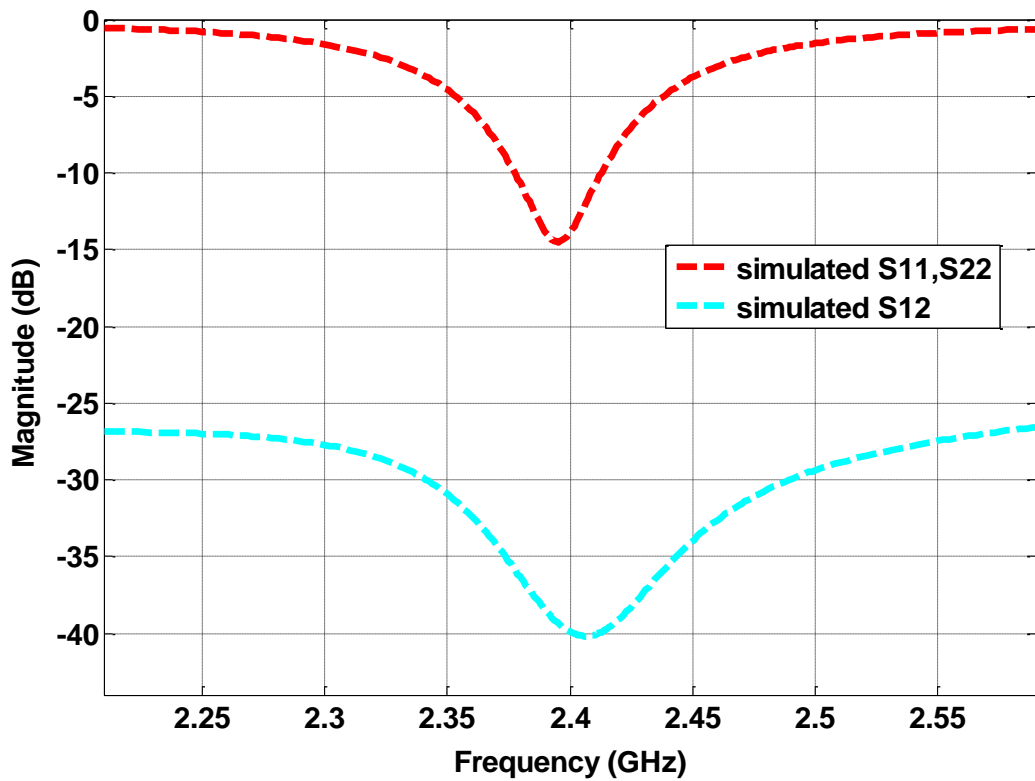
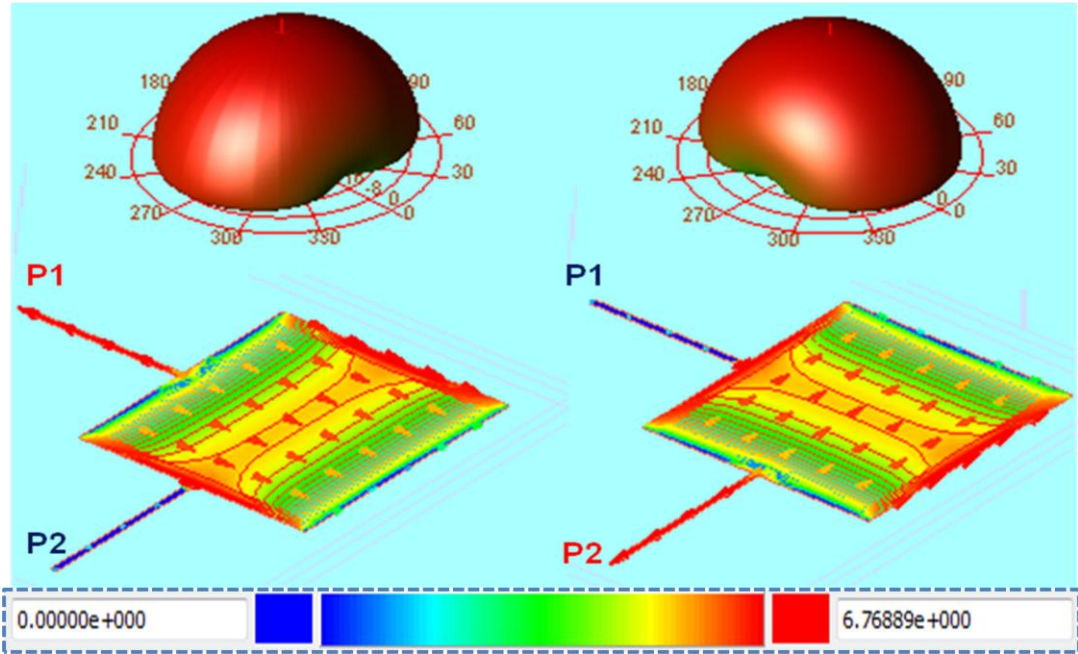


Figure 3.3: Simulated and measured S11, S22 and S12 for dual polarized microstrip antenna with both quarter wave microstrip feeds

ADS Momentum simulated S-parameters results for each port matching performance and port to port RF isolation are shown in Fig.3.3. Simulated interport isolation is better than 40dB for antenna's 10dB input impedance bandwidth of 50MHz as shown in Fig.3.3. This isolation results from polarization diversity. External self interference cancellation circuitry can be deployed [49] with implemented antenna to achieve additional interport isolation for in band full duplex applications

ADS Momentum simulated gain patterns and surface currents of dual polarized microstrip patch antenna fed through quarter wave length impedance transformer microstrip transmission lines are shown in Fig.3.4 for each port excitation while the other port is terminated in 50 ohms. HFSS simulated co-polarization and cross polarization gain patterns are shown in Fig.3.5 for each port excitation with other port terminated in 50 ohms. The proposed antenna is clearly dual polarized (orthogonal polarization) as it is linear vertical polarized for excitation from one port and linear horizontal polarized for other port excitation as shown in Fig.3.4 and Fig.3.5. The simulated gain is 4.1dBi for each port excitation. The antenna transmits and receives with orthogonal polarization and it effectively provides propagation domain isolation between transmit and receive RF signals.



(a) Port 1 excitation

(b) Port 2 excitation

Figure 3.4: Simulated gains and surface currents of dual polarized antenna with $\lambda/4$ microstrip feeds for each port excitation

HFSS simulated co-polarization and cross polarization gain patterns for dual polarized antenna with $\lambda/4$ microstrip feeds are shown in Fig.3.5. The antenna has good polarization purity as it provides very low cross polarization level for each port excitation.

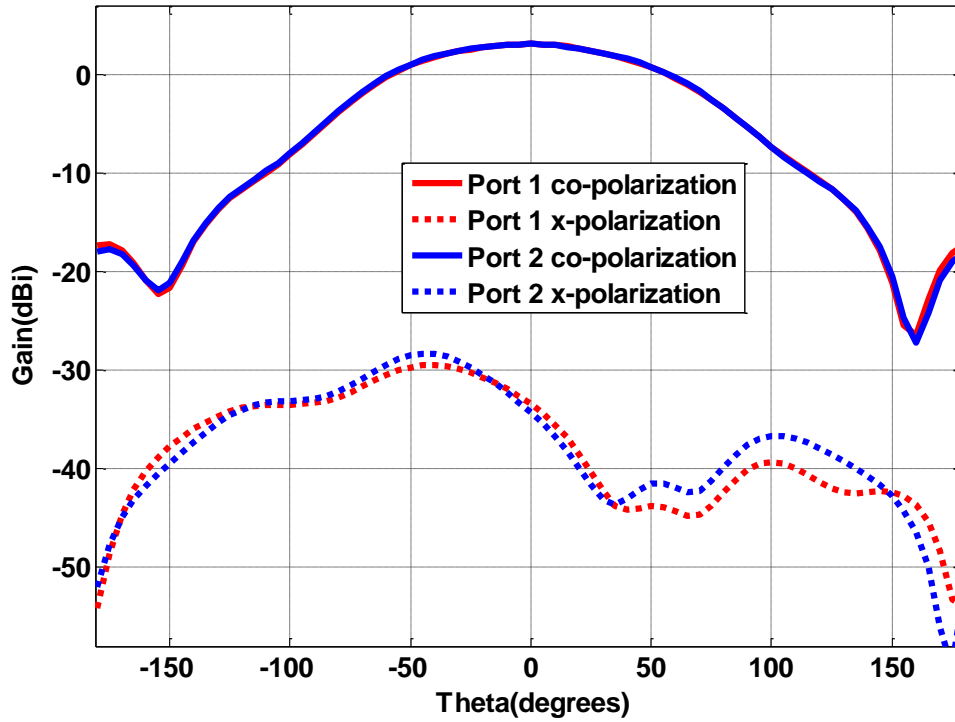


Figure 3.5: HFSS simulated co-polarization and cross polarization gain patterns for dual polarized antenna with $\lambda/4$ microstrip feeds

3.1.2 Dual port ,dual polarized Antenna fed with microstrip-T feeds

A dual polarized 2.4GHz square microstrip patch fed with two T-shaped microstrip feeds from two orthogonal edges [59-60] as shown in Fig.3.6, was simulated using Keysight Advanced Design System (ADS) Momentum software. T-shaped microstrip lines excite the antenna through EM coupling. The dimensions of antenna are kept identical in order to operate antenna at the same transmit and receive frequencies.

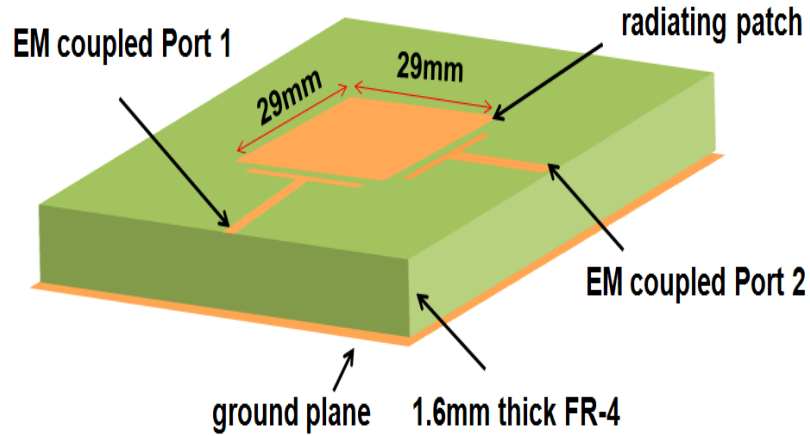


Figure 3.6: Geometry of dual port microstrip antenna with both microstrip-T coupled ports

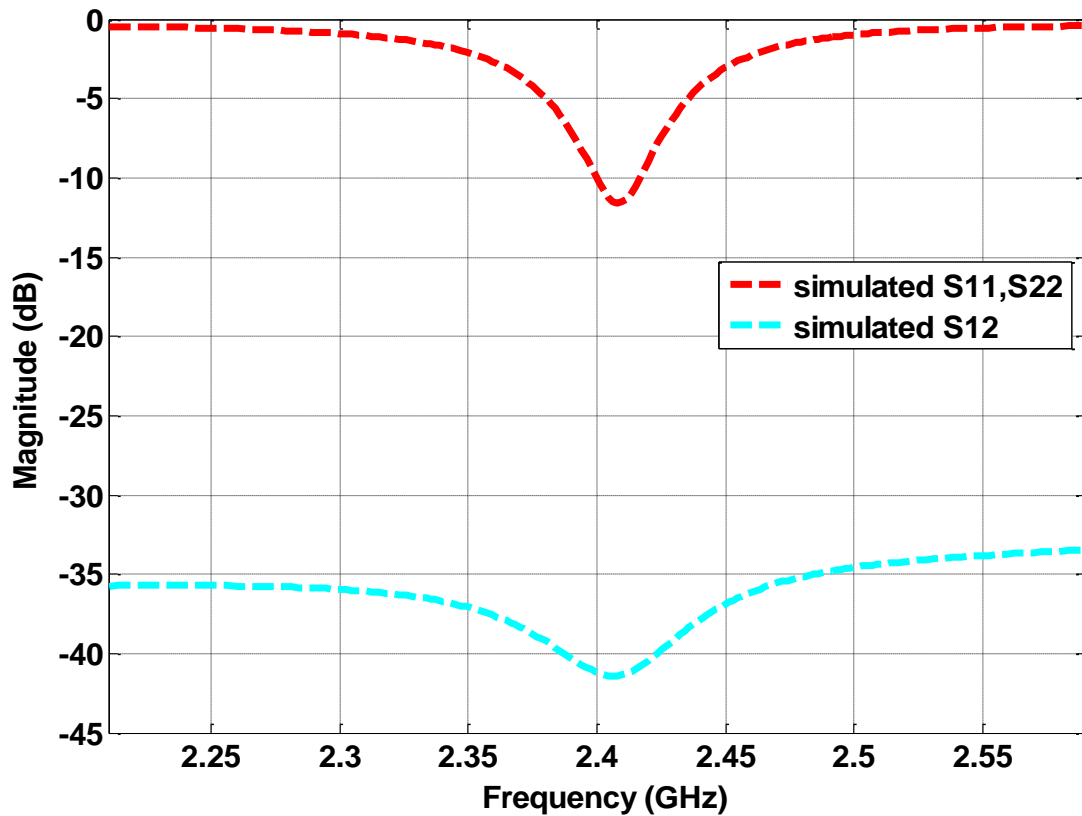


Figure 3.7: Simulated S11, S22 and S12 for dual polarized microstrip antenna with both microstrip-T feeds

ADS Momentum simulated S-parameters results for each port matching performance and port to port RF isolation are shown in Fig.3.7. Simulated interport isolation is better than 42dB for antenna's 10dB input impedance bandwidth of 50MHz as shown in Fig.3.7. As both

ports excite the radiating patch through EM coupling so this antenna provides DC isolation along with 42dB RF isolation at centre frequency through orthogonal polarization. External self interference cancellation circuitry can be deployed [49] with implemented antenna to achieve additional interport isolation for in band full duplex applications

The proposed 2.4GHz dual polarized single layer patch antenna structure shown in Fig.3.8 utilizes different feeding technique for each port excitation. The square microstrip patch is fed with quarter wave microstrip line from one port while the other port is microstrip-T coupled as shown in Fig.3.8. Both ports exist on centre of respective orthogonal edges. The antenna still provides DC interport isolation due to non-existence of direct path between port 1 and port 2. RF isolation is again achieved by dual polarization. Keysight Advanced Design System (ADS) Momentum software was again used to verify port matching and radiation properties of proposed antenna configuration.

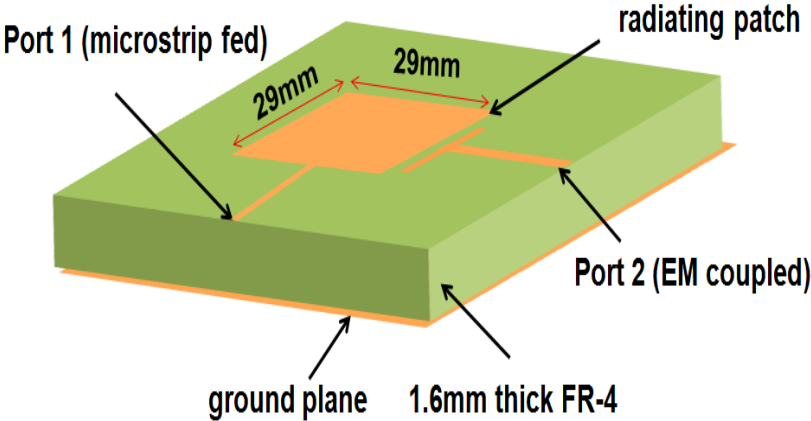


Figure 3.8: Geometry of dual port microstrip patch antenna with one $\lambda/4$ microstrip feed and one microstrip-T feed

Simulated input matching for each port and RF interport isolation results are shown in Fig. 3.9. The antenna has good matching for both ports and measured interport isolation (S12) is 40dB at resonant frequency. The antenna still provides DC interport isolation due to non-existence of direct path between port 1 and port 2. RF isolation is again achieved by dual polarization. The implemented antenna with two DC and RF isolated ports can be deployed

for active antenna applications and also for realization of dual port antennas with high interport isolation for in band full duplex applications as discussed earlier.

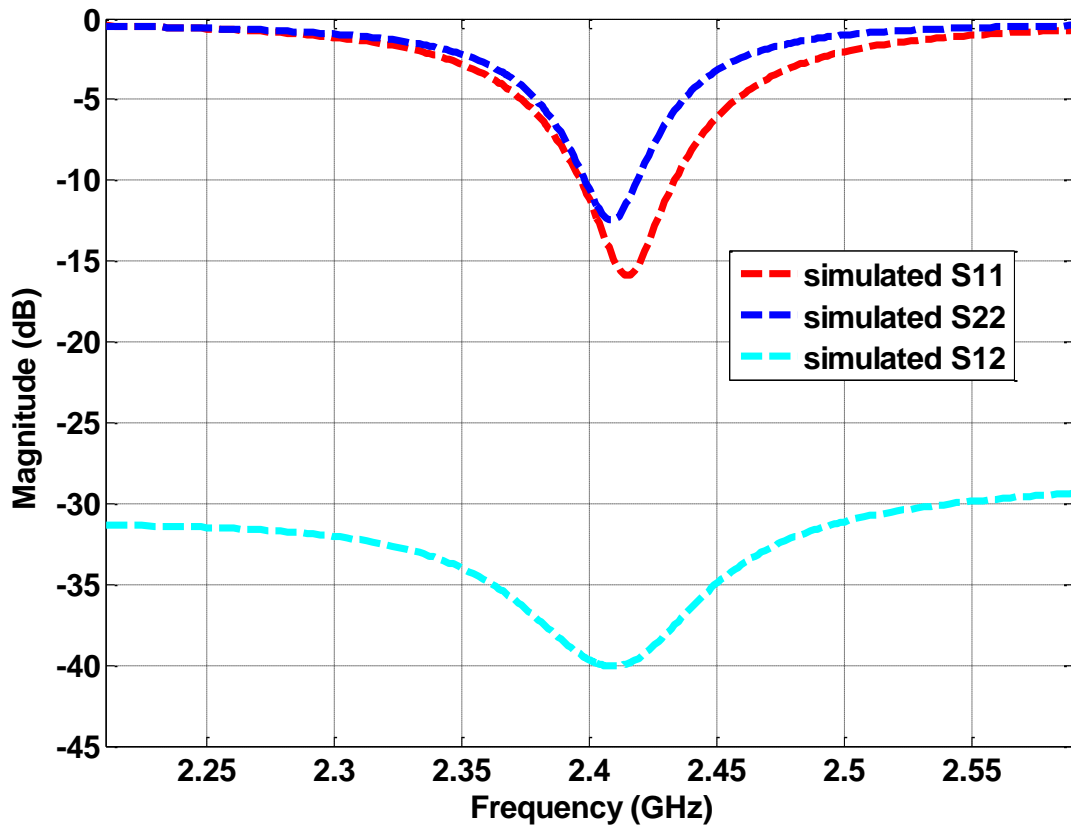


Figure 3.9: Simulated S11, S22 and S12 for dual polarized microstrip antenna with one $\lambda/4$ microstrip feed and one microstrip-T feed

3.1.3 Dual port Orthogonal Polarized Antenna with feed forward loop

A dual port orthogonal polarized single Microstrip patch antenna for IBFD communication has been proposed which uses external feed forward loop for self interference cancellation in RF domain. Initially, a dual port orthogonal polarized 2.4GHz square microstrip patch antenna was designed and simulated using Agilent Advanced Design System (ADS) Momentum software. One port is used as transmit and other as receive port for IBFD operation. The dimensions of antenna are kept equal to have the same transmit and receive operating frequency. Antenna's EM model and ADS simulation results are shown in Fig.3.10.

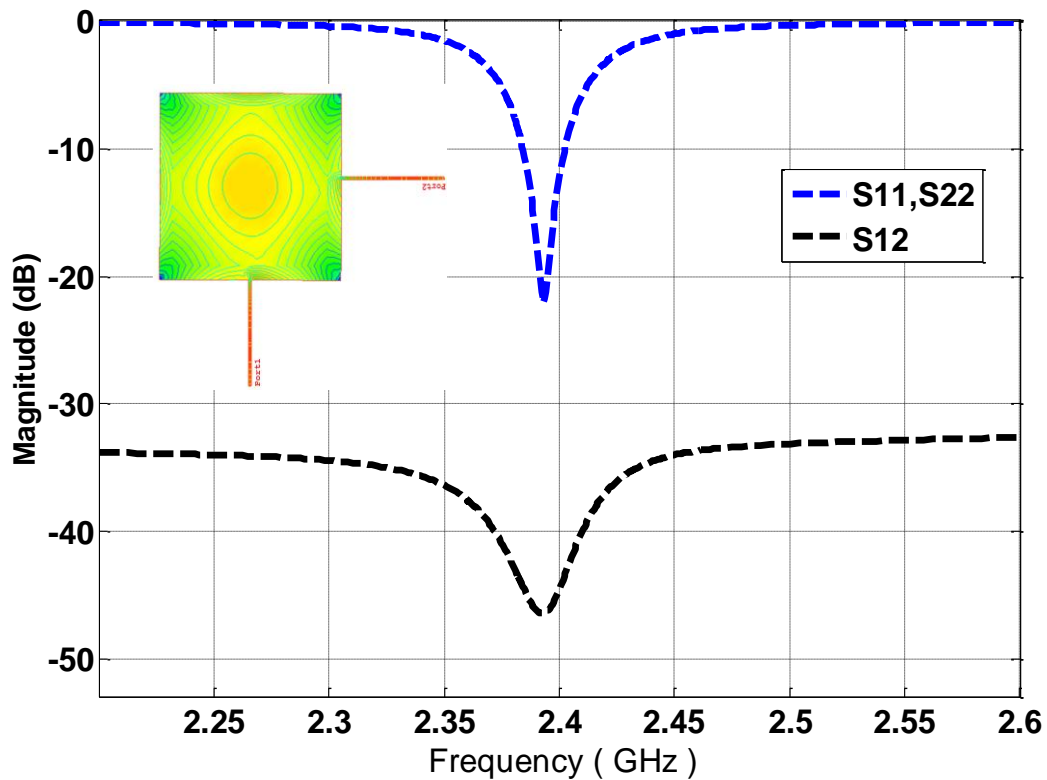


Figure 3.10: Simulated S11, S22 and S12 parameters for dual port patch antenna

The design was simulated for different feeding locations of Port 2 on respective antenna edge to optimize S12 for required operating frequency. Feeding offset distances from the edges for the two ports should be identical and are critical for the design of the antenna for required operating frequency. For this purpose, ADS Momentum Simulation results for different feeding locations of Port2 (offset distances=0.5mm, 1mm, 1.5mm and 2.0mm) on respective antenna edge are obtained and shown in Fig.3.11. It is evident that maximum interport isolation(S12) is attained for required operating frequency of 2.4GHz when both antenna edges are centre fed from the respective edge. It is also noticed that the value of isolation changes as the feed point changes w.r.t the corner. As shown in Fig.3.11, for the 2mm offset from antenna edge centre, the interport isolation is 56dB as compared to 46dB for centre fed case; however, the resonance frequency is also changed from 2.4GHz to 2.6GHz. The optimized S12 was obtained when both antenna edges are centre fed from respective edge as shown in Fig.3.11.

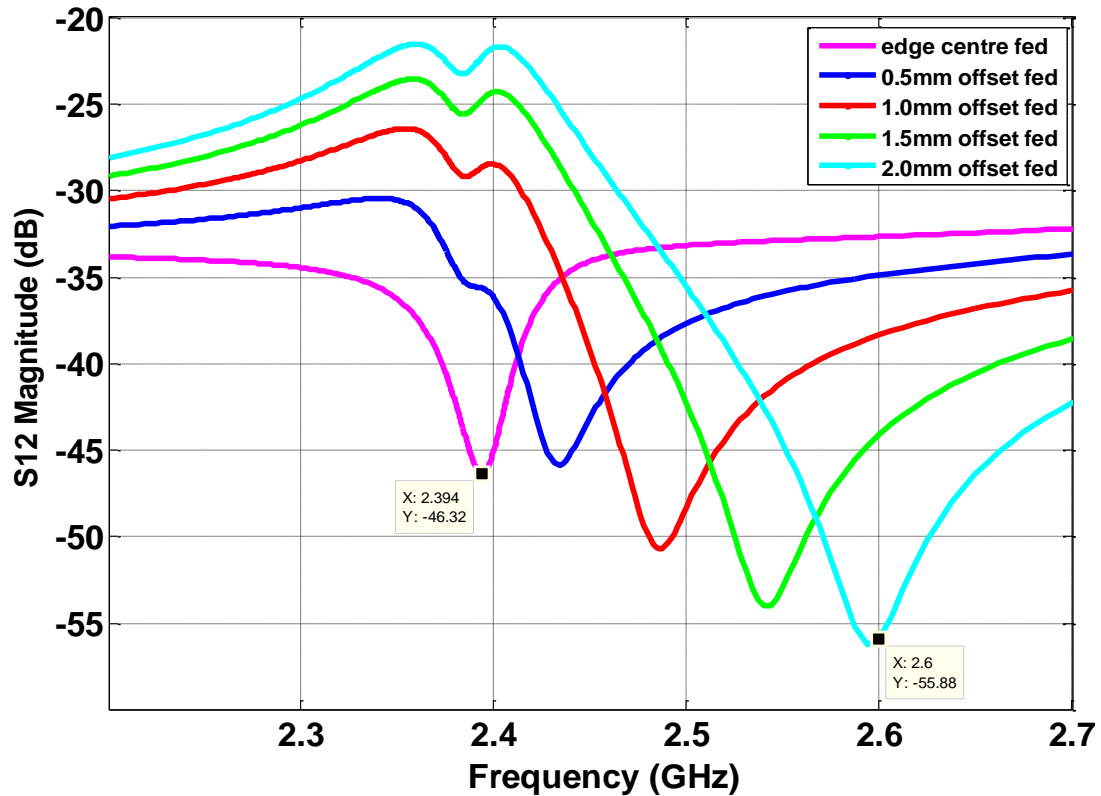


Figure 3.11: Simulation results for Interport isolation variations vs. port 2 feeding positions

Then EM model of dual port antenna was simulated with external feed forward loop. The ADS schematic and simulation setup are shown in Fig.3.12. The signal is sampled from transmit chain and added to sampled signal from receive chain using RF couplers. To adjust the amplitude and phase of the signal, variable phase shifter and variable attenuator are used. The variable phase shifter and variable attenuator used in feed forward loop adjust the phase and magnitude of both sampled signals in such a way that they are equal in magnitude but 180 degrees out of phase so that they interfere destructively to cancel SI. Simulation Results for this setup are shown in Fig.3.13.

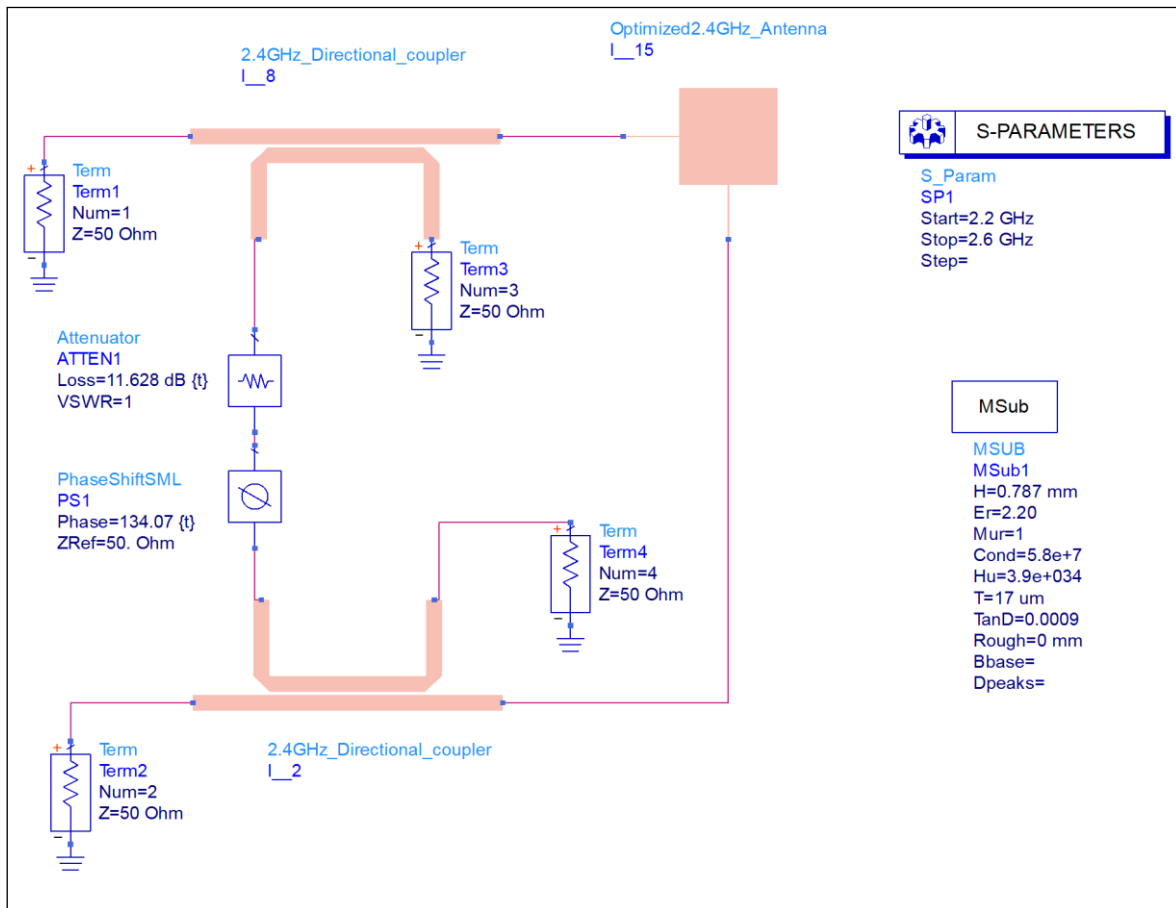


Figure 3.12: ADS schematic and simulation setup for dual port patch antenna with feed forward loop

It is important to note that interport isolation is very sensitive to even slight changes in loop attenuation and phase shift. As shown in Fig.3.13, simulated interport isolation is more than -95dB at 2.4GHz when loop attenuator and phase shifter are set to 11.16dB and 135.15⁰, respectively. However, when loop attenuator and phase shifter values are changed slightly and set to 11dB and 135⁰ the simulated interport isolation degrades by almost 20dB and simulation and measurement results for interport isolation closely follow each other when attenuator and phase shifter in feed forward loop are set to 11dB and 135 degree respectively as clearly shown in Fig.3.13. For better interport isolation values, one can use more precise variable attenuators and phase shifters.

The complete PCB layout for all components including patch antenna, RF couplers and layouts for attenuator and phase shifter is shown in Fig.3.14

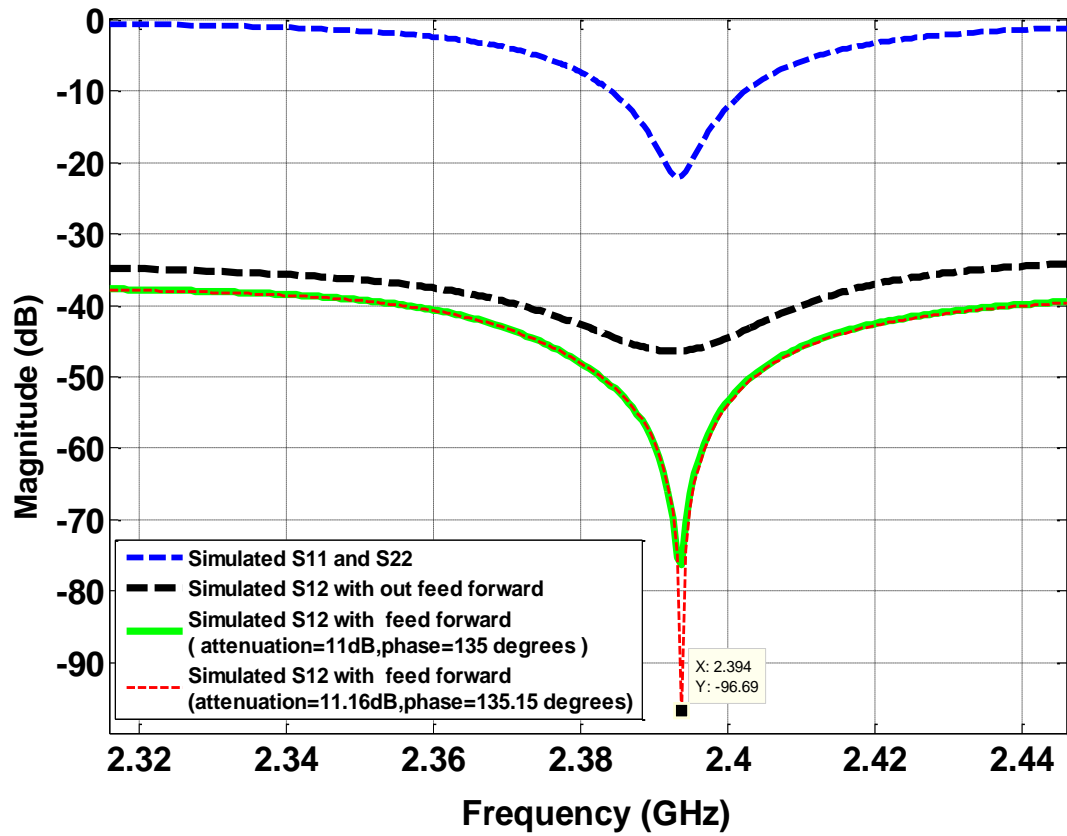


Figure 3.13: Simulated S11, S22 ,S12 for dual port patch antenna with feed forward loop

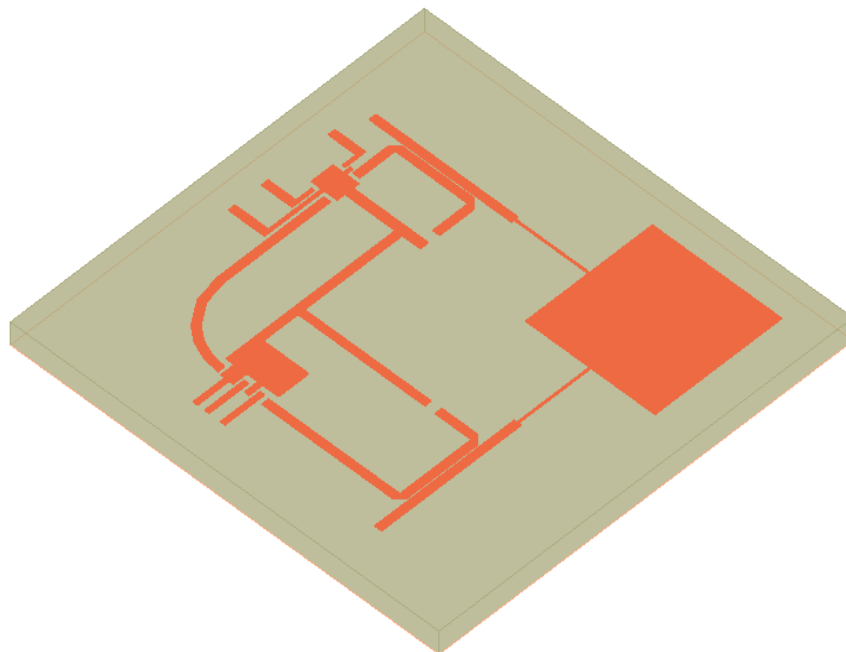


Figure 3.14: Complete PCB layout for antenna with feed forward loop

3.1.4 Dual Port Linearly Co-Polarized Patch Antenna with High Inter-Port Isolation using External SIC Circuit

In the case of IBFD Transceivers with single antenna architecture, most of the reported antenna systems use polarization diversity along with SI cancellation mechanism to decouple transmit and receive ports. In contrast to such designs, in this section a dual port linear co-polarized single microstrip patch antenna has been proposed which uses three ports microstrip patch antenna with 3-dB Ring Hybrid Coupler as SIC circuit to achieve high interport isolation.

As compared to antenna presented in section 3.1.3 which uses external feed forward loop comprised of surface mount components (directional couplers, tuneable phase shifter and variable RF attenuator) in order to achieve high interport isolation for microstrip patch antenna with two orthogonal ports for dual polarization, the presented structure in this work uses patch antenna fed from the same edge and dual polarization is obtained by differential excitation of two side ports using ring hybrid coupler. As compared to external loop used in for self interference suppression, ring hybrid coupler performs self interference cancellation in wider bandwidth to achieve improved interport isolation over large frequency range for three ports microstrip antenna which deploys differential excitation for dual polarization and self interference cancellation using two Rx ports placed symmetrically with respect to centre port (Tx port).

ADS Momentum model of three port microstrip antenna is shown Fig 3.15 (a). By exciting any individual port and terminating the other two ports in 50 ohms, the antenna is linearly vertically polarized as each port feeds the microstrip patch from the same edge. But if we differentially excite the two side ports (port 2 and port 3), then antenna is linearly horizontally polarized. This polarization diversity is clearly depicted in ADS simulated gain patterns and surface currents as shown in Fig 3.16. For our proposed design, port 1 will be used as Tx port and port 2 and port 3 as Rx port for transmission and reception of RF signal with single antenna at same frequency (2.5GHz) as shown in Fig 3.15 (a).

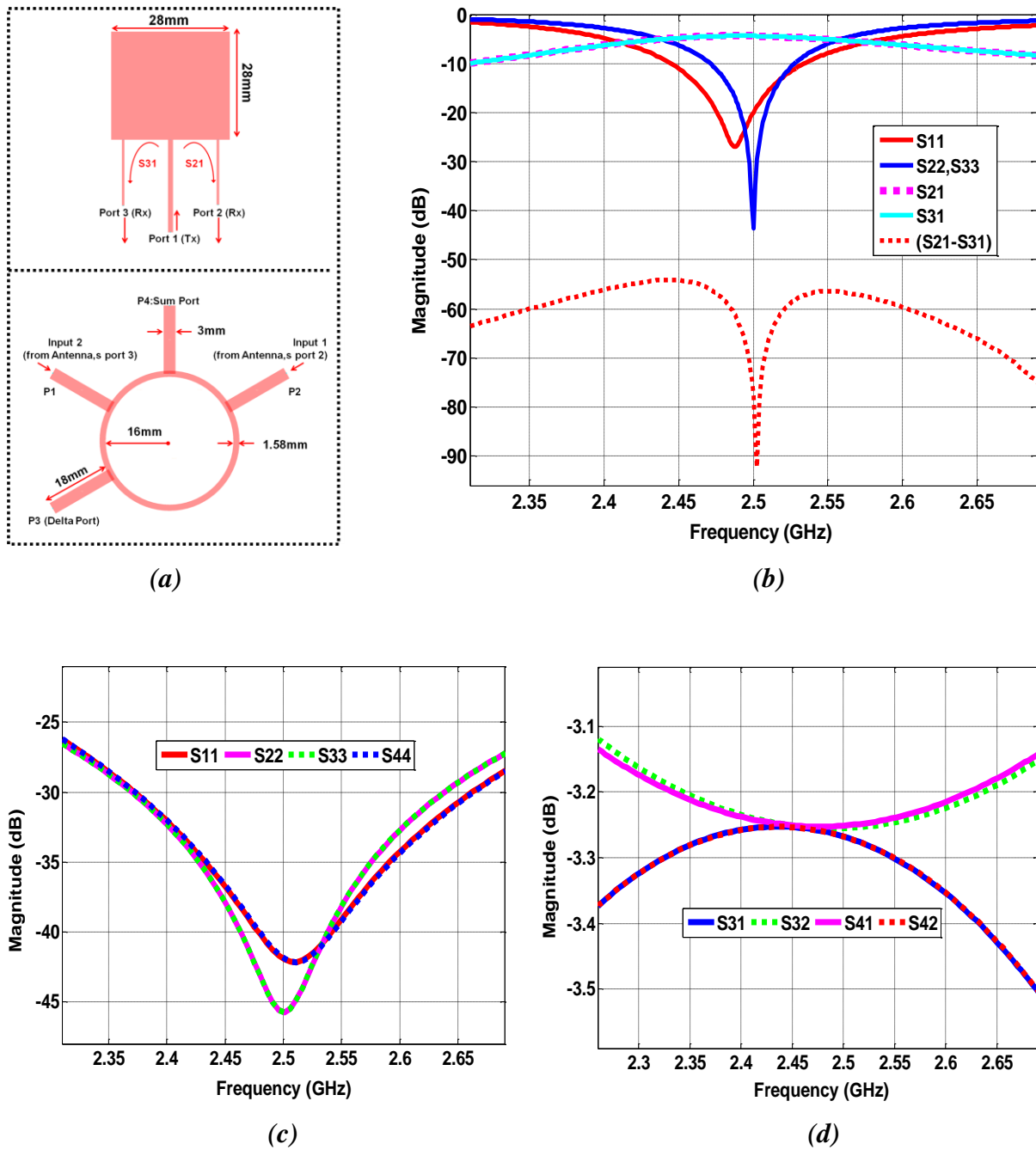
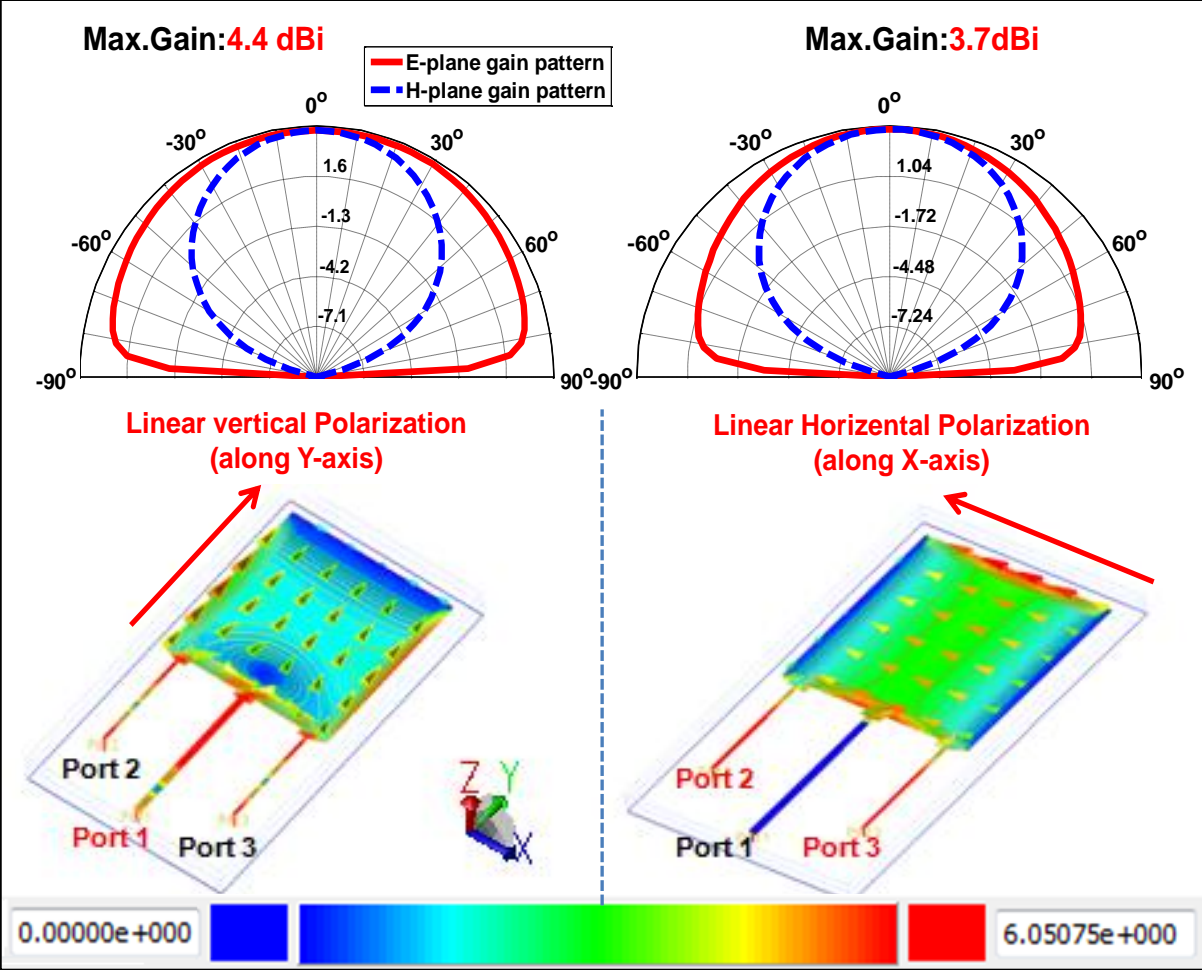


Figure 3.15: (a) ADS Momentum Models of antenna and Hybrid coupler, (b) Simulated S-Parameters Results for antenna (c),(d) Simulated S-Parameters Results for Ring Hybrid coupler

Same amount of RF signal is coupled from port 1 to port 2 and port 3 due to symmetrical configuration of two side ports with respect to the centre port i.e. $S_{21}=S_{31}$. The 3-dB ring hybrid coupler shown in Fig 3.15 (a) is used as SI canceller. Simulated S-Parameters results for ring hybrid coupler are shown in Fig 3.15 (c) and Fig.3.15 (d). If we use port 2

and port 3 of antenna as inputs to hybrid coupler, it performs (S_{21} - S_{31}) operation if delta port is used as Rx port as clearly shown in Fig.3.15(b) with simulated S-Parameters results for three ports antenna. In this way the coupling from Tx to Rx port is effectively cancelled in addition to polarization diversity obtained by differential feeding mechanism, so high interport isolation is achieved to enable single microstrip patch antenna for full duplex operation at same frequency.



(a) Port 1 excitation

(b) Differential excitation of Port 2 & Port 3

Figure 3.16: Simulated gain patterns and current distribution of three port antenna for each port excitation

As shown in Fig.3.16 by simulated E-plane and H-plane radiation patterns and current distributions of three ports antenna, when port 1 is excited and port 2 and port 3 are terminated in 50 ohms then antenna is vertical linearly polarized ($E_y \neq 0$ and $E_x=0$) with

4.4dBi gain while terminating port 1 with 50 ohms and differential excitation of port 2 and port 3 leads to horizontal polarized patch antenna ($E_x \neq 0$ and $E_y=0$) with 3.7dBi gain. This indicates that although patch is fed from same edge for both Tx and Rx modes, it is dual polarized due to differential excitation configuration for Rx mode.

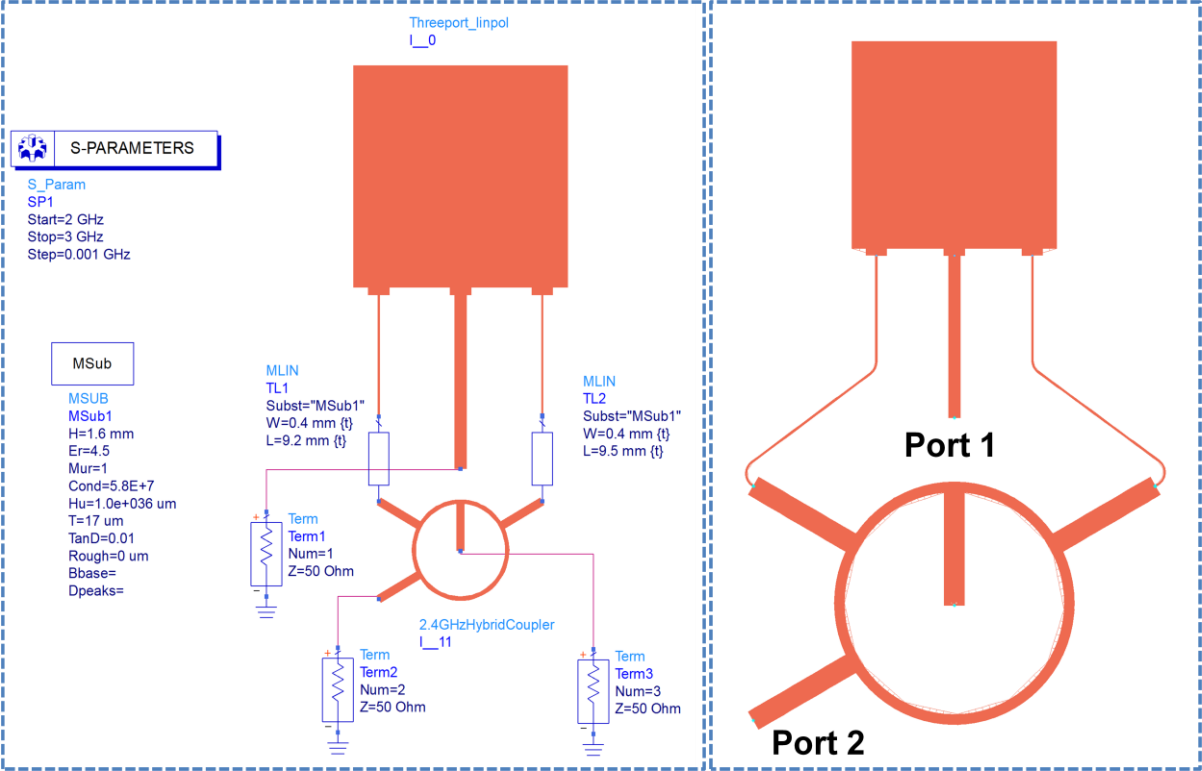


Figure 3.17: (a) ADS Schematic and simulation set up (b) PCB layout for compact Design

ADS simulation has been performed by connecting the EM models of both three ports linear co-polarized antenna and 3-dB Ring Hybrid coupler as shown in Fig.3.17 (a). Simulation results for this setup are shown in Fig.3.18. Compact antenna structure can be realized by etching three port antenna and ring hybrid coupler on the same PCB. PCB layout for such compact structure is shown in Fig.3.17 (b). The simulation results achieve 70 dB isolation for ADS schematic setup and more than 60dB isolation at centre operating frequency for compact design. The simulated isolation is more than 45dB in 50MHz antenna input impedance bandwidth for compact antenna shown in Fig.3.18.

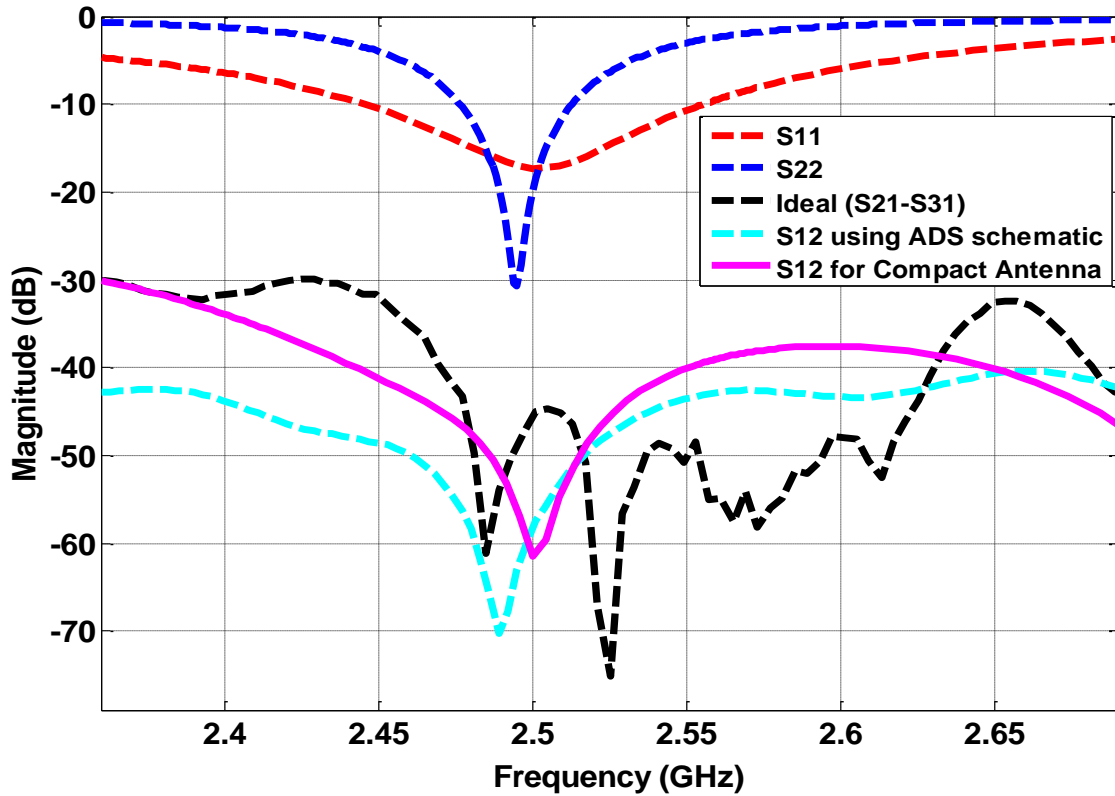


Figure 3.18: Simulated S11, S22 ,S12 for dual port linear co-polarized patch antenna using SIC circuit

3.1.5 Dual port ,dual Polarized Antenna with quarter wave microstrip (MS) feeds using single SIC Circuit for high Inter-Port isolation

For the proposed antenna design, a Ring hybrid coupler has been used as an external SIC with three ports orthogonal polarized patch antenna. The EM model for three port orthogonal polarized antenna is shown in Fig.3.19 which uses quarter wave microstrip feeds for all ports excitation. The polarization diversity provides almost 40dB isolation between port 1 and port 2 and same is the case for port 3 and port 1 as clearly shown in Fig.3.21 .If an external SIC circuit is connected between port 2 and port 3 which can perform ($S_{21} - S_{31}$) operation then SI from transmit to receive port can be cancelled then additional isolation can be achieved by this SIC circuit as depicted in Fig.3.21. A 3-dB Ring Hybrid coupler has been used as an external SIC circuit which performs ($S_{21}-S_{31}$) operation when Δ port of coupler is used.

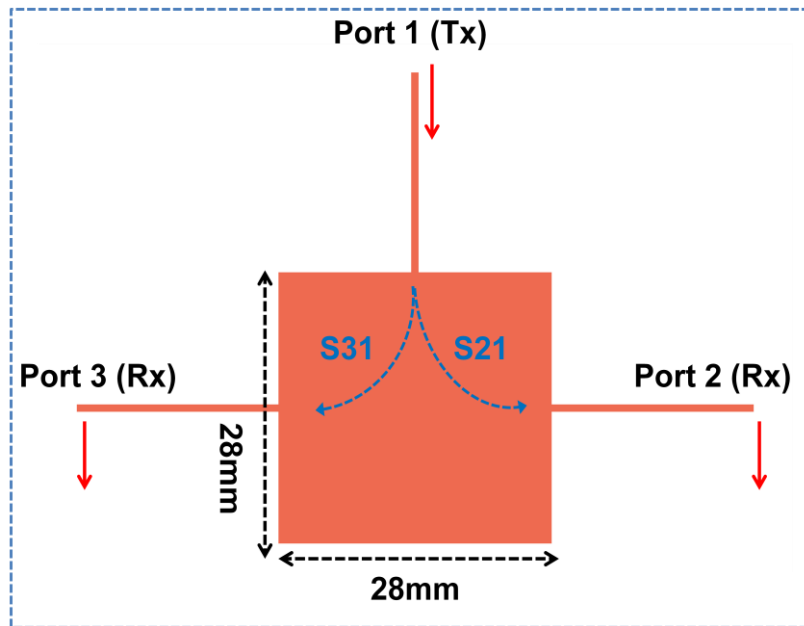


Figure 3.19: EM Model for three port dual polarized antenna with quarter wave microstrip feeds

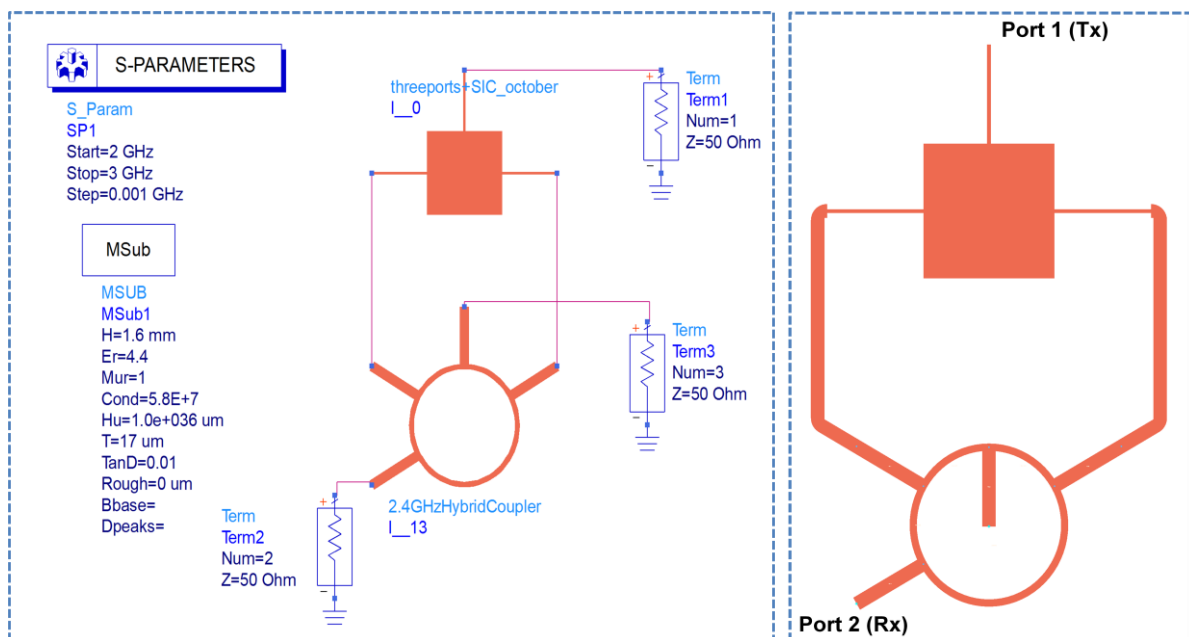


Figure 3.20: (a) ADS schematic and simulation setup (b) PCB layout for compact antenna

ADS simulation has been accomplished by interconnections of EM models of both three ports orthogonal polarized antenna and 3-dB Ring Hybrid coupler as shown in Fig.3.20 (a). The compact antenna can be fabricated by etching the three port antenna and SIC circuits on the same PCB. The PCB layout for the compact antenna is shown in Fig.3.20 (b).The simulation results for the compact antenna structure provide more than 75dB isolation at the centre operating frequency as shown in Fig.3.21. So, more than 35dB additional isolation is obtained by SIC circuit. The simulated isolation is more than 65dB in 50MHz antenna input impedance bandwidth.

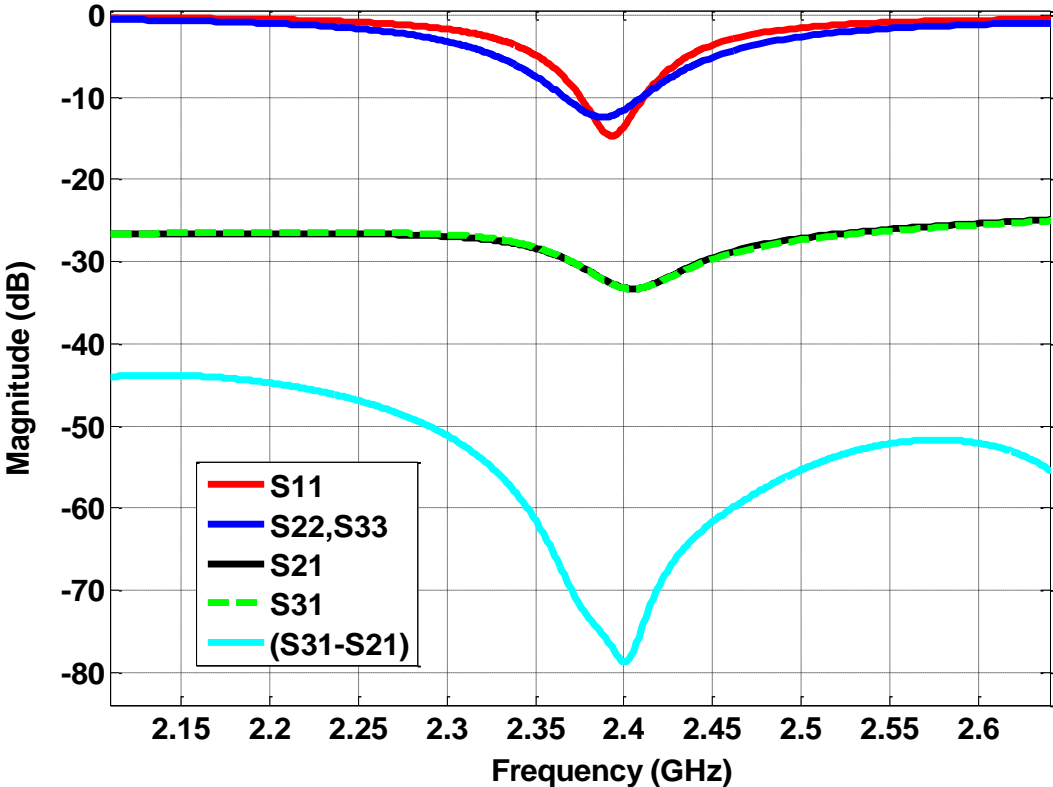


Figure 3.21: Simulated S-Parameters for three port dual polarized patch antenna with quarter wave microstrip feeds and differentially excited by ring hybrid coupler

HFSS simulated co-polarization and cross polarization gain patterns for dual polarized differential fed microstrip patch antenna with $\lambda/4$ microstrip feeds are shown in Fig.3.22. The antenna has good polarization purity as it provides very low cross polarization level for each port excitation and especially for excitation port with differential feeding configuration.

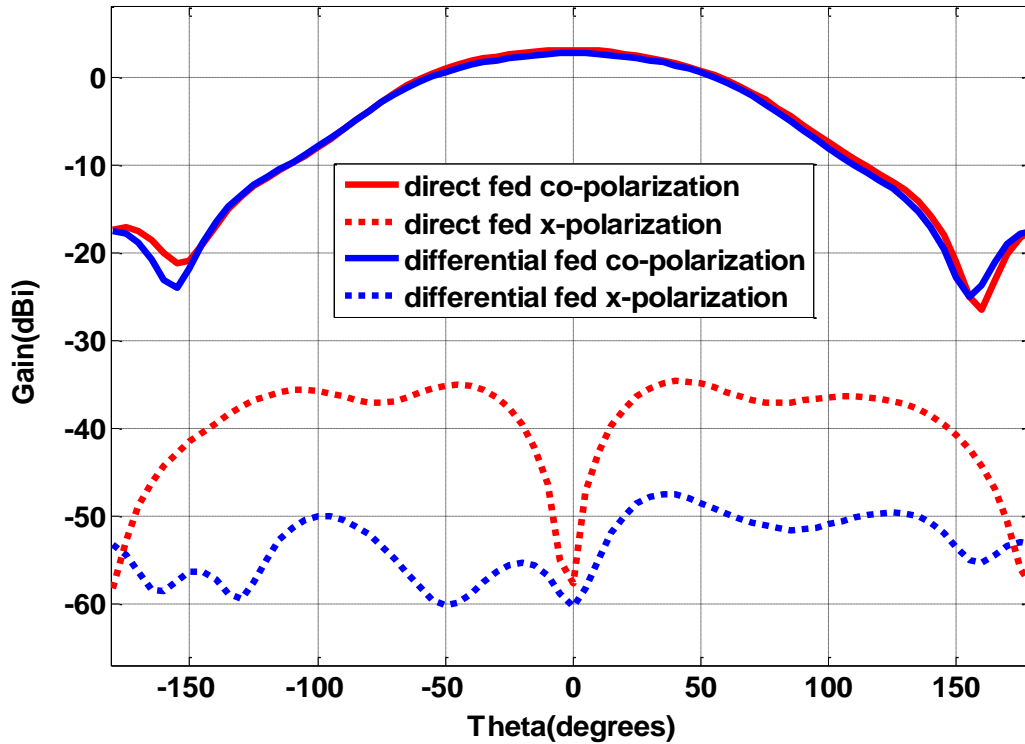


Figure 3.22: HFSS simulated co-polarization and cross polarization gain patterns for dual polarized differential fed antenna with $\lambda/4$ microstrip feeds

3.1.6 Dual port ,dual Polarized Antenna with microstrip-T (MS-T) feeds using single SIC Circuit for high Inter-Port isolation

This antenna architecture deploys microstrip-T shaped structure for each port to excite radiating patch through electromagnetic coupling instead of quarter wave microstrip feed lines and thus provides DC isolation between transmit and receive ports. For the proposed antenna design, a ring hybrid coupler has been used as an external SIC with three port orthogonal polarized patch antenna fed through MS-T from each port. The EM model for three port orthogonal polarized antenna is shown in Fig.3.23 which uses microstrip-T feeds for all ports excitation. Port 2 and port 3 are used for differential excitation and due to this differential configuration, RF leakage from port1 is suppressed at receive port as already discussed for three port antenna with thin quarter wave feeds. This configuration provides high RF port to port isolation along with DC isolation.

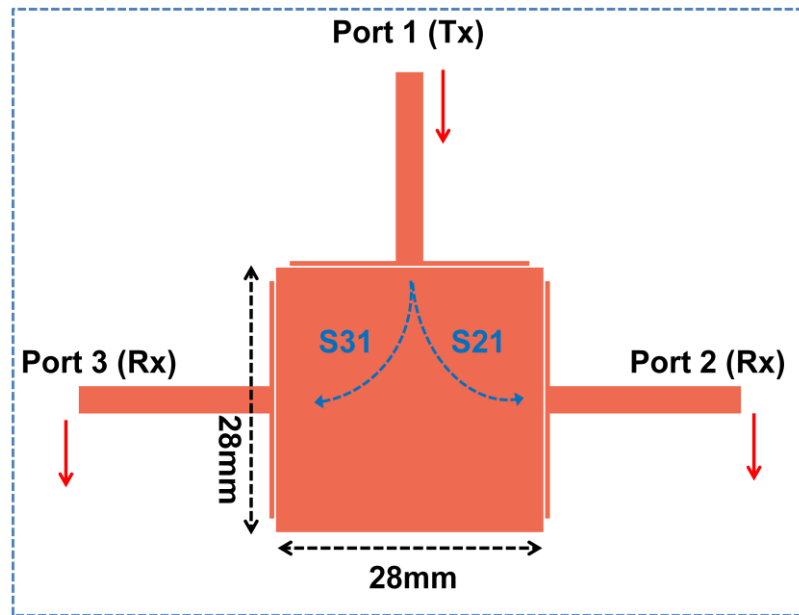


Figure 3.23: EM Model for three port dual polarized antenna with microstrip-T feeds

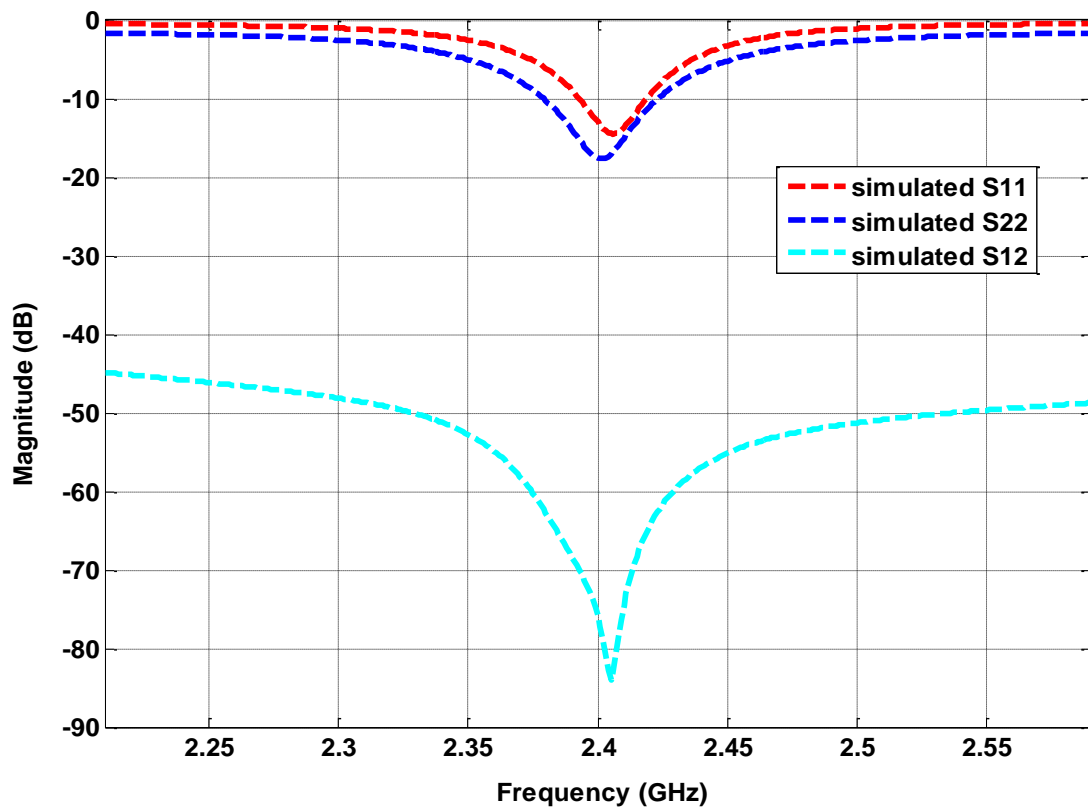


Figure 3.24: Simulated S-Parameters for three port dual polarized patch antenna with microstrip-T feeds and differentially excited by ring hybrid coupler

Again ADS simulation has been accomplished by interconnections of EM models of both three ports orthogonal polarized antenna and 3-dB ring hybrid coupler. The polarization diversity provides almost 40dB isolation between port 1 and port 2 and same is the case for port 3 and port 1. If an external SIC circuit is connected between port 2 and port 3 which can perform $(S_{21} - S_{31})$ operation, SI from transmit to receive port can be cancelled then additional isolation can be achieved by this SIC circuit. A 3-dB Ring Hybrid coupler has been used as the external SIC circuit which performs $(S_{21}-S_{31})$ operation when Δ port of coupler is used. The simulation results provide more than 80dB isolation at the centre operating frequency as shown in Fig.3.24. Thus, more than 40dB additional isolation is obtained by SIC circuit. The simulated isolation is more than 60dB in 50MHz antenna input impedance bandwidth. The compact antenna can be fabricated by etching the three port antenna and SIC circuits on the same PCB. The PCB layout for the compact antenna is shown in Fig.3.25.

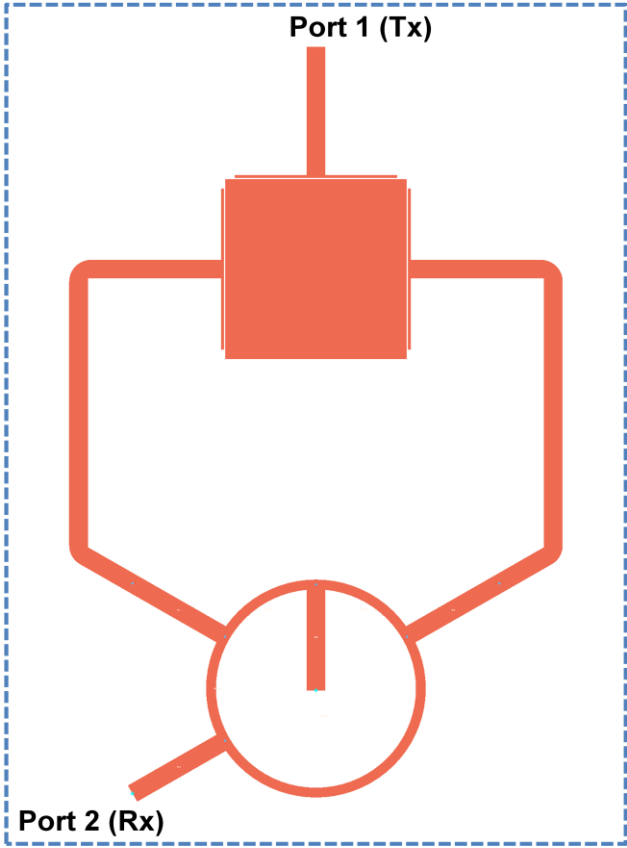


Figure 3.25: PCB layout for compact antenna structure with MS-T feeds and SIC circuit

3.1.7 Dual port, dual Polarized microstrip patch antenna with quarter wave feeds and using two SIC circuits

For the antenna discussed in section 3.1.5 and section 3.1.6, the external SIC circuit has been used as Differential Feeding Network (DFN) for suppressing the mutual coupling by destructive interference of two signals which are obtained by coupling from single port to two input ports of SIC circuit. For the antenna discussed in section 3.1.5 and section 3.1.6, the total achieved isolation is resulted from polarization diversity and SIC circuit. In both cases, the SIC circuit with Differential Feeding Network (DFN) mechanism has been used at either transmit port or receive port. If we use Differential Feeding Network (DFN) at both transmit and receive ports simultaneously then extra interport isolation can be achieved as compared to proposed design in previous section for orthogonal polarized antenna. The extra isolation results from double suppression of mutual coupling between the antenna ports.

For the proposed antenna design, four port microstrip patch antenna with thin $\lambda/4$ feeds shown in Fig.3.26 (a) has been used. One SIC circuit with DFN mechanism is connected between port 1 and port 2 for transmission while the other SIC is connected between port 3 and port 4 for reception signals. Again 3dB Ring Hybrid coupler has been used as discussed earlier to differentially excite the respective antenna ports.

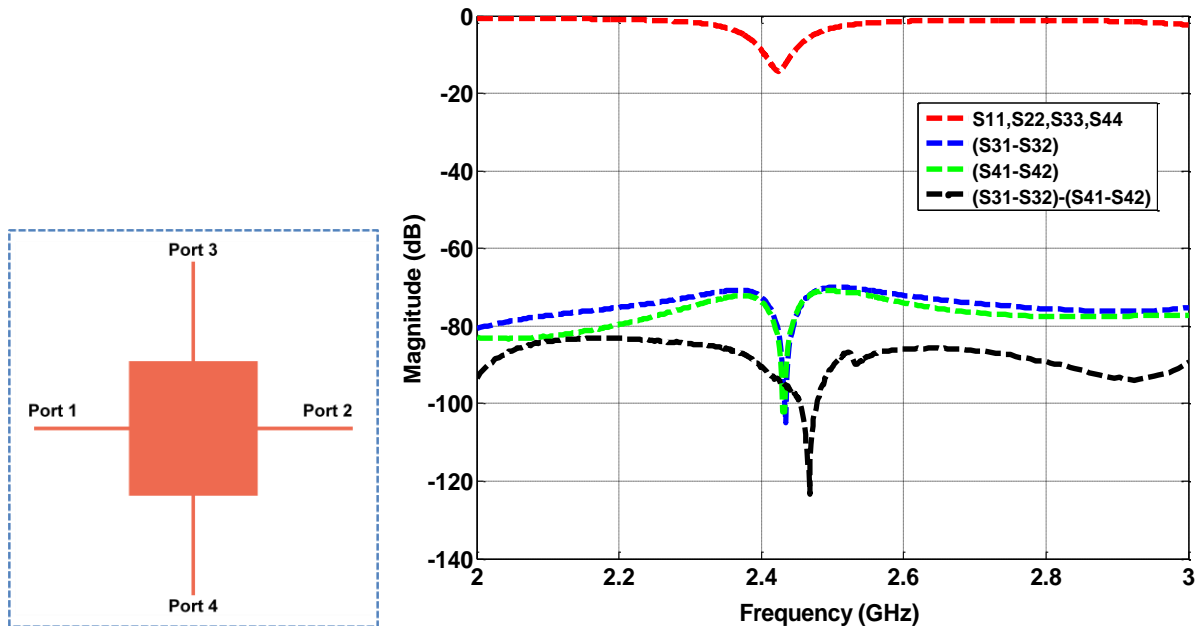


Figure 3.26: (a) Four ports Antenna's EM Model

(b) ADS Simulation Results

The RF leakage from port 1 to port 3 i.e. S31 and from port 2 to port 3 i.e. S32 interfere destructively to cancel each other i.e. S31-S32 operation is performed at Δ port of SIC Circuit due to differential excitation of port 1 and port 2 as already discussed for three port orthogonal polarized antenna in previous section. Similar operation is performed at port 4 and we get S41-S42. Then the second SI suppression results from other SIC Circuit and we get (S31-S32)-(S41-S42) using Δ port of this SIC Circuit.

ADS schematic and simulation setup for the proposed antenna is shown in Fig.3.27. The simulation results in Fig.3.28 show that 80dB isolation over wider bandwidth as compared to 65dB isolation in 50MHz antenna input impedance bandwidth for the antenna discussed in section 3.1.5. The proposed antenna with two SIC Circuits can not be implemented in compact form on single PCB on single side due to cross over of microstrip interconnects for SICs interfacing with antennas. It is possible to implement antenna and one SIC on the same layer and connect the second SIC through equal length RF cables from the back side of the PCB.

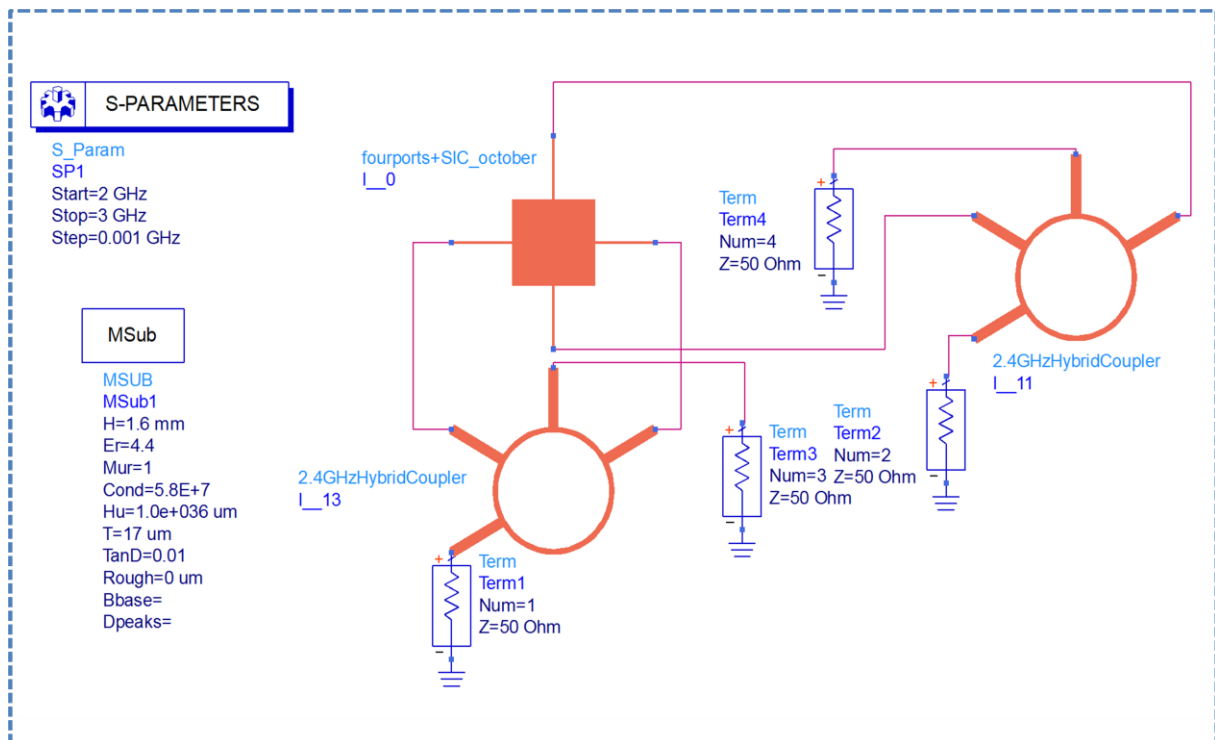


Figure 3.27: ADS schematic and simulation setup for four ports patch antenna with two SIC Circuits

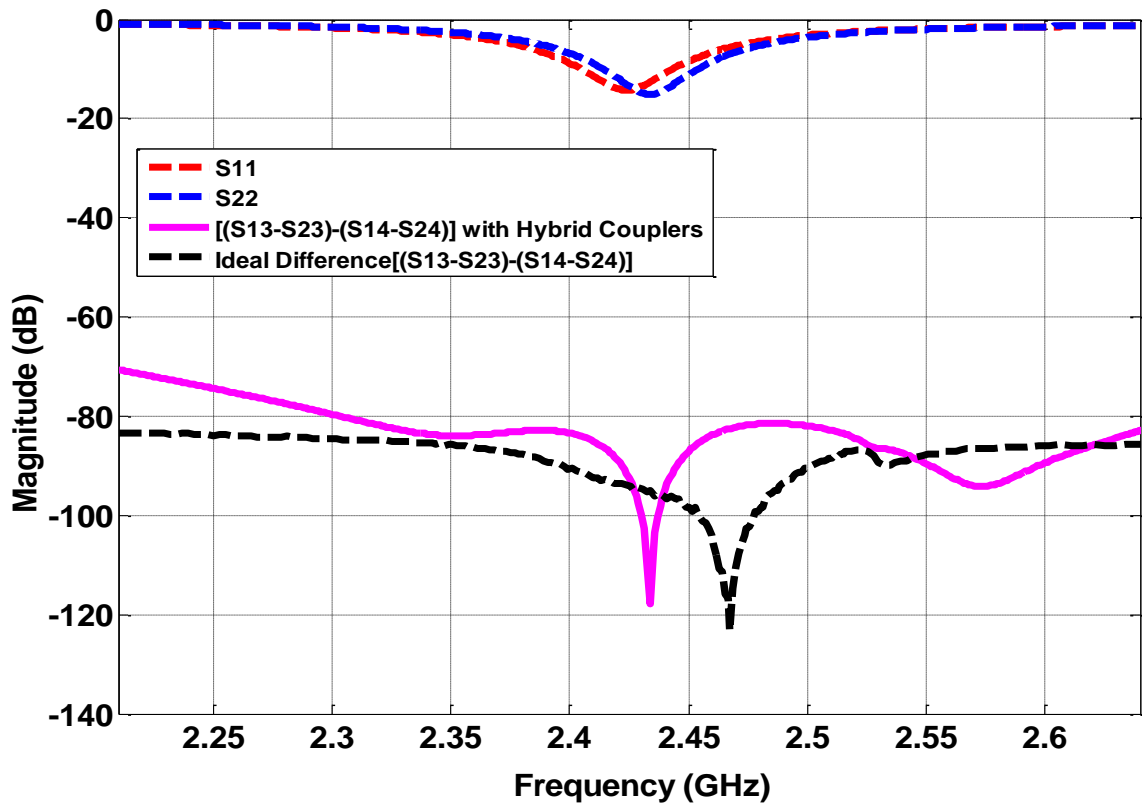


Figure 3.28: Simulation results for dual polarized patch with two SIC Circuits

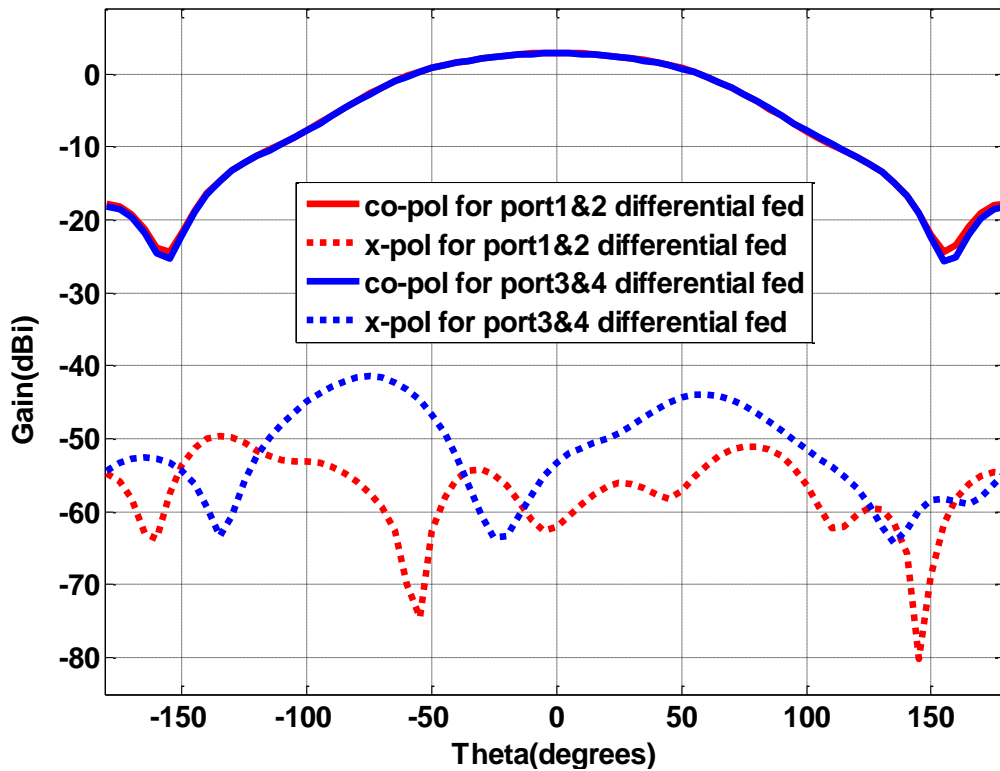


Figure 3.29: HFSS simulated co-polarization and cross polarization gain patterns for dual polarized differential fed antenna with $\lambda/4$ microstrip feeds

HFSS simulated co-polarization and cross polarization gain patterns for dual polarized double differential fed microstrip patch antenna with $\lambda/4$ microstrip feeds are shown in Fig.3.29. The antenna has very nice polarization purity for both ports as it provides very low cross polarization level for both differential feeding configurations.

3.1.8 Dual port ,dual Polarized Antenna array with quarter wave microstrip (MS) feeds using single SIC Circuit for high Inter-Port isolation

The proposed antenna array design in this section achieves almost the same performance as that of the antenna discussed in section 3.1.5 by using single ring hybrid coupler with two element microstrip antenna array as shown in Fig.3.30. The additional advantage of this design is high gain due to array setup.

ADS schematic and simulation setup for the proposed antenna array is shown in Fig.3.31 with a single hybrid coupler which operates at 2.4GHz frequency. The spacing between array-elements is $\lambda_0/4$ where λ_0 is the free space wave length corresponding to 2.4GHz operating frequency. The RF leakages from port 1 to port 3 i.e. S31 and from port 1 to port 2 i.e. S21 interfere destructively to cancel each other i.e. S31-S21 operation is performed at Δ port of SIC Circuit due to differential excitation of port 2 and port 3 as already discussed for three port orthogonal polarized antenna.

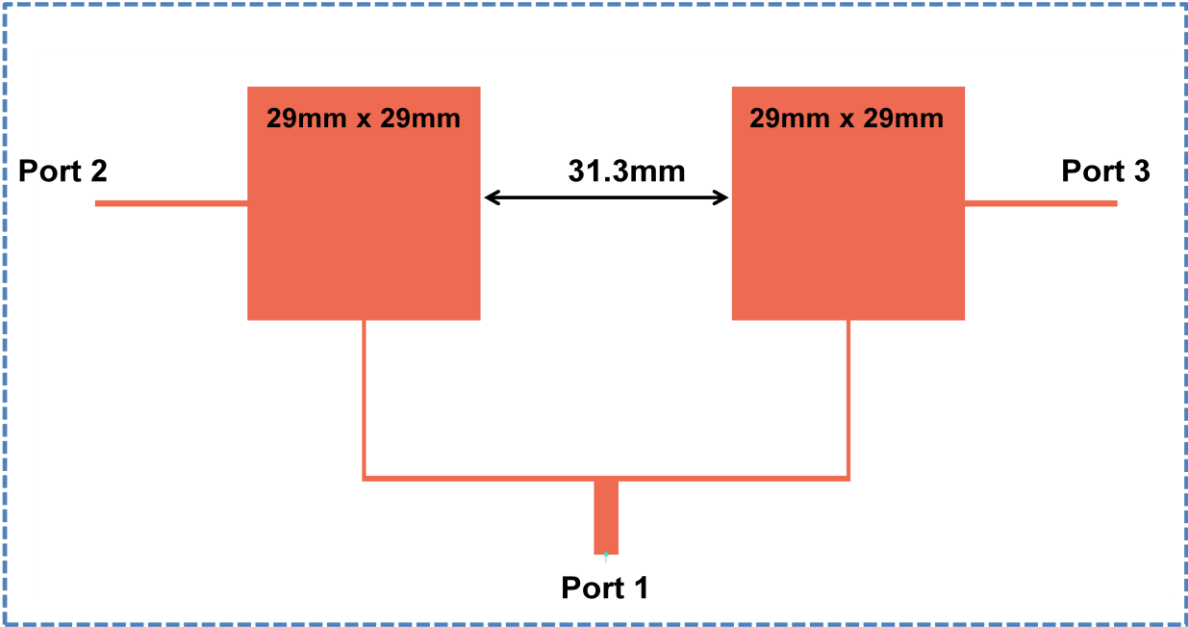


Figure 3.30: EM Model for dual polarized differential fed microstrip patch antenna array

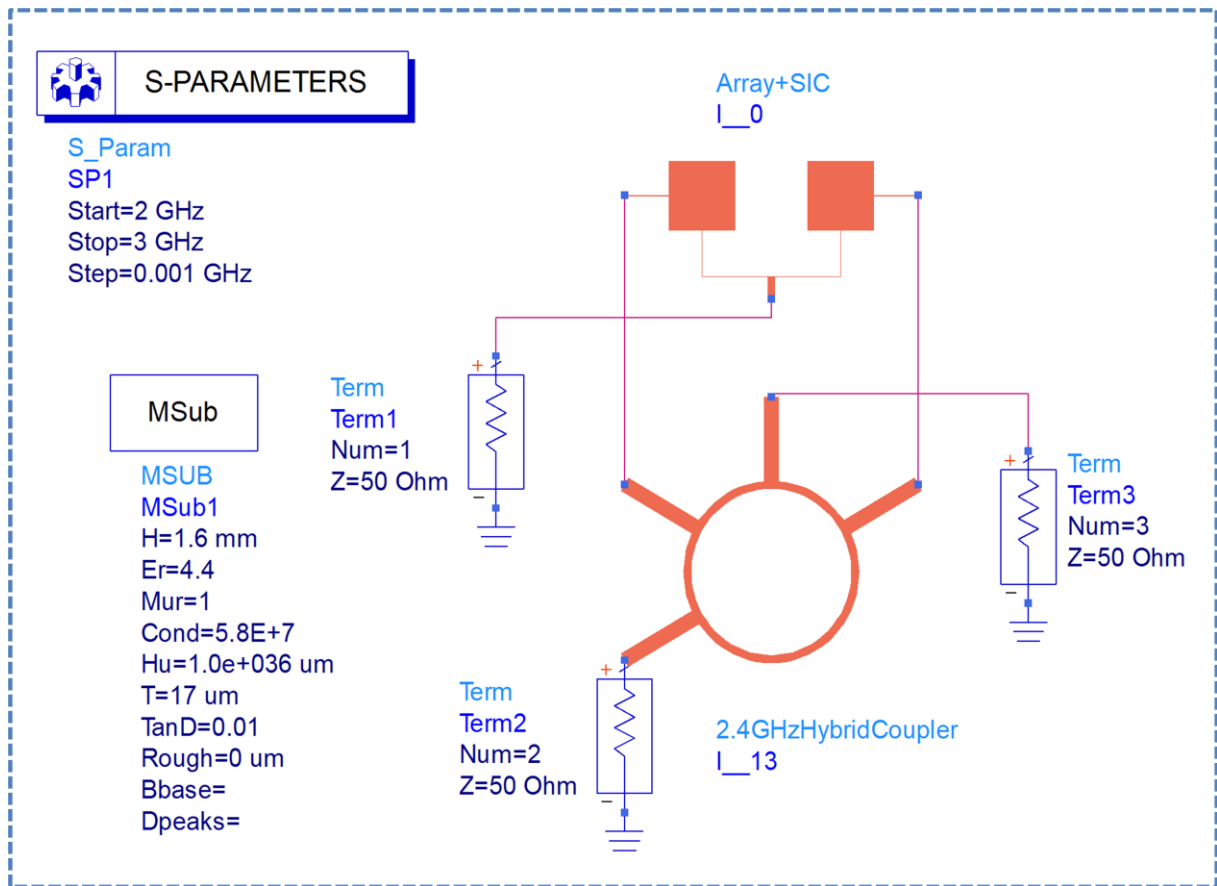


Figure 3.31: ADS schematic and simulation setup for antenna array with SIC Circuit

The simulation results in Fig.3.32 show that more than 120dB isolation is obtained for the centre frequency and simulated isolation is more than 75dB over wider bandwidth as compared to 65dB isolation in 50MHz antenna input bandwidth for the antenna proposed in section 3.1.5. The proposed setup has comparable performance in terms of antenna input impedance bandwidth and interport isolation with the antenna discussed in section 3.1.5 with improved antenna gain performance. The proposed antenna system can be implemented in compact form by etching both hybrid couplers and the antenna array on the same side of FR4 substrate with other side of PCB as ground plane.

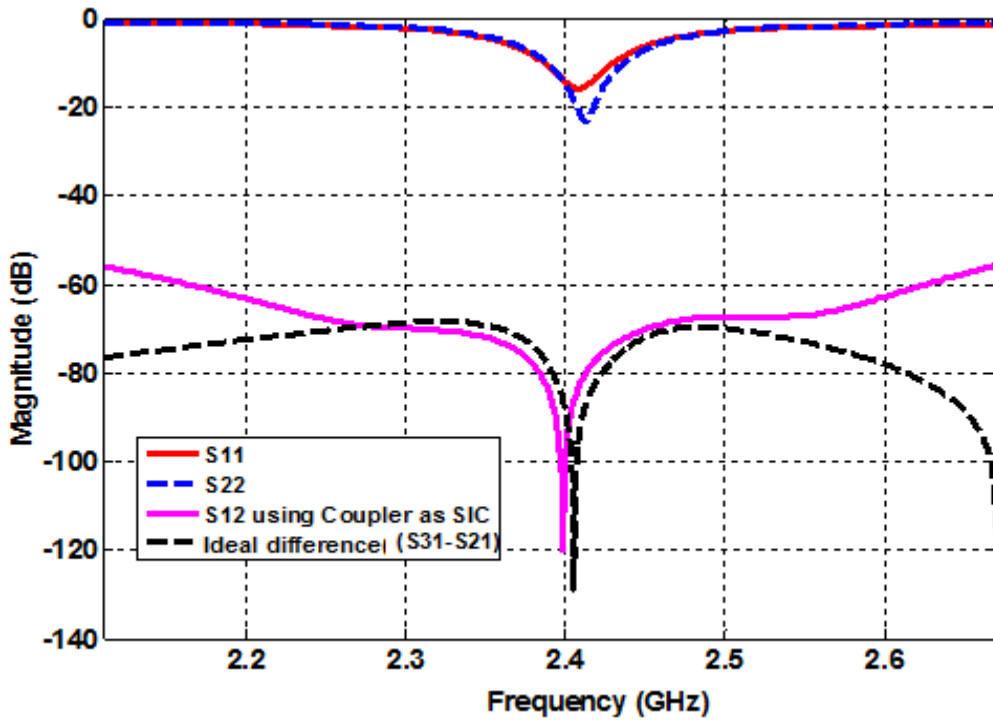


Figure 3.32: Simulation results for patch antenna array with SIC Circuit

3.1.9 Dual port, orthogonal Polarized Slot Coupled Microstrip Patch Antenna

In this design, dual port orthogonal polarized antenna has been designed without any SIC circuit where one polarization mode is excited by Microstrip (MS) feed coupling while the other polarization mode is energized by aperture coupling feeding technique as shown in Fig.3.33. The interport isolation of orthogonally fed patch antenna can be improved significantly if one port is slot/aperture coupled instead of feeding with quarter wave microstrip feed line. The slot coupled port excites the antenna through a small aperture in the ground plane. The shape of coupling slot greatly affects the amount of coupling from feed line to radiating element and the rectangular slot has better coupling efficiency as compared to circular coupling slot for a given area of aperture [61]. Such structure consists of two substrate layers as shown in Fig.3.33. The top substrate layer has radiating element on upper side. The second substrate has ground plane with rectangular coupling slot on top side and 50 ohms microstrip feed line on its lower part. The length of the slot determines the amount of coupling and level of back radiation. The coupling level also depends upon the width of the slot but it is less sensitive as compared to its dependency on slot length and the maximum amount of coupling is achieved when the feed line is placed perpendicular to centre of the

coupling slot [62]. The width of feed line defines its impedance and also affects the coupling level between feed line and radiating patch.

In our implemented structure, both substrate layers are comprised of 1.6mm thick FR-4 substrate ($\epsilon = 4.4$, tangent loss = .02) as shown in Fig.3.33. The optimized dimensions for both radiating element and feeding structures are also shown in Fig.3.33.

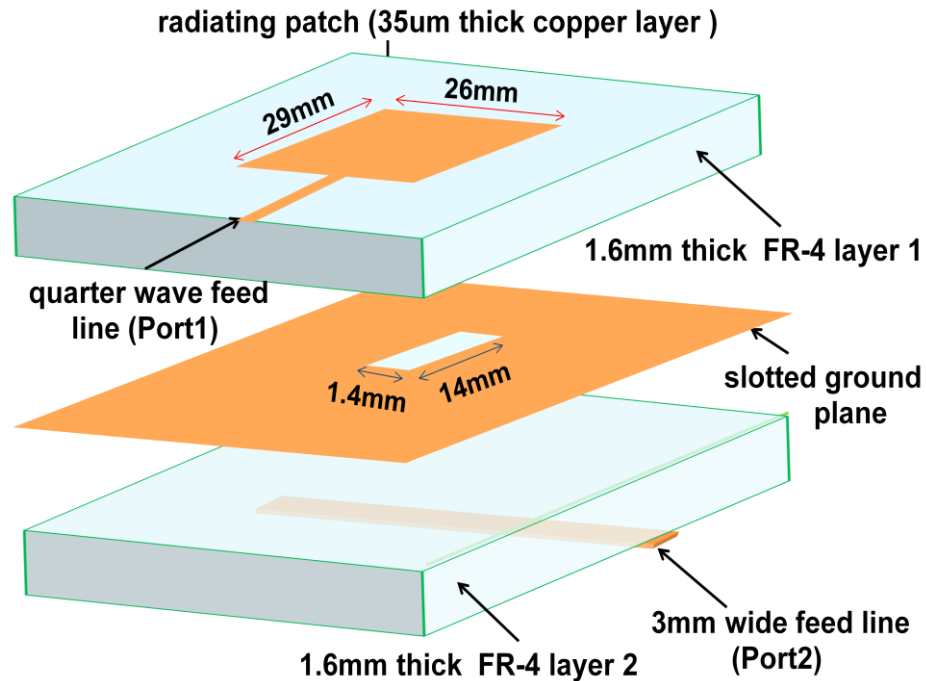


Figure 3.33: Geometry of dual port microstrip antenna with one microstrip fed port and other port is slot coupled

The slot/aperture coupled microstrip patch antenna provides improved input impedance bandwidth as compared to single layer microstrip fed patch antennas [63-64]. This improvement results from tuning stub which is used to tune the reactance of aperture coupled antenna (which is mainly resulted from thick substrates) to achieve optimum input matching [64].

The dual polarized slot coupled antenna with optimized dimensions as shown in Fig.3.34 (a) was simulated using Keysight Advanced Design System (ADS) Momentum software. The simulations were performed with infinite slot ground plane. As clear from simulation results shown in Fig 3.34 (b), high interport isolation (S_{12}) can be achieved by this

configuration as compared to simple antenna with two thin quarter wave microstrip feeds. In the case of antenna with two MS coupled orthogonal ports, the interport isolation is achieved only through polarization diversity but for the antenna proposed in this section, the simulated high interport isolation is the combination of both polarization diversity and isolation resulted from physical disconnection of two ports through radiating element. The simulated interport isolation is better than 65dB by using this antenna feeding configuration for 50MHz antenna Input 10dB bandwidth as compared to 45dB in the case of antenna with two MS coupled orthogonal ports.

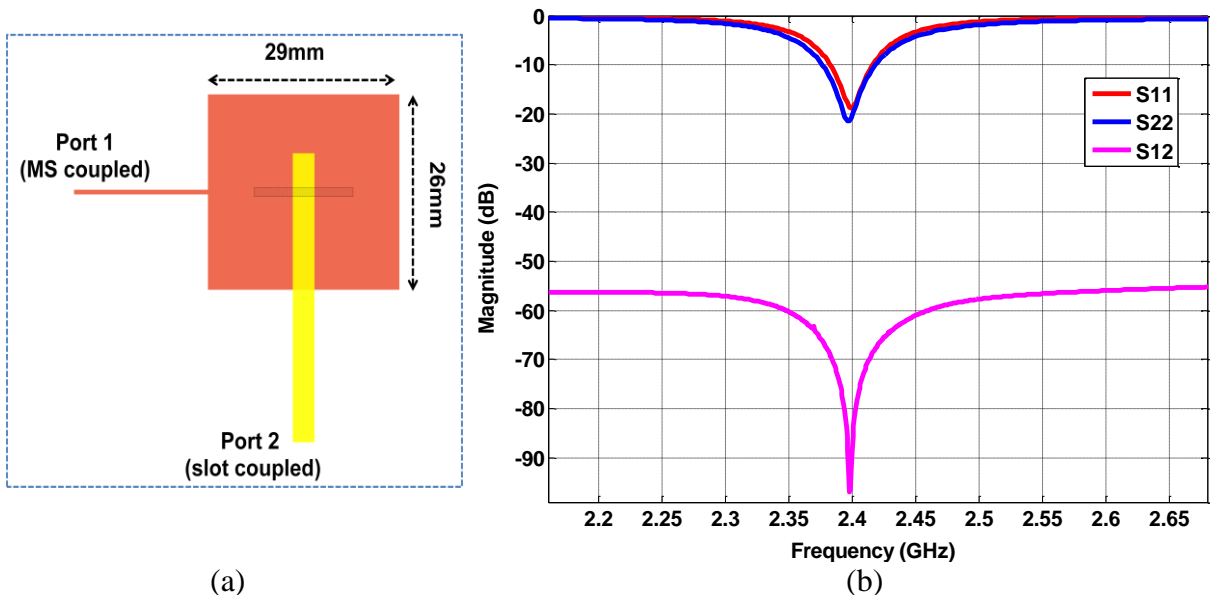
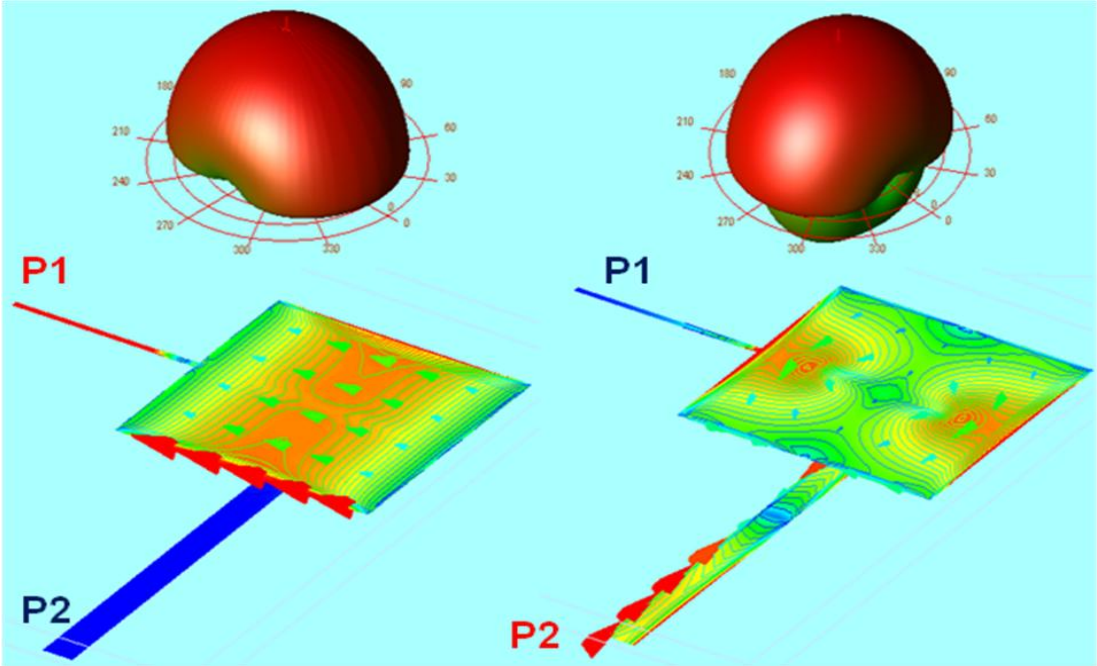


Figure 3.34: (a) EM Model of proposed antenna (b) Simulation Results

The simulated surface currents and gain patterns of dual polarized microstrip patch antenna are shown in Fig.3.35 for each port excitation with the other port terminated in 50 ohms. Port1 feeds the antenna through a quarter wave microstrip transmission line but port 2 is slot coupled and excites the radiating element by electromagnetic coupling through a slot in the ground plane. The back side radiations are clearly visible in Fig.3.35 (b) when the slot coupled port is used to excite the radiating element.

HFSS simulated co-polarization and cross polarization gain patterns for dual polarized slot coupled patch antenna shown in Fig.3.36 clearly shows the low cross polarization level

for the proposed antenna configuration. Thus this structure has nice polarization purity and the antenna is clearly dual polarized (orthogonal polarization).



(a) Port 1 excitation

(b) Port 2 excitation

Figure 3.35: Simulated Radiation characteristics of slot coupled microstrip patch antenna for each port excitation

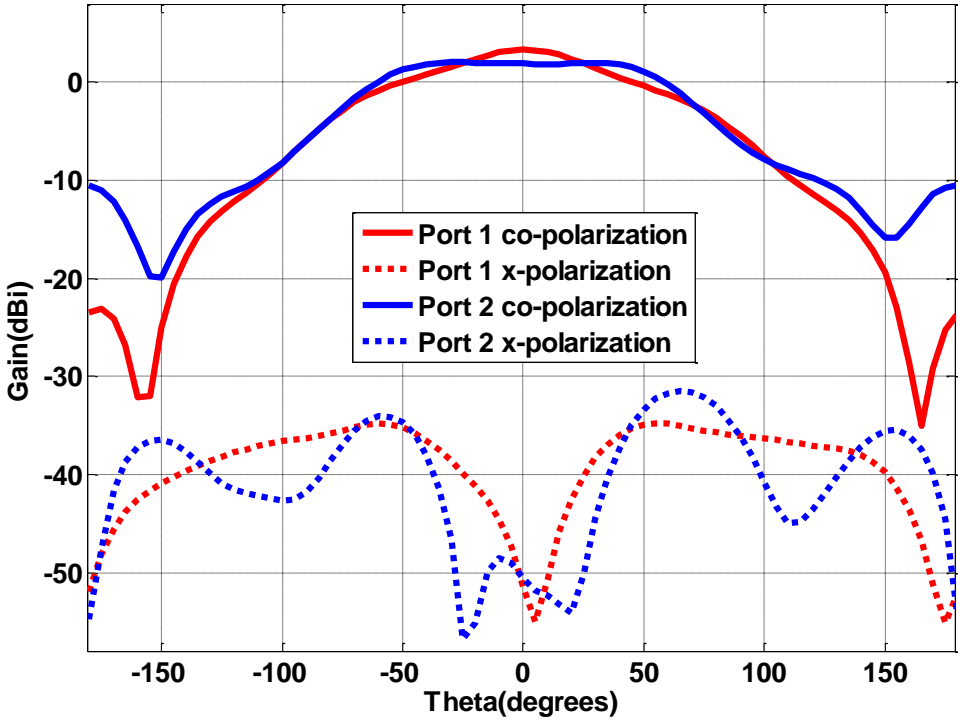


Figure 3.36: HFSS simulated co-polarization and cross polarization gain patterns for dual polarized slot coupled patch antenna

The simulated E-plane gain patterns (for $\Phi=0^0$ and $\Phi=90^0$) for dual polarized slot coupled microstrip antenna operating at 2.4GHz frequency are shown in Fig.3.37. The simulated gain is 4.1dBi for microstrip fed port and 3.85dBi for slot coupled port as shown in Fig.3.37.

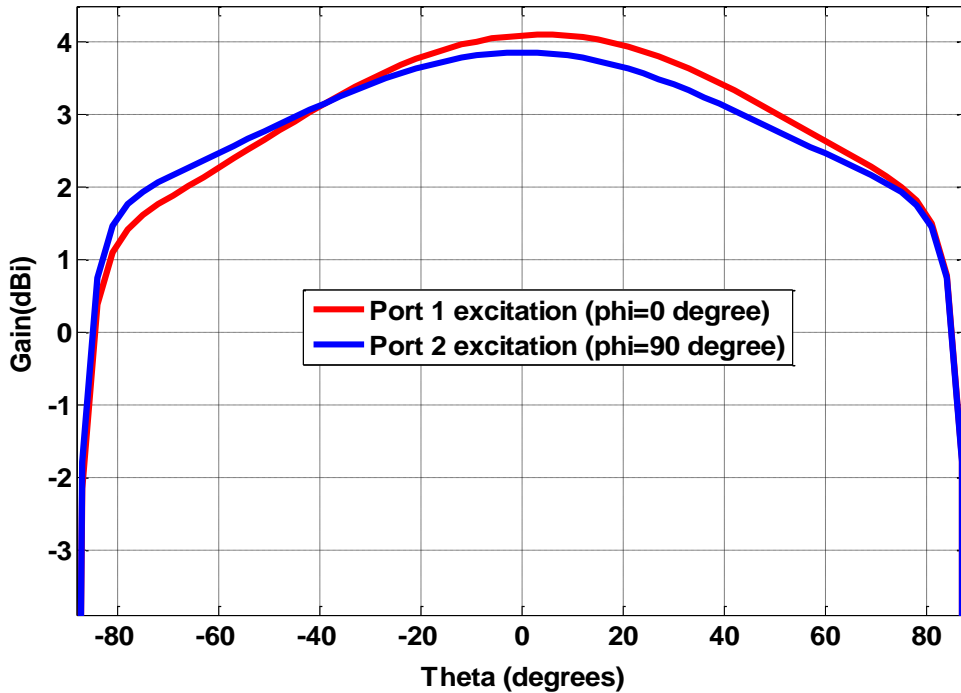


Figure 3.37: Simulated 2D gain pattern for dual polarized slot coupled microstrip antenna at 2.4GHz

3.1.10 Dual Port, orthogonal Polarized Slot Coupled Antenna with SIC Circuit

In this design, dual port orthogonal polarized antenna with external SIC circuit has been proposed. The EM model for three port slot coupled antenna is shown in Fig.3.38 (a) where port 1 and port 3 are MS coupled while port 2 is aperture coupled. There is more than 60dB isolation (S_{12}) between port 1 and port 2 and there is similar case for port 3 and port 2 i.e. S_{32} . If we use an external SIC circuit connected between port 1 and port 3 which deploys DFN configuration then very high interport isolation is resulted by ($S_{12} - S_{32}$) operation because S_{12} and S_{32} are symmetrical. The simulation results for three port antenna are shown in Fig.3.38 (b) along with ideal ($S_{12} - S_{32}$) results.

Again the 3-dB Ring Hybrid coupler has been used as the external SIC circuit to differentially feed port 1 and port 3 to get ($S_{12} - S_{32}$) operation. ADS simulation has been

performed by interconnections of EM models of both three port antenna and Ring Hybrid coupler as shown in Fig.3.39.

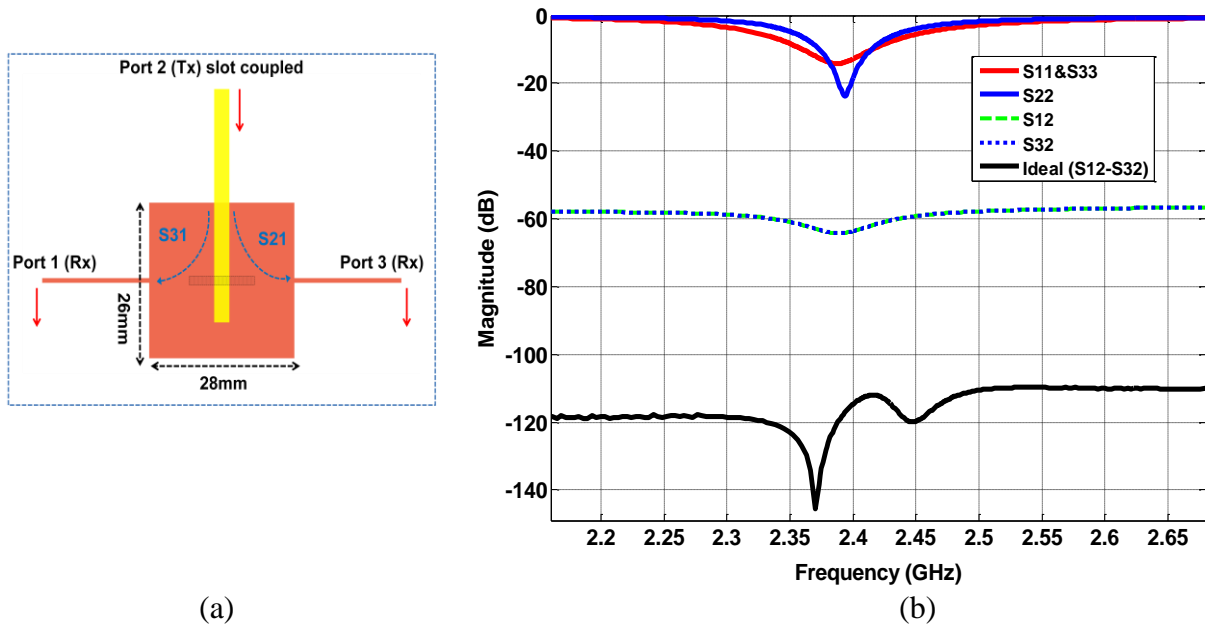


Figure 3.38: (a) EM Model for three port antenna (b) Simulation results

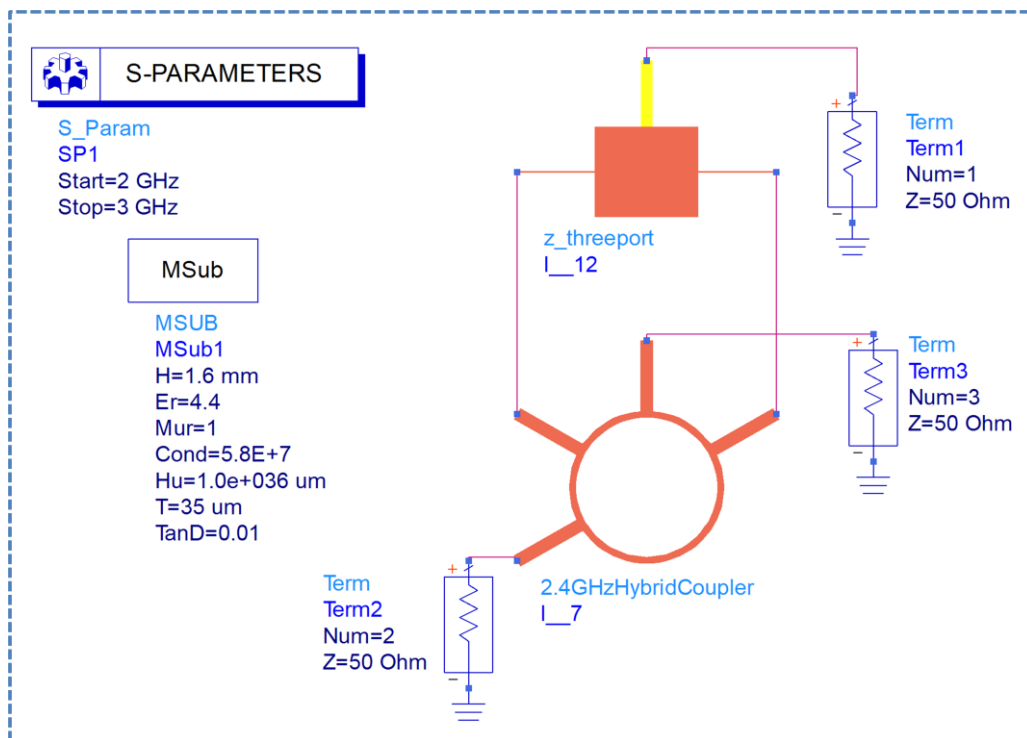


Figure 3.39: ADS schematic and simulation setup for proposed slot coupled antenna

Simulation results for this setup are shown in Fig.3.40. Although perfect difference of S12 and S32 can provide more than 140dB isolation at the centre operating frequency, using 3-dB ring hybrid coupler as SIC circuit, interport isolation of more than 120dB at centre frequency has been observed. The simulated isolation using SIC is more than 95dB in 50MHz antenna input impedance bandwidth. This additional interport isolation results from cancellation mechanism. Three port antenna model used for ADS schematic simulations was simulated in ADS Momentum with infinite slotted ground plane but implemented antenna will be finite slotted ground plane which will result some reduction in port to port RF isolation. As given in the next chapter, the measurements results for this antenna structure will be compared with three port antenna simulated using HFSS software with finite slotted ground plane which provides nice agreement between measured and simulated results. PCB layout for compact antenna structure is shown in Fig.3.41.

HFSS simulated co-polarization and cross polarization gain patterns for dual polarized differential fed slot coupled patch antenna shown in Fig.3.42 clearly show the low cross polarization level for each port. Thus this structure has excellent polarization purity.

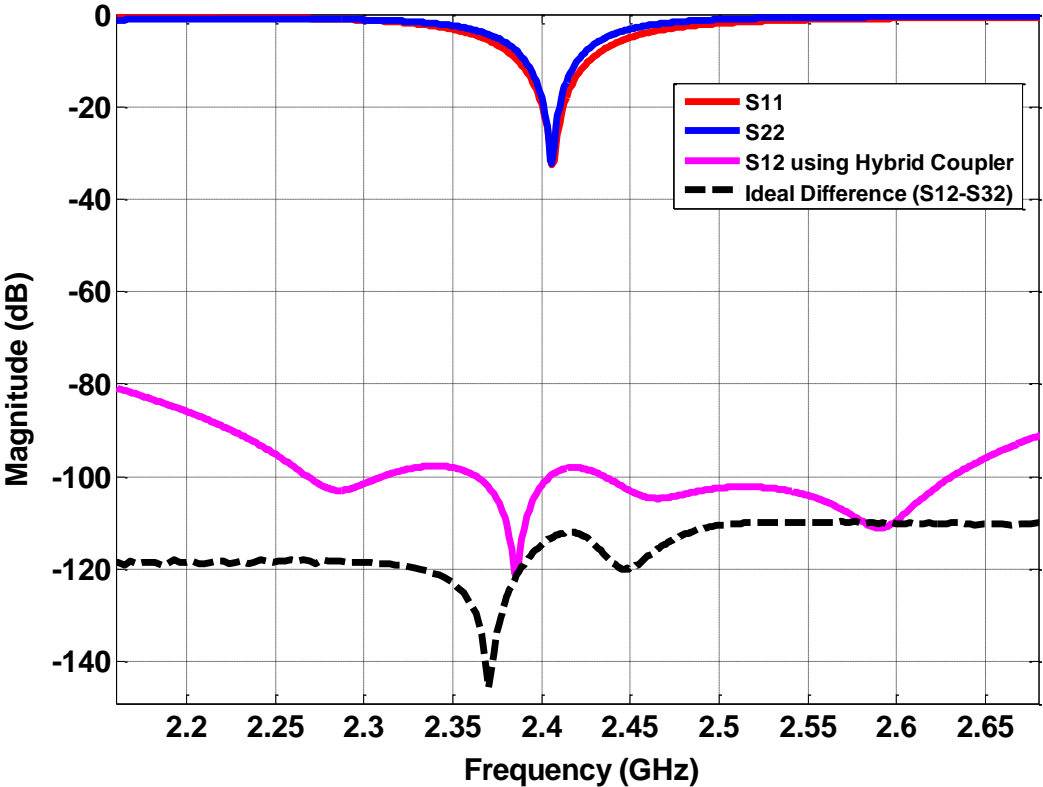


Figure 3.40: Simulation results for dual port dual polarized antenna with SIC Circuit

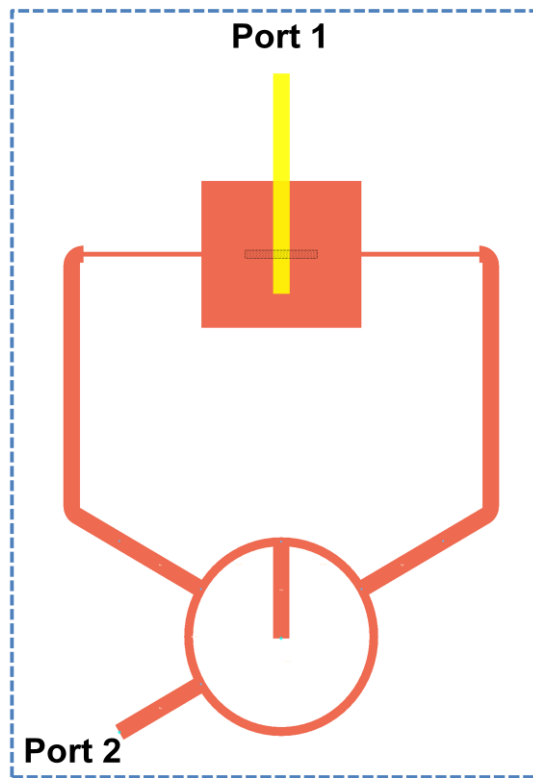


Figure 3.41: PCB layout for compact differential fed slot coupled microstrip patch antenna

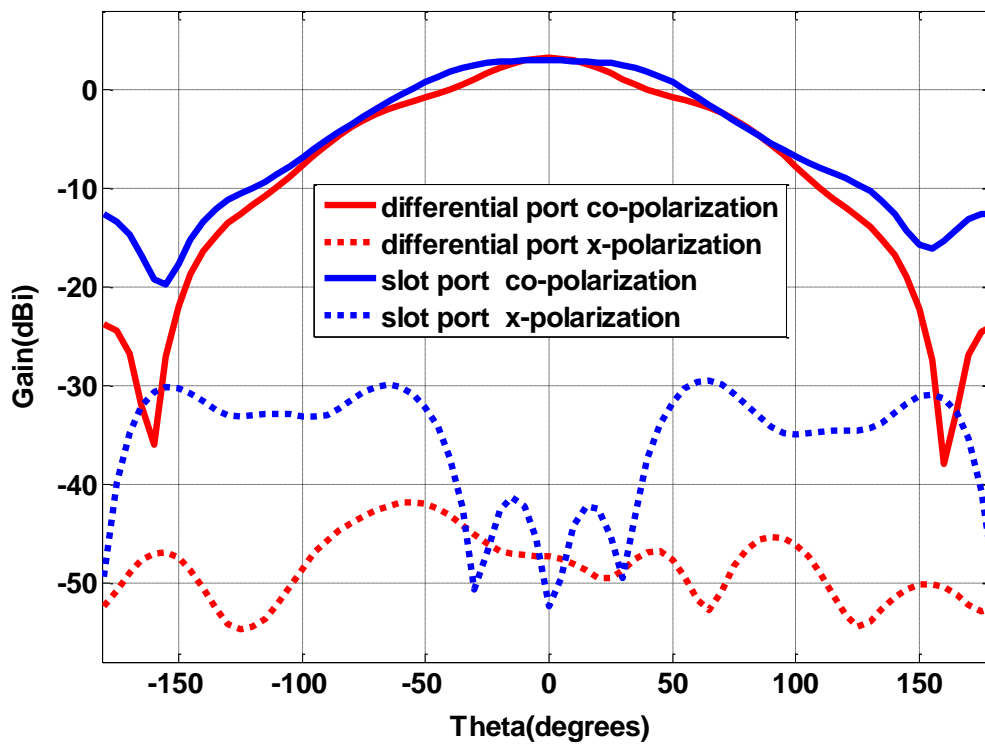


Figure 3.42: HFSS simulated co-polarization and cross polarization gain patterns for dual polarized differential fed slot coupled patch antenna

3.1.11 Three ports microstrip patch antenna with dual linear and linear co-polarization characteristics

In the case of IBFD transceivers with single antenna architecture, most of the reported antenna systems use polarization diversity along with SI cancellation mechanism to decouple transmit and receive ports. Three ports proximity coupled microstrip patch antenna with linear co-polarization and linear dual polarization characteristics has been presented for in-band full duplex and active antenna applications. Depending upon the excitation ports, antenna can perform both transmit and receive operation either with dual linear polarization or linear co-polarization at same carrier frequency with DC isolated ports in both cases. It provides more than 10dB interport isolation with linear co-polarization as compared to around 2.5dB port to port isolation of simple linear co-polarized antenna with two anti-parallel feeds. With dual polarization, interport isolation is more than 43dB at the centre frequency as compared to 36dB port isolation provided by dual polarized antenna with two orthogonal feeds. Proposed antenna has been implemented on FR4 substrate in order to compare its simulated and measured input matching and port to port isolation performances

The antenna structure uses three port microstrip patch antenna with 3-dB Ring Hybrid Coupler as SIC circuit to achieve good interport isolation with same polarization for both Tx and Rx operation. The proximity coupled antenna configuration is shown in Fig. 3.43. Proximity coupled antenna has been used due to its improved gain and input impedance due to thick substrate.

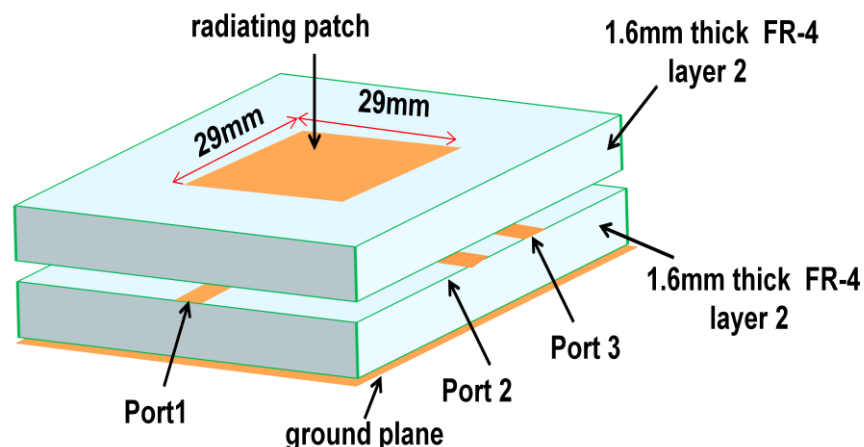


Figure 3.43: Three ports 2.4GHz proximity coupled microstrip patch antenna

Proposed three port proximity antenna in our work provides two DC isolated linear co-polarized ports with more than 10dB RF isolation achieved through differential feeding used for co-polarized antenna configuration while more than 43dB isolation is achieved for DC isolated linear dual polarized ports.

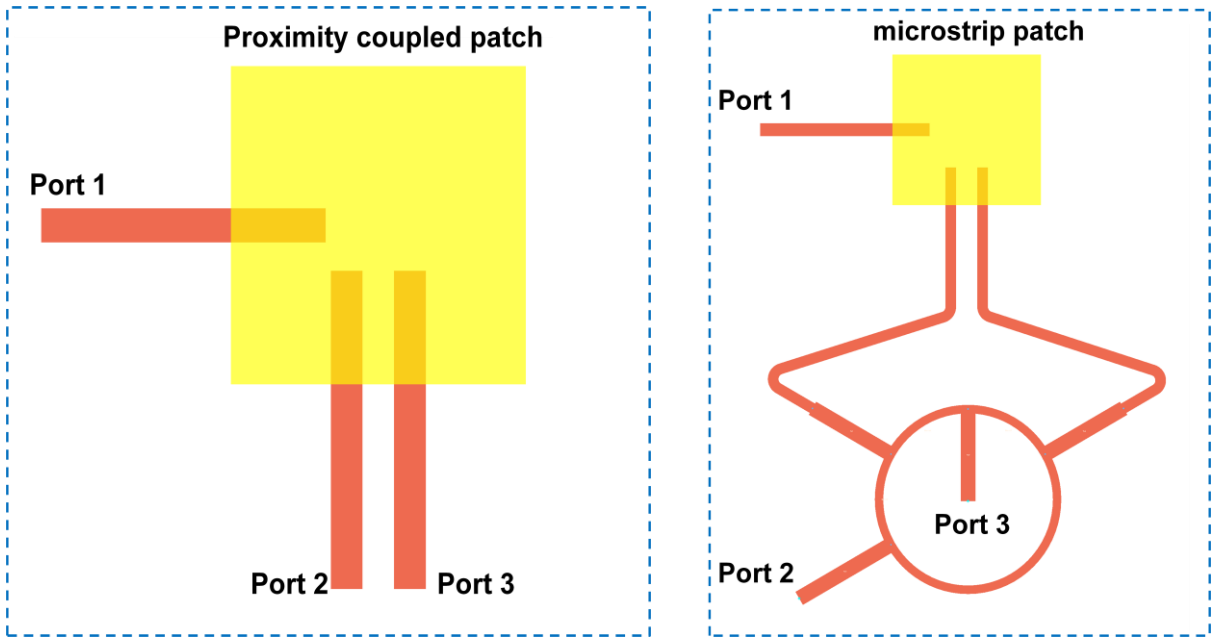


Figure 3.44: (a) EM Model for three port antenna (b) EM model for compact structure

The delta port of 3-dB Ring Hybrid Coupler is used to excite the antenna from port 2 and port 3 as shown in Fig.3.44. Due to differential excitation at port 2 and port 3, the antenna has same polarization as when excited from port 1 but DFN provides improved isolation between port 1 and port 2(delta port of coupler) as RF leakage from port 1 to port 2 and port 3 of antenna is cancelled.

The EM model for compact structure having three port antenna and ring hybrid coupler on the same PCB is shown in Fig.3.44 (b). The simulation results for this setup are shown in Fig.4.47 (a). The interport isolation performance of this antenna has been compared with that shown in Fig. 3.47 (a) which achieves linear co-polarization using direct feeding. The antenna achieves 10dB interport isolation as compared to 2.5dB isolation provided by direct fed antenna.

Antenna's structure and working: Three port proximity coupled microstrip antenna along with a 3-dB ring hybrid coupler has been used to obtain linear dual polarization and linear co-polarization radiation characteristics. Three port 2.4GHz proximity coupled microstrip antenna is shown in Fig.3.44 (a) where port 2 and port 3 are placed on same edge but perpendicular to port 1. All ports excite the radiating patch through EM coupling [65] and radiating patch has equal dimension in order to obtain same resonating frequencies with feeding from two orthogonal edges. Differential excitation of port 2 and port 3 (same magnitude with 180° phase) produce same polarization as produced by port 1 excitation as shown in Fig.3.45 where coupler's difference port(port 2 of coupler) has been used to feed antenna's port 2 and port 3 with equal magnitude but 180° phase difference. Differential feeding provides improved interport isolation between antenna's port 1 and port 2 of coupler even with both linear co-polarized ports due to (S21-S31) operation for three ports antenna. Linear co-polarized radiation characteristics for proposed compact antenna configuration are clearly depicted in Fig.3.45 for excitation of both port 1 and port 2 while terminating port 3 with 50Ω .

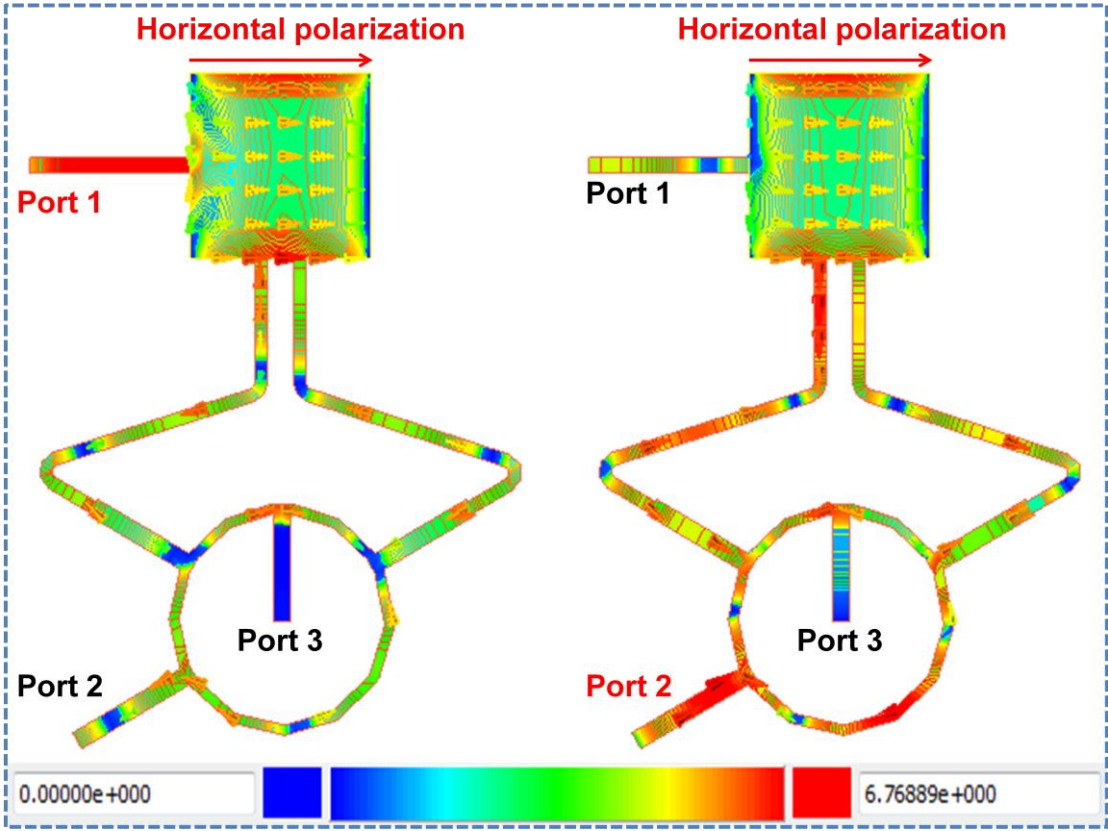


Figure 3.45: Linear co-polarized radiation characteristics of proposed proximity coupled antenna with port 1 and port 2 excitations

On the other hand, port 1 and port 3 of the proposed compact structure shown in Fig.3.44 (b) are dual polarized as this configuration excites port 2 and port 3 of proximity coupled antenna with same magnitude and phase. Ring hybrid coupler simply acts as 3-dB power divider in this case. Excitation from Port 1 and port 3 of structure shown in Fig.3.44 (a) produces orthogonal polarization (horizontal and vertical polarization respectively). This configuration provides more port isolation between dual polarized port1 and port 3 due to polarization diversity. Linear dual polarized radiation characteristics for proposed compact antenna configuration are clearly depicted in Fig.3.46 for excitation of both port 1 and port 3 while terminating port 2 with 50Ω. External SI cancellation circuit [58] or port decoupling network [66] can be deployed to achieve additional interport isolation in order to use this antenna for in band full duplex and active antenna applications.

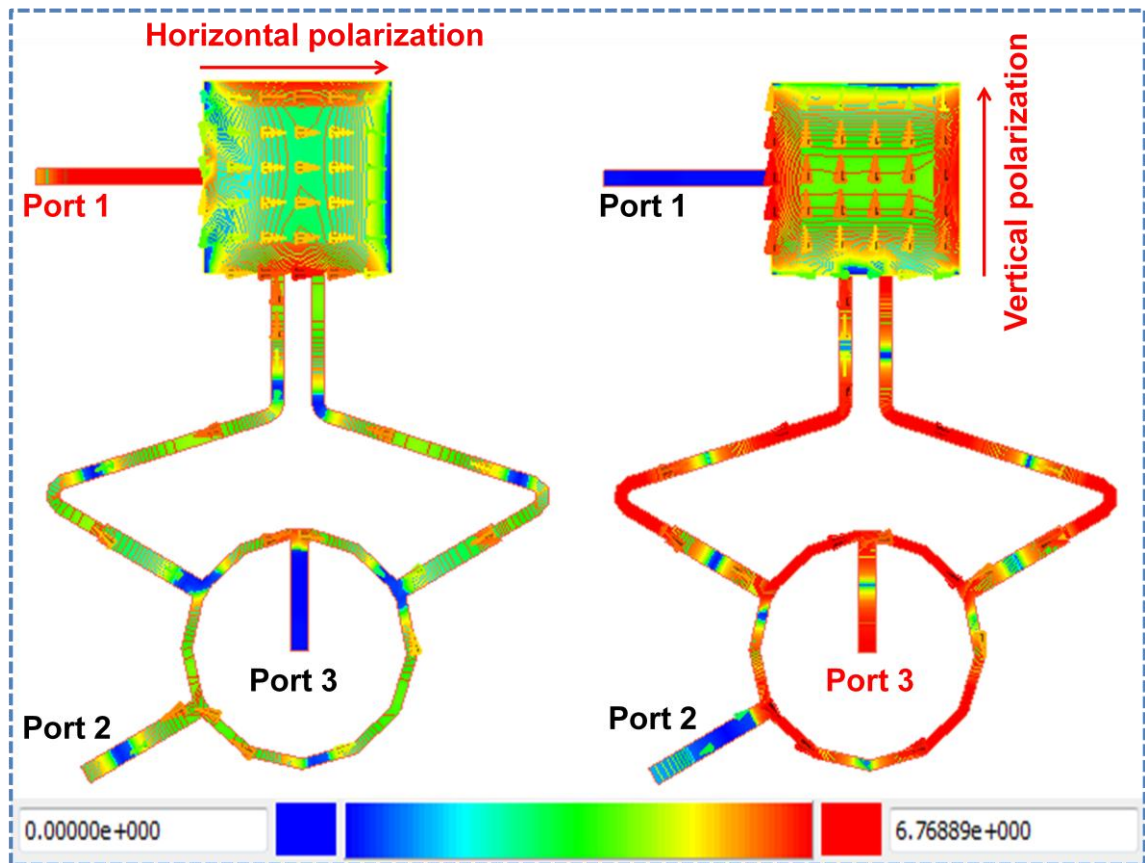


Figure 3.46: Linear dual polarized radiation characteristics of proposed proximity coupled antenna with port 1 and port 3 excitations

For linear co-polarized configuration, simulated input matching (S_{11} , S_{22}) and port to port RF isolation (S_{12}) results are shown in Fig.3.47 (a). Antenna's 10dB impedance

bandwidth is more than 60MHz for both linear co-polarized ports. Simulated RF isolation between port1 and port 2 is better than 10dB in 60MHz bandwidth as compared to 2.5dB interport isolation provided by two ports linear co-polarized proximity coupled patch antenna with dual anti-parallel feeds (shown as antenna A in Fig.3.47 (a)). Thus, interport isolation improvement of around 8dB is obtained for linear co-polarized configuration using differential feeding as discussed earlier. In addition to RF isolation, both linear co-polarized ports are DC isolated due to proximity feeding mechanism for each port.

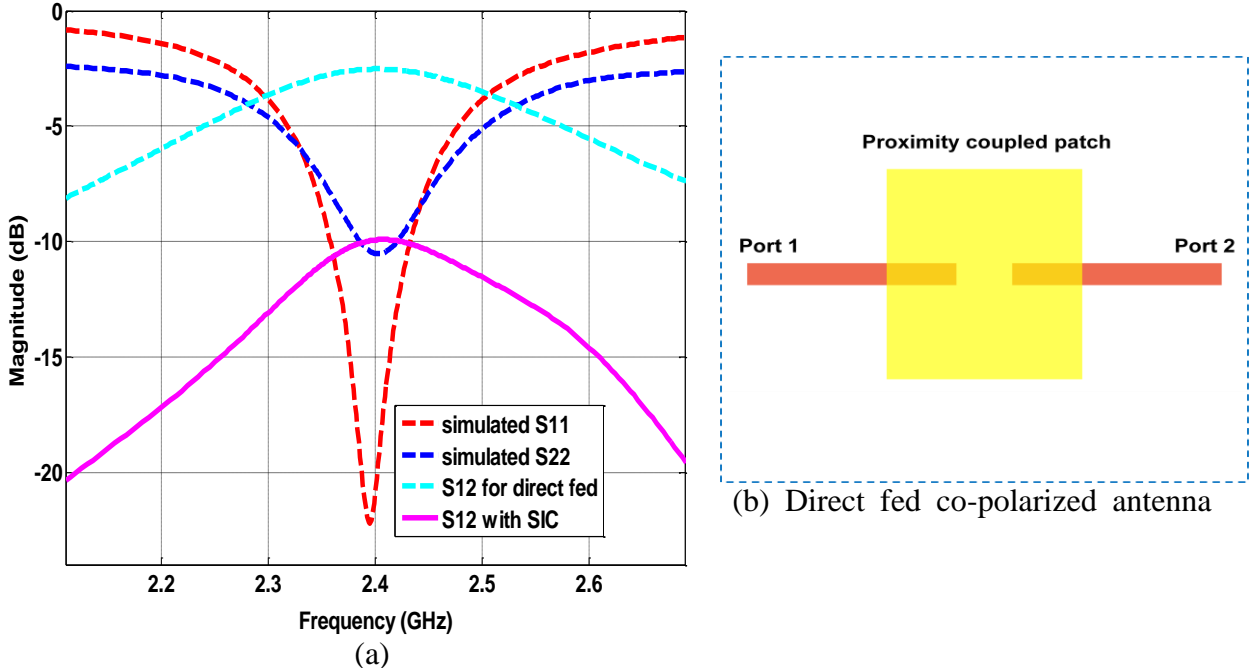
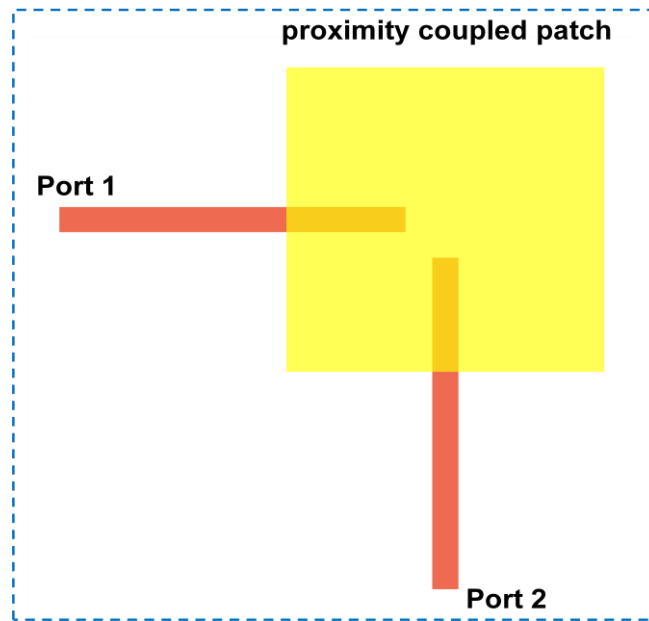


Figure 3.47: (a) Simulated S-parameters results for linear co-polarized antenna configuration as compared with direct fed linear co-polarized antenna

Simulated input matching (S11, S33) and interport RF isolation (S13) characteristics for dual polarized case are shown in Fig.3.48 (b). Simulated 10dB impedance bandwidth is again more than 60MHz for both port 1 and port 3 while simulated RF isolation between dual polarized ports is more than 43dB at centre frequency as compared to 36dB interport isolation provided by dual polarized proximity coupled antenna B which deploys two perpendicular feeds to excite two orthogonal TM_{01} and TM_{10} modes for dual polarization (shown as antenna B in Fig.3.48 (a)). Simulated interport isolation for dual polarization case is better than 40dB for 60MHz band-width as was the case for antenna B. Again both ports are DC isolated due to EM excitation of radiating patch through proximity coupled port 1 and port 3.



(a)

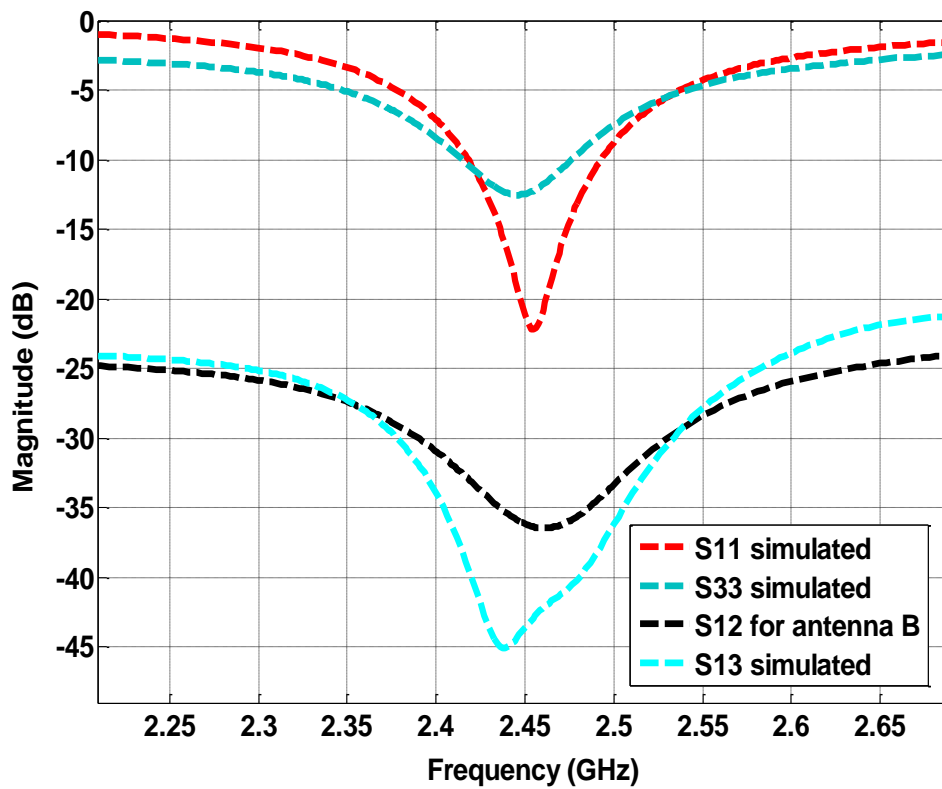


Figure 3.48: (a) Dual polarized antenna B with orthogonal feeds (b) Simulated S-parameters results for linear dual polarized antenna configuration as compared with direct fed linear dual polarized antenna B

CHAPTER 4

IMPLEMENTATION DETAILS & PERFORMANCE EVALUATION OF IMPLEMENTED ANTENNAS

Microstrip patch antennas (dual polarized, linear co-polarized) those discussed in chapter 3, have been implemented and their performance has been evaluated by comparing the measured and simulated input matching, interport isolation, gains, co-polarization vs. cross polarization matrices. Additionally design and implementation of a wide-band dual port monopole antenna based on single circular disc radiating element has been presented for Multi Input Multi Output (MIMO) configured 4G mobile and wireless communication systems. This antenna structure was fabricated on 1.575mm thick RT5880 substrate. In last section, the effect of antenna's impedance bandwidth on interport isolation has been investigated for dual port, dual linear polarized square microstrip antenna which deploys symmetrical feeding structure on two orthogonal ports on respective edges of patch.

The implementation details and measurement results for following antennas have been presented and discussed in this chapter:

- (i) Dual port ,dual polarized Antenna fed with quarter wave Microstrip feeds
- (ii) Dual port ,dual polarized Antenna fed with T-shaped microstrip feeds
- (iii) Dual port Orthogonal Polarized antenna with feed forward mechanism
- (iv) Dual Port dual Polarized Patch Antenna with high Inter-Port isolation using feeding from same edge
- (v) Dual port ,dual Polarized Antenna with quarter wave microstrip (MS) feeds using single SIC Circuit for high Inter-Port isolation
- (vi) Dual port ,dual Polarized Antenna with microstrip-T (MS-T) feeds using single SIC Circuit for high Inter-Port isolation
- (vii) Dual port ,dual Polarized Antenna with quarter wave feeds (MS) using two SIC Circuits for high Inter-Port isolation
- (viii) Dual port ,dual Polarized Antenna array with quarter wave microstrip (MS) feeds using single SIC Circuit for high Inter-Port isolation
- (ix) Dual port ,orthogonal Polarized Slot Coupled Antenna

- (x) Dual port ,orthogonal Polarized Slot Coupled Antenna with SIC Circuit
- (xi) Three ports microstrip patch antenna with dual linear and linear co-polarization characteristics
- (xii) Dual port circular Monopole antenna implemented on 1.575mm thick RT/Duroid® 5880

4.1 Dual port ,dual polarized Antenna fed with quarter wave Microstrip feeds

The geometry and simulated characteristics of dual polarized 2.4GHz square microstrip patch fed with two quarter wave microstrip lines from two orthogonal edges has been discussed in chapter 3. The dual polarized 2.4GHz square microstrip patch fed with two quarter wave microstrip feeds from two orthogonal edges was implemented on 1.6mm thick FR-4 substrate ($\epsilon = 4.4$, tangent loss =.02) as shown in Fig.4.1. One port is to transmit RF signal and other is used to receive radio signal.

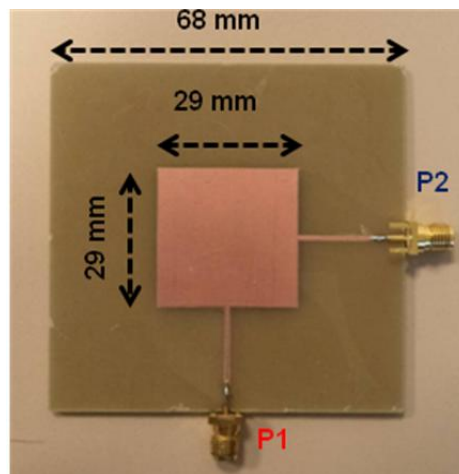


Figure 4.1: Dual polarized 2.4GHz patch antenna implemented on 1.6mm thick FR-4 substrate

E5062A RF Network Analyzer was used for S11 and S22 measurements for port 1 and port 2 respectively and isolation (S12) between the two ports. SOLT calibration for network was performed using Keysight 85032E calibration kit.

As shown in Fig.4.2, the measured return loss (S11, S22) and interport isolation (S12) are around 20dB and 43dB respectively at centre frequency. The interport isolation is better than 35dB for 50MHz antenna's 10dB input impedance bandwidth. The simulated and measured results are in close agreement with each other.

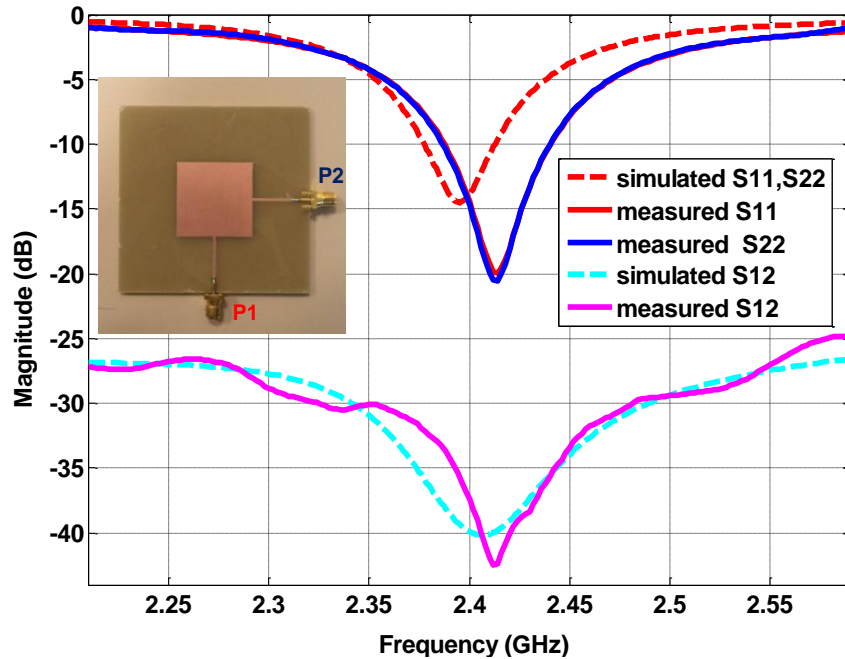


Figure 4.2: Simulated and measured S11, S22 and S12 for dual polarized microstrip fed microstrip patch antenna

4.2 Dual port ,dual polarized Antenna fed with both microstrip-T feeds

The quarter wave feeds are normally very thin as they are deployed to match 50Ω input impedance with high impedance of radiating edge. These feeds may cause power loss so a dual polarized 2.4GHz square microstrip patch fed with two microstrip-T feeds instead of quarter wave feeds from two orthogonal edges has been fabricated and measured. Microstrip-T feeds are relatively thick and above mentioned power loss problem can be avoided for dual port microstrip patch antenna design. Also this configuration provides DC isolation between transmit and receive ports which is normally required to deploy these antennas for active applications. The implemented antenna on 1.6mm thick FR-4 substrate ($\epsilon = 4.4$, tangent loss =.02) is shown in Fig.4.3. Again for full duplex operation, one port is to transmit RF signal and other is used to receive radio signal.

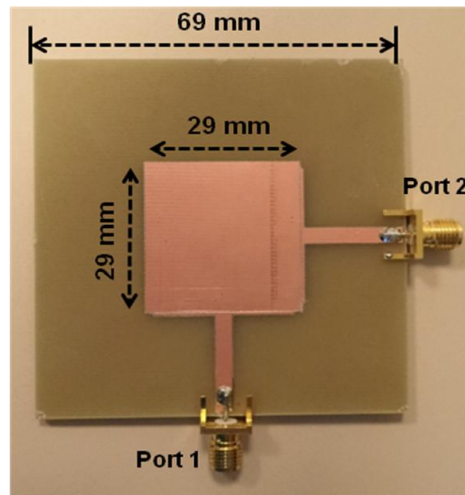


Figure 4.3: Implemented Dual polarized 2.4GHz patch antenna with both EM coupled ports

As shown in Fig. 4.4, the measured return loss (S_{11} , S_{22}) and interport isolation (S_{12}) are around 20dB and 43dB respectively at centre frequency along with DC isolated ports as discussed earlier. The interport isolation is better than 35dB for 50MHz antenna's 10dB input impedance bandwidth.

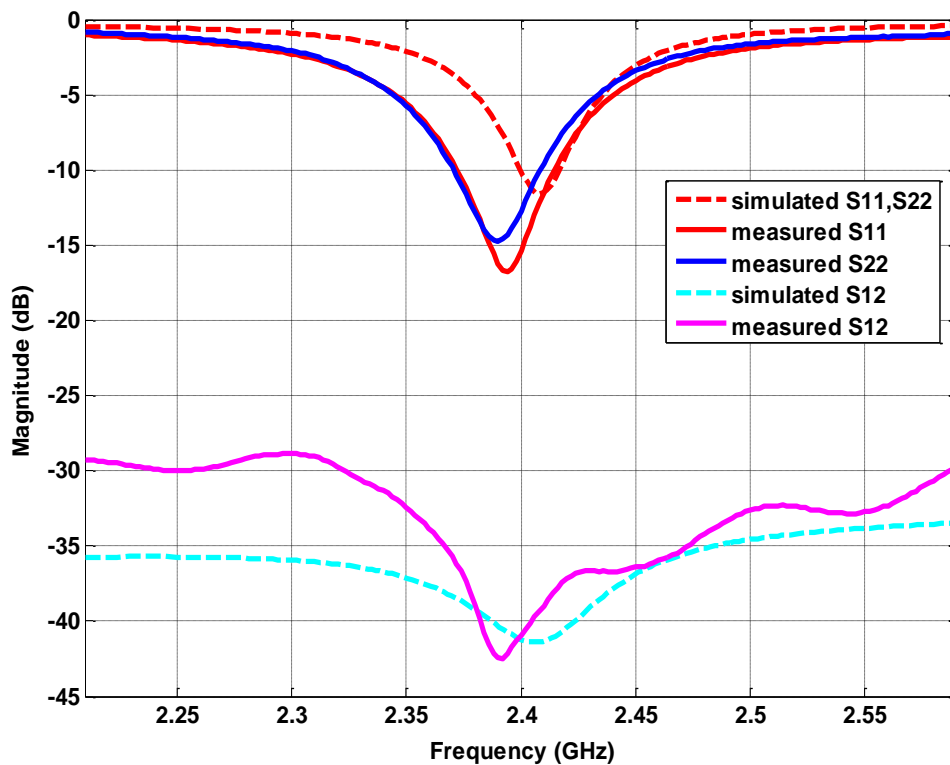


Figure 4.4: Simulated and measured S_{11} , S_{22} and S_{12} parameters for dual polarized microstrip patch antenna with both EM coupled ports

In another configuration, a dual polarized 2.4GHz square microstrip patch using a hybrid feeding configuration where one port excites the antenna through quarter wave microstrip feed while the other port uses T-shaped microstrip feed through EM excitation. The antenna was implemented on 1.6mm thick FR-4 substrate as shown in Fig.4.5.

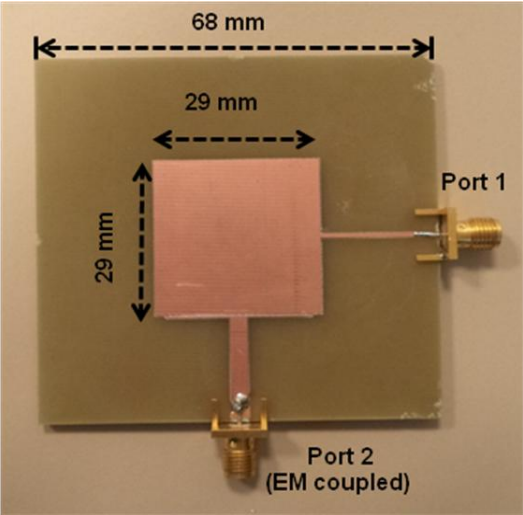


Figure 4.5: Implemented Dual polarized 2.4GHz antenna with one MS-T and one $\lambda/4$ feed

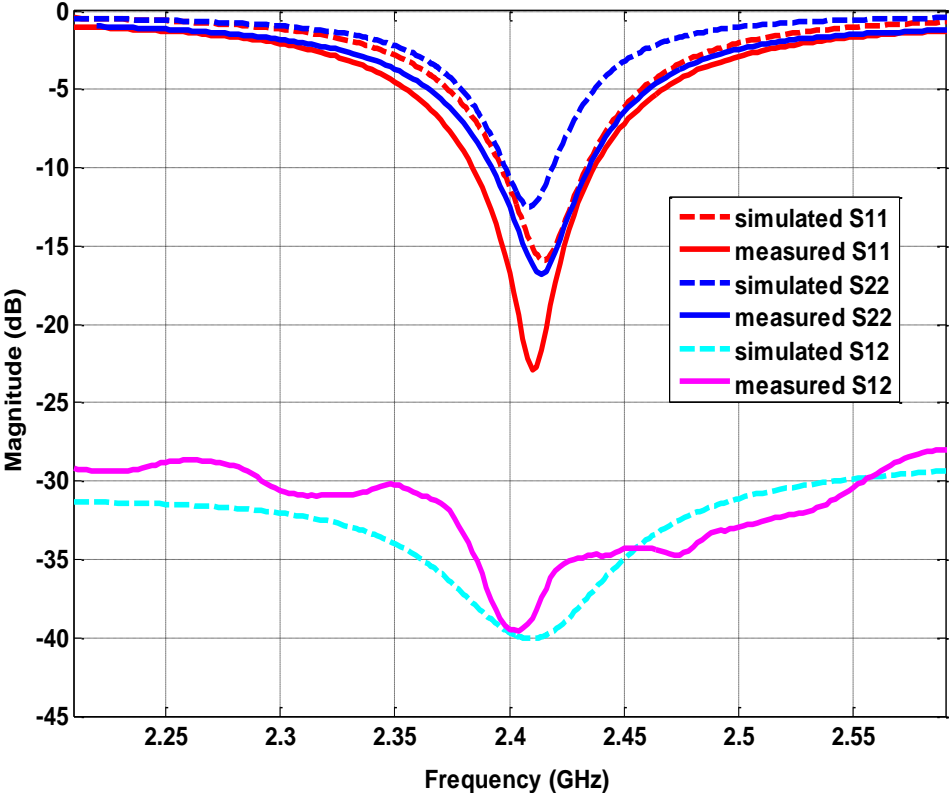


Figure 4.6: Simulated and measured S11, S22 and S12 parameters for dual polarized microstrip patch antenna with one EM coupled port and one microstrip fed port

Measured results for implemented antenna are shown in Fig.4.6. The antenna has good matching for both ports and measured interport isolation (S_{12}) is around 40dB at centre frequency. The interport isolation is better than 35dB for 100MHz band-width.

4.3 Dual port Orthogonal Polarized antenna with feed forward mechanism

A dual port orthogonal polarized 2.4GHz square microstrip patch antenna as shown in Fig.4.7 was implemented on RT/Duroid® 5880 substrate (with $\epsilon=2.2$, tangent loss =.0009 and thickness (h)= 0.787mm). RT/Duroid® 5880 substrate has been used for implementation of this antenna to achieve improved antenna's again due to low loss of this substrate. Port 1 is used as transmit and Port 2 as receive port for IBFD operation. The dimensions of antenna are kept equal to have same transmit and receive operating frequency.

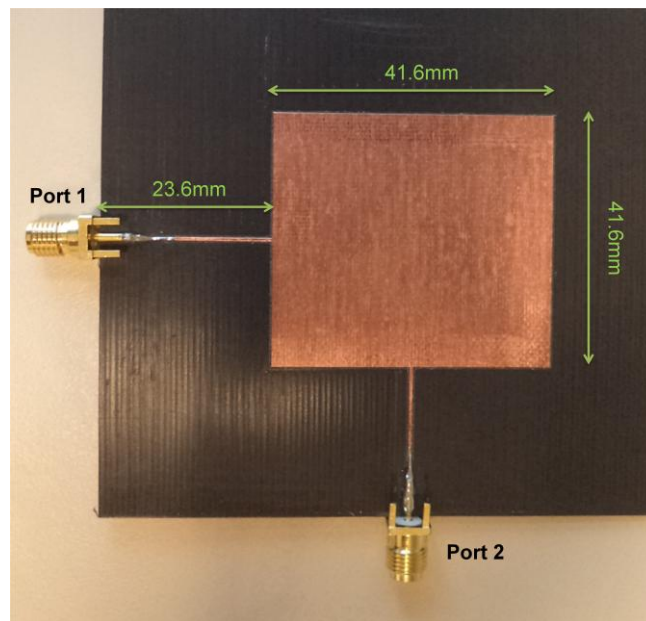


Figure 4.7: Implemented 2.4GHz dual port patch antenna on RT5880 substrate

As seen in Fig. 4.8, the measured return loss (S_{11}) is 38.37dB and interport isolation (S_{12}) is 47.56dB at centre frequency and the interport isolation is better than 40dB for 24MHz 10dB impedance bandwidth at 2.4 GHz. Simulated and measured E-Plane radiation patterns for 2.4GHz dual port orthogonal polarized microstrip patch antenna are also shown in Fig.4.9 for each port excitation. The implemented antenna provides 6.5dB maximum gain and Half

Power Beam Width (HPBW) is 65degree when one of the ports is fed and the other port is terminated with 50 ohms. The radiation pattern is symmetrical for each port.

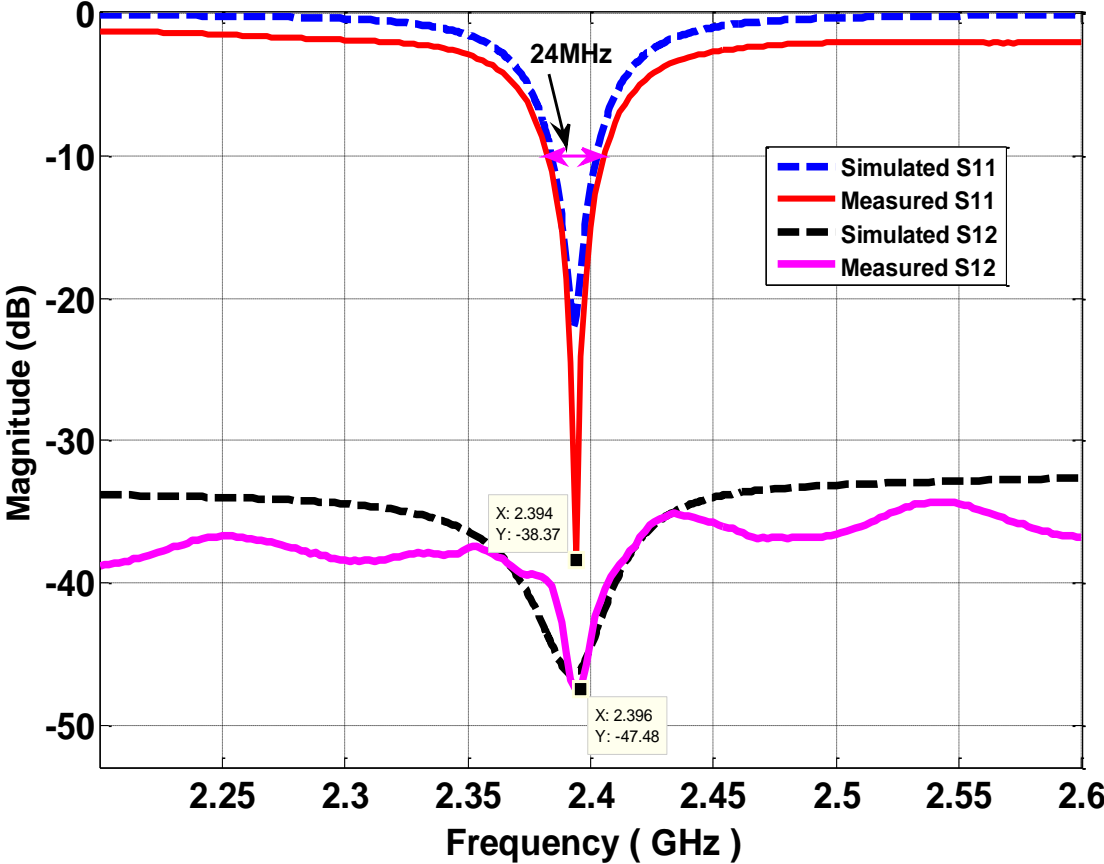


Figure 4.8: Simulated and measured S11 and S12 for a dual port orthogonal polarized patch antenna

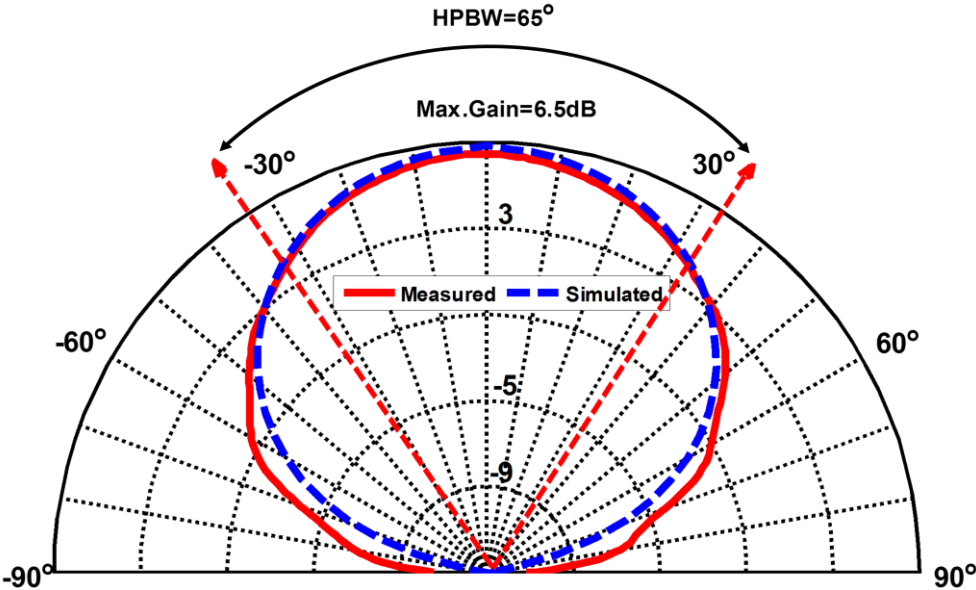


Figure 4.9: E-plane radiation pattern at 2.4GHz for a dual port orthogonal polarized antenna

Measured co-polarization and cross polarization gain patterns for dual polarized antenna with $\lambda/4$ microstrip feeds and fabricated on 0.787mm thick RT5880 are shown in Fig.4.10. Implemented antenna has improved gain and very low cross polarization level thus provides good polarization purity for dual polarized applications.

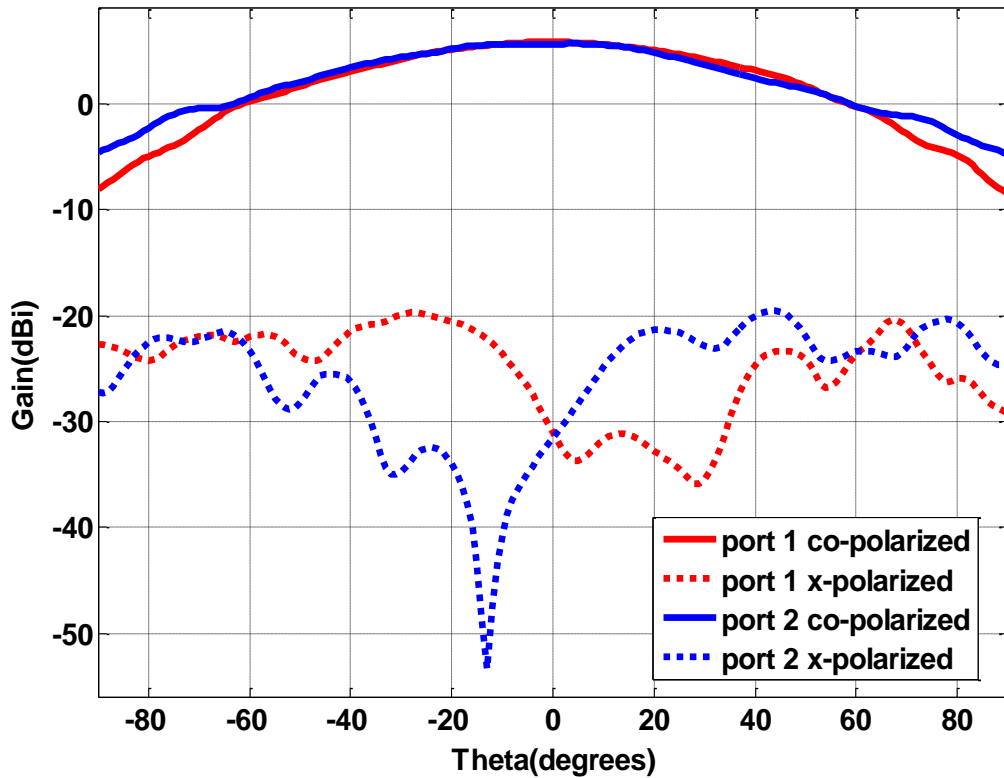


Figure 4.10: Measured co-polarization and cross polarization gain patterns for dual polarized antenna with $\lambda/4$ microstrip feeds and fabricated on 0.787mm thick RT5880

After analyzing the performance of two port patch antenna, external feed forward loop between transmit and receive ports was implemented to improve the interport isolation by attenuating the RF leakage from transmit to receive ports. The signal is sampled from transmit chain and added to sampled signal from receive chain using RF couplers. To adjust the amplitude and phase of the signal, variable phase shifter and variable attenuator are used as shown in Fig.4.11. The variable phase shifter and variable attenuator used in feed forward loop adjust the phase and magnitude of both sampled signals in such a way that they are equal in magnitude but 180° out of phase so that they interfere destructively. The two port antenna coupling is around 40dB, so we need to have around 40dB coupling to cancel further and

obtain much higher (70-80dB) isolation. We have used two fixed 15dB couplers and a variable attenuator which we can change attenuation between 3.5 and 24dB such that we can obtain higher cancellation. RF directional couplers with 15dB coupling were designed using microstrip coupled lines. EVA-3000+ and JSPHS-2484+ from Mini-circuits were used as surface mount voltage variable attenuator and surface mount variable phase shifter, respectively. The variable attenuator provides typical attenuation from 24dB to 3.5dB with input 0-8 Vdc as tuning voltage. The phase shifter can provide 0° - 180° phase change with 0-15Vdc control voltage. The complete design including patch antenna, RF couplers and layouts for attenuator and phase shifter was analyzed in ADS Momentum. The final PCB layout was etched on RT/Duroid® 5880 substrate. Variable phase shifter and variable attenuator were soldered and SMA connectors had been fixed for transmit and receive ports. The implemented dual port orthogonal polarized antenna with feed forward loop is shown in Fig.4.11.

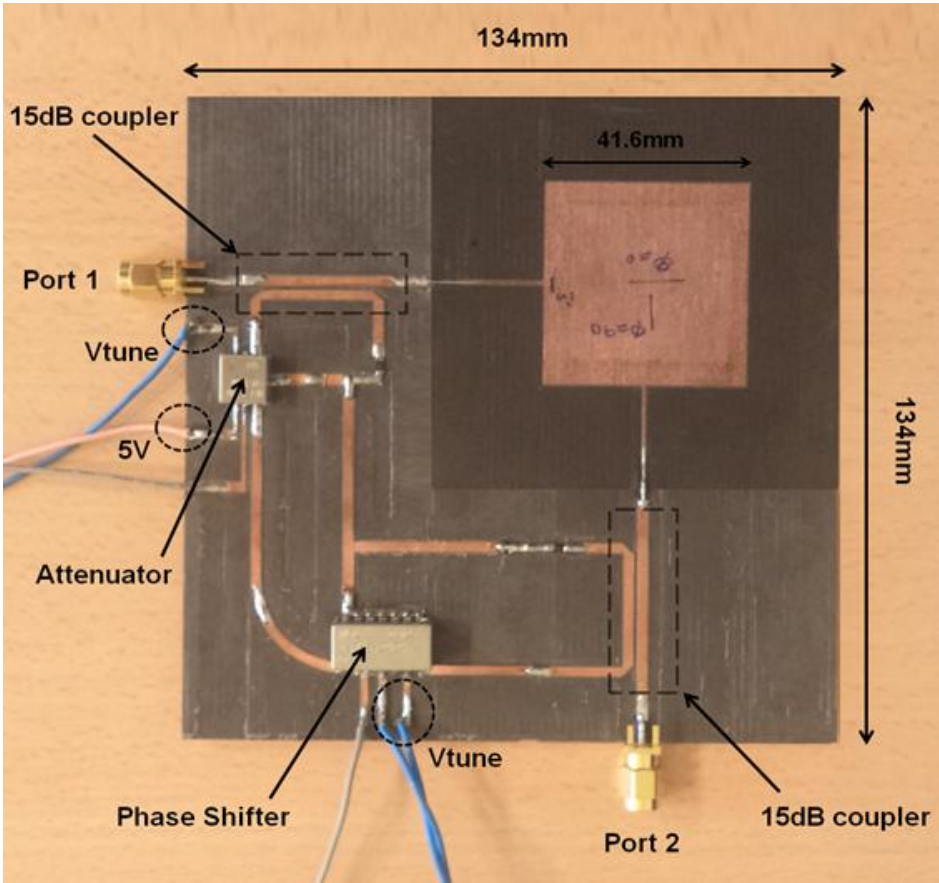


Figure 4.11: Implemented two port ,dual polarized 2.4GHz antenna with feed forward loop

Simulation and measurement results for simple dual port orthogonal polarized antenna with and with out feed forward loop are depicted and compared in Fig.4.12. The implemented antenna provides 47.5dB interport isolation without feed forward loop and 73.5dB isolation between transmit and receive ports at 2.4GHz when external feed forward loop is activated. In both cases, the interport isolation is better than 40dB for 24MHz antenna 10dB input impedance bandwidth. The peak isolation operating frequency can be adjusted by changing the loop attenuation and phase shift to operate antenna at any frequency with in 24MHz antenna 10dB input impedance bandwidth as shown in Fig.4.12.

As stated earlier, interport isolation is very sensitive to even slight changes in loop attenuation and phase shift so peak interport isolation can be improved further by using more precise variable attenuators and phase shifters as discussed in chapter 3.

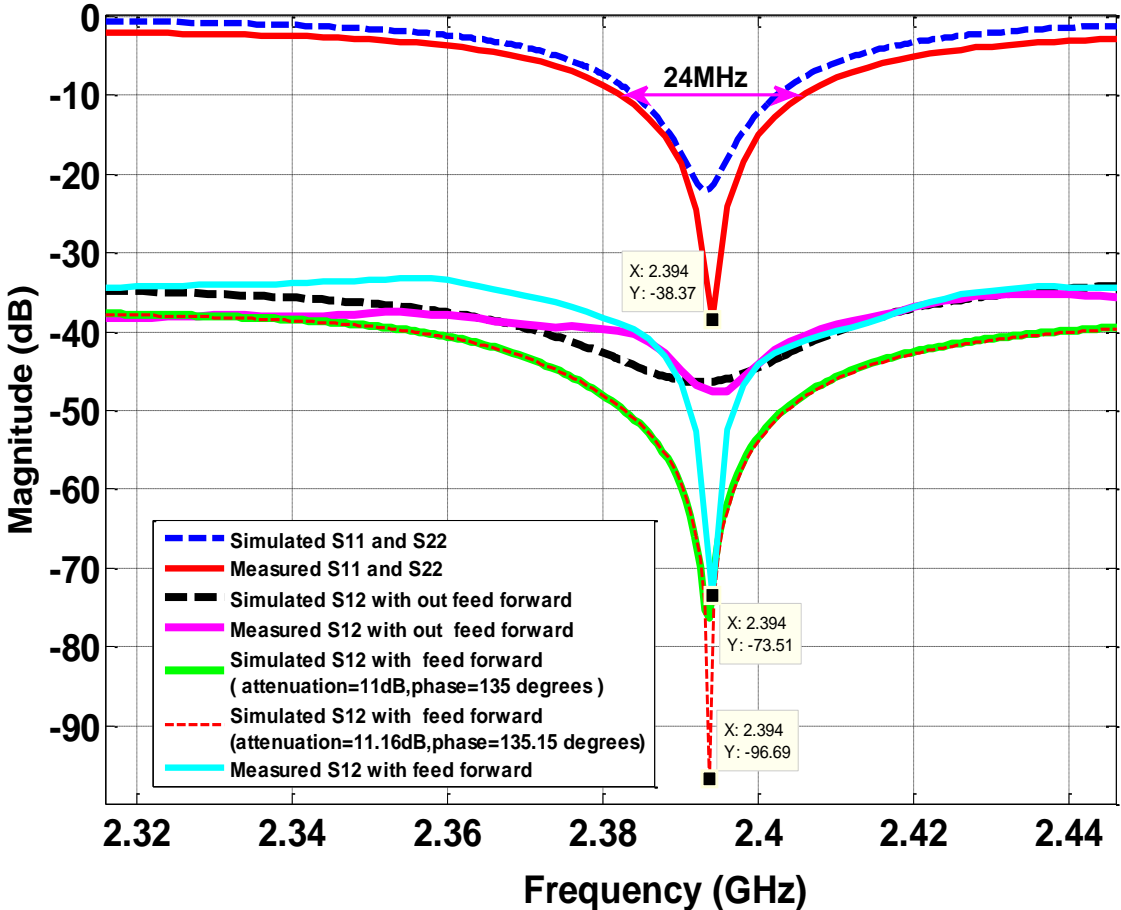


Figure 4.12: Simulated vs. Measured S11, S22 and S12 parameters for antenna with feed forward loop

The peak isolation operating frequency can be adjusted by changing the loop attenuation and phase shift. As antenna input impedance bandwidth is 24MHz so peak interport isolation operating frequency in the span of 2.382GHz to 2.406GHz can be obtained by tuning loop attenuator and phase shifter. For example, the interport isolation measurement results adjusted through loop tuning to get peak isolation at lower cutoff and upper cutoff frequencies are shown in Fig.4.13. The measured interport isolation is -80dB at lower cutoff frequency of 2.382MHz and -67dB at upper cutoff frequency of 2.406MHz.

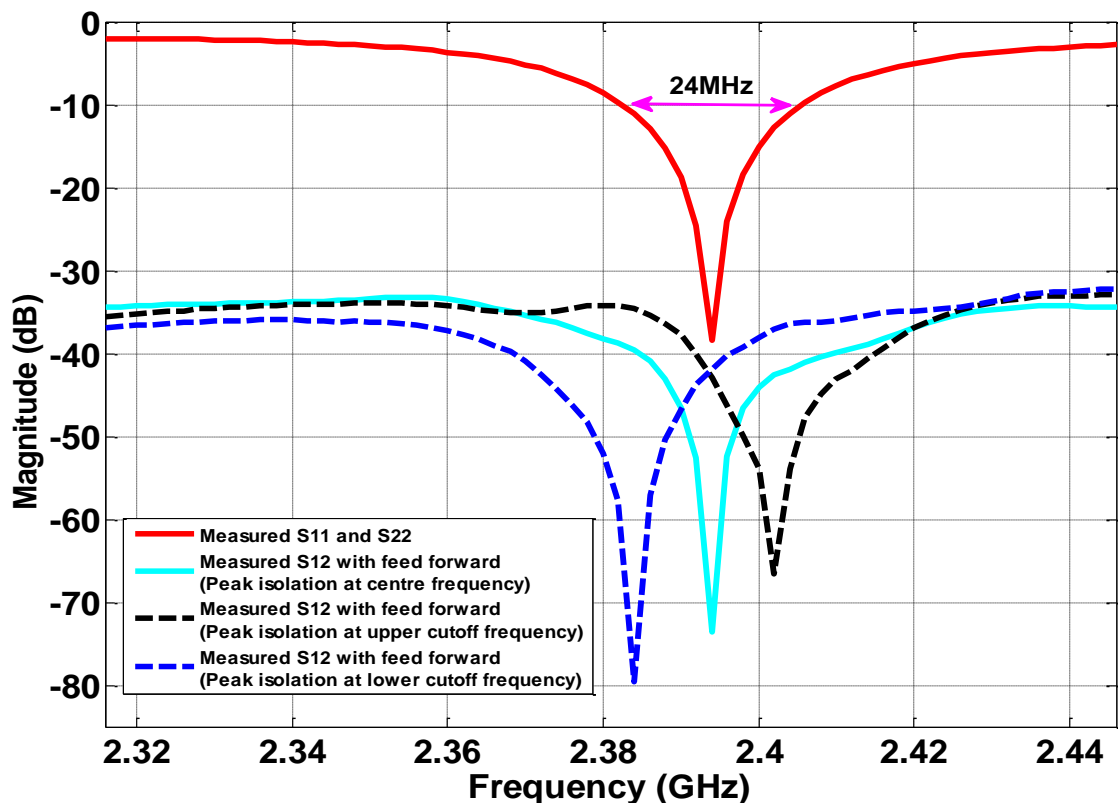


Figure 4.13: Measured interport isolation (S12) with peak isolation at lower cutoff and upper cutoff operating frequencies adjusted through loop tuning

As Antenna is fed from two orthogonal ports so it transmits and receives with orthogonal polarization which provides additional isolation between transmit and receive signals in propagation domain. The designed antenna with feed forward loop has no effect on antenna received signal as it only cancels the RF leakage from transmit port to receive port to provide high interport isolation for IBFD operation with single antenna without circulator/diplexer.

4.4 Dual Port dual Polarized Patch Antenna with high Inter-Port isolation using feeding from same edge

A compact two ports, dual polarized microstrip patch antenna has been designed and implemented. The implemented antenna has comparatively wider 10dB input bandwidth (50MHz) along with high interport isolation. The proposed and implemented dual port, dual linear polarized single microstrip patch antenna uses three ports microstrip patch antenna with 3-dB Ring Hybrid Coupler as SIC circuit to achieve high interport isolation.

Three ports linear co-polarized microstrip patch antenna and 3-dB ring hybrid coupler for 2.4GHz frequency were implemented on FR4 Epoxy substrate (with $\epsilon=4.4$, tangent loss $=.01$ and thickness (h)= 1.6 mm). Measured results for three ports linear co-polarized microstrip patch antenna are shown in Fig.4.14.

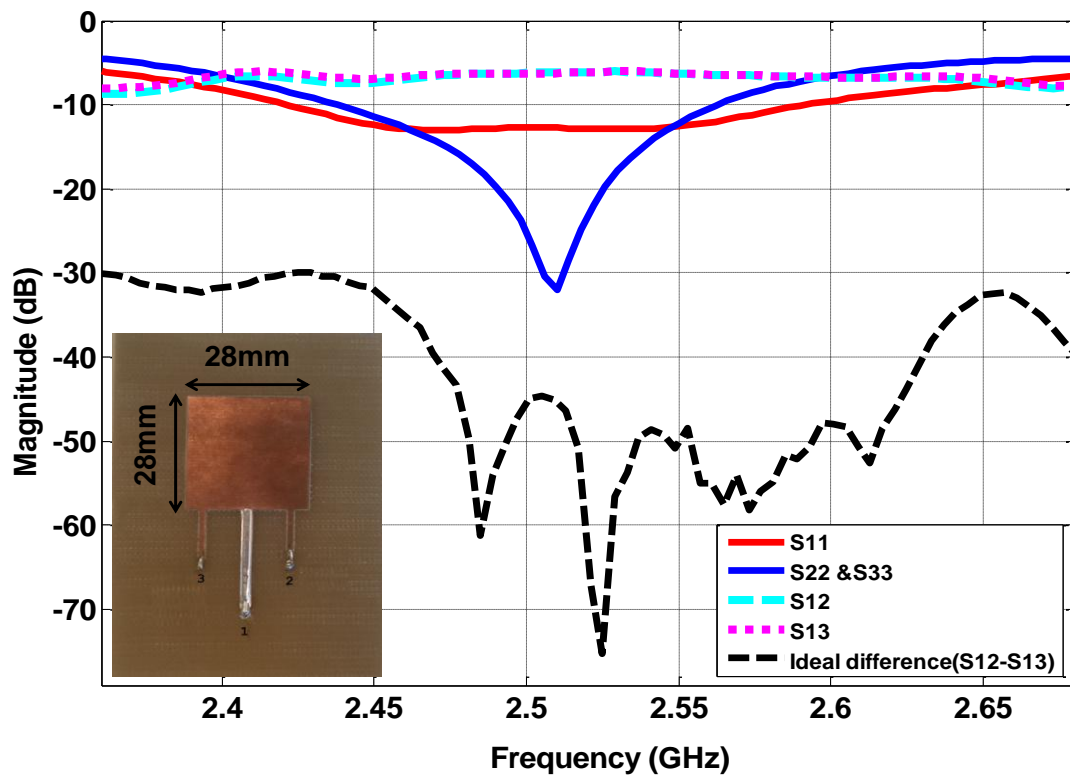


Figure 4.14: Measured S-Parameters for three port linear co-polarized antenna

Simulated and measured 2D gain patterns for three port implemented microstrip antenna are also shown in Fig.4.15 for each port excitation while the other two ports are terminated with 50 ohms. Antenna radiates in z-direction and ports are along y-axis. Antenna polarization direction is along y-axis and yz pattern is measured as E-plane pattern. The antenna provides

4.4 dB and 3.3dB maximum gain for port 1 and port2/port3 respectively at 2.5GHz thus antenna's efficiency is around 74%.

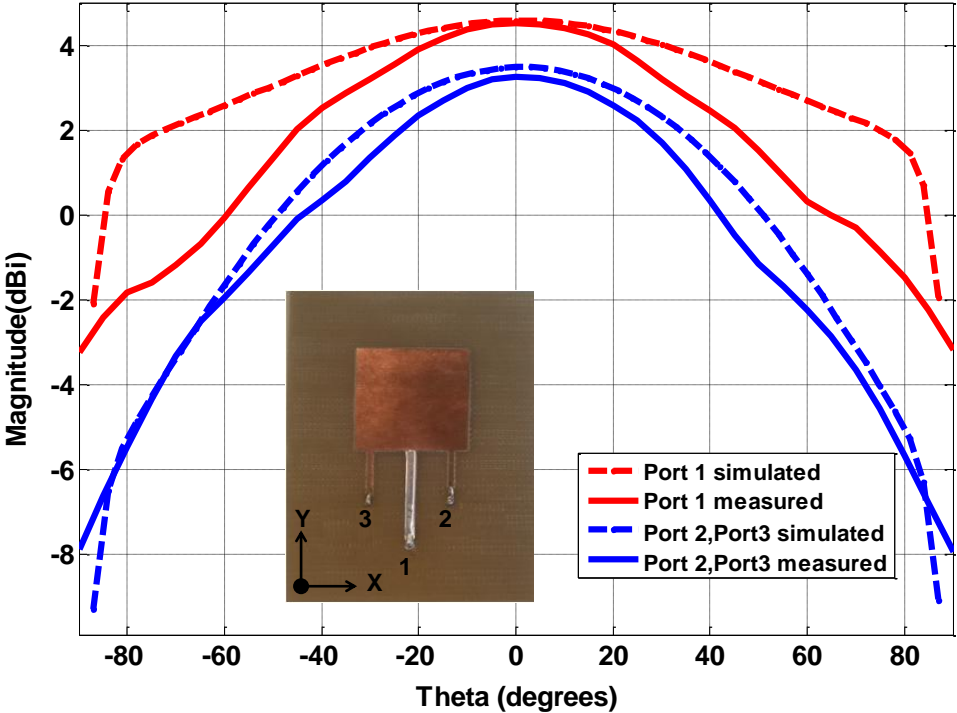


Figure 4.15: Simulated vs. measured 2D gain patterns at 2.5GHz for three port antenna

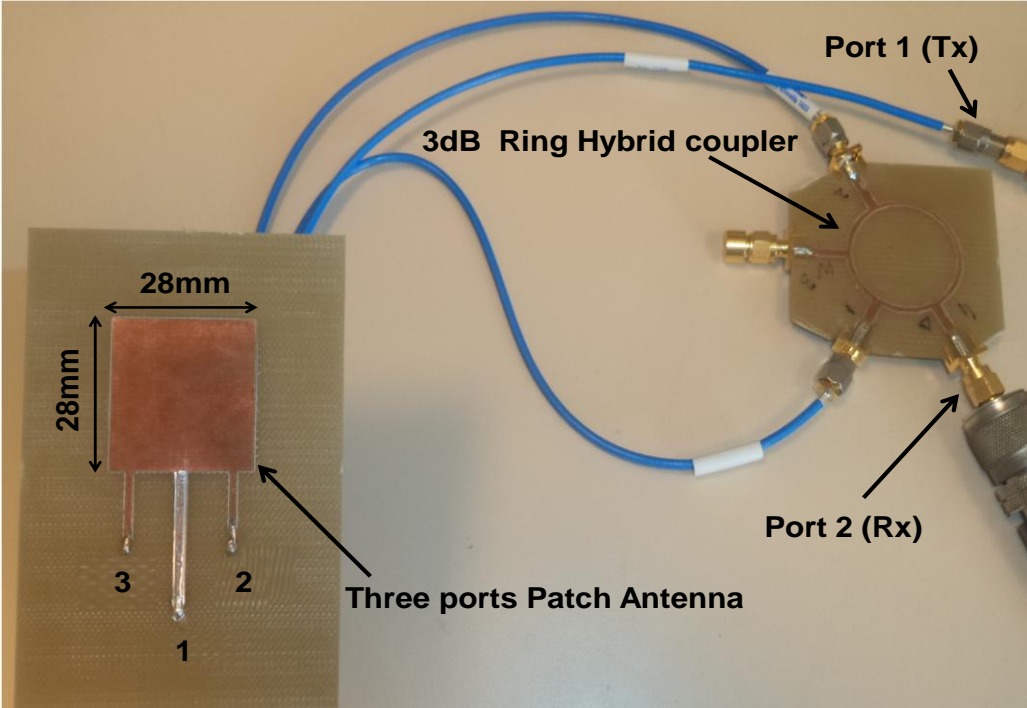


Figure 4.16: Test and measurement of three port antenna with SIC Circuit

After analyzing the performance of three ports linear co-polarized microstrip patch antenna, the implemented antenna has been interfaced with 3-dB ring hybrid coupler through two RF cables of equal length as shown in Fig.4.16. The ring hybrid coupler has been used as SIC Circuit. The two receive ports which feed the 3-dB Ring Hybrid coupler are located on same antenna edge at equal distance from transmit port, hence same amount of RF power is coupled to each receive port from transmit port. This coupled signal is then suppressed by differential mode operation of hybrid coupler as Δ port of Ring hybrid coupler has been used as receive port (Port 2).

Measured interport isolation between transmit and receive ports is greater than 60dB at centre frequency and interport isolation is better than 40dB for 55MHz with in antenna 10 dB input impedance bandwidth as shown in Fig.4.17. For the sake of comparison, ideal achievable isolation (S12-S13) is also sketched again in Fig.4.17.

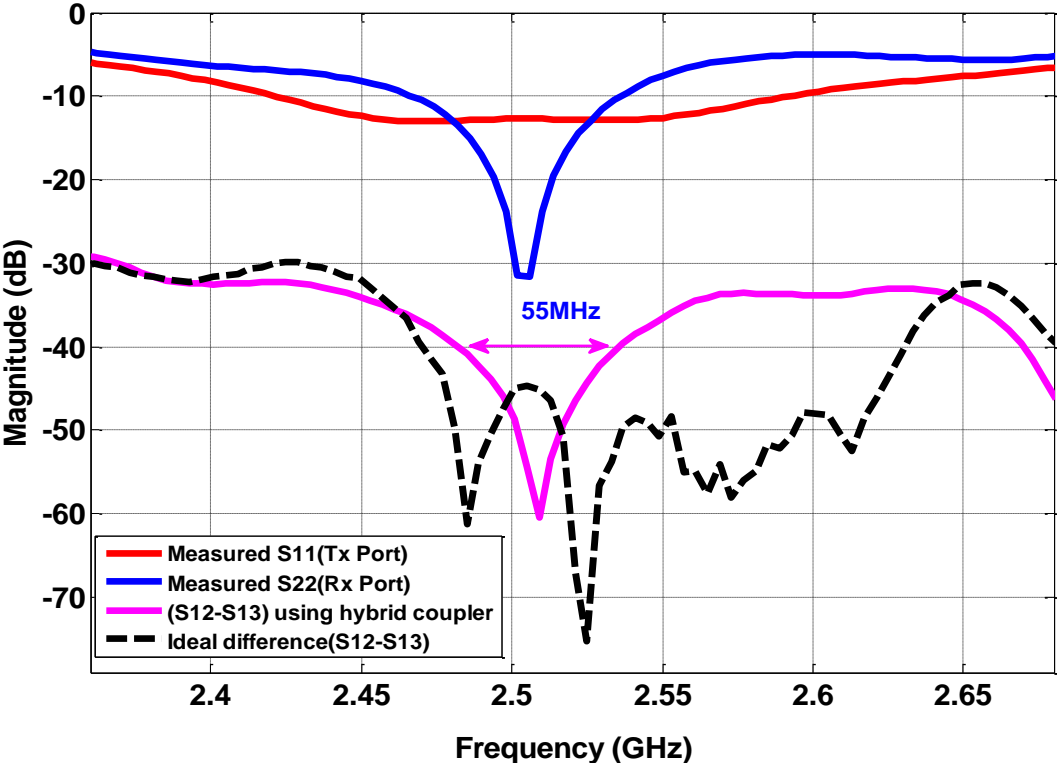


Figure 4.17: Simulated and measured S11, S22 and S12 parameters for linear co-polarized Microstrip patch antenna interfaced with SIC Circuit through RF cables

The compact dual port dual polarized antenna has been implemented by etching the antenna and Ring Hybrid coupler on single PCB along with interconnecting microstrip lines

to get rid of RF cables for interfacing of three ports antenna with ring hybrid coupler. The complete design was fabricated on FR4 Epoxy substrate (with $\epsilon=4.4$, tangent loss =.01 and thickness (h) = 1.6 mm) as shown in Fig.4.18 (a). As shown in Fig.4.18 (a), port1 excites the antenna from respective corner centre for Tx operation and port 2 excites the antenna by differentially feeding the corner ports of three port microstrip patch antenna for Rx mode. The Σ port of hybrid coupler is terminated with 50 ohms. Simulation and measurement S-Parameters results for compact dual port dual polarized antenna are shown in Fig.4.18 (b). Measured interport isolation between transmit and receive ports is greater 57.3dB at centre frequency of 2.5GHz and interport isolation is better than 40dB for 50MHz antenna 10 dB input impedance bandwidth as shown in Fig.4.18 (b).

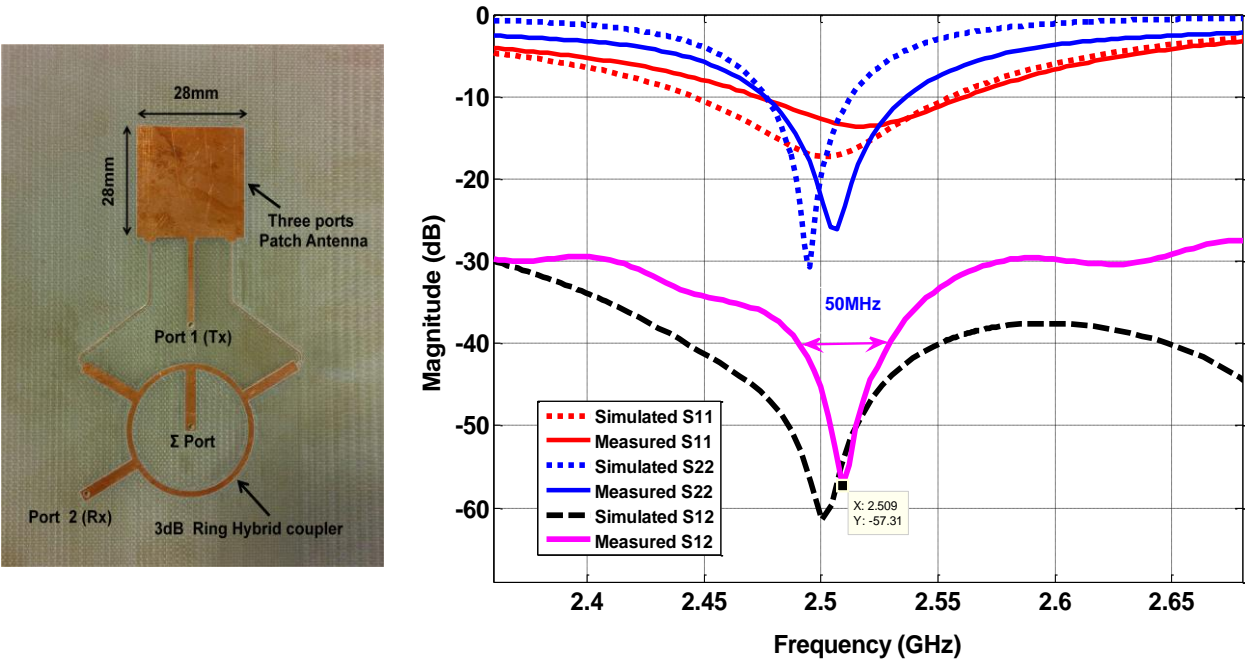


Figure 4.18: (a) Implemented compact dual port dual polarized microstrip patch antenna and 3dB Ring Hybrid coupler (b) Simulated and measured S11, S22 and S12 for dual polarized patch antenna

The gain patterns for each port were measured by exciting one port and terminating other port with 50 ohms. Again antenna radiates in z-direction and ports are along y-axis. For port 1(Tx port) excitation, antenna polarization direction is along y-axis and yz pattern is measured and mentioned as E-plane pattern while for differential excitation of two side ports of antenna through port 2 of ring hybrid coupler, antenna is polarized along x-axis and xz pattern is measured as E-plane pattern for second polarization. Measured 2D E-plane and H-

plane gain patterns at 2.5GHz for both horizontal and vertical polarizations when Port 1 is excited and other ports terminated with 50 ohms are shown in Fig.4.19(a), where pole1 and pole2 represent horizontal and vertical polarization respectively while $\Phi=90^\circ$ and $\Phi=0^\circ$ correspond to antenna's E-plane and H-plane respectively. As expected and clearly visible from the Fig.4.19 (a), the antenna is linear vertically polarized for port 1 excitation and there is a null at $\Theta=0^\circ$ as most of the Tx power diminishes for $\Theta=0^\circ$ due to differential feeding mechanism for two side ports of antenna.

For the case of differential excitation of antenna from two side ports through hybrid Coupler for receive mode configuration, measured 2D E-plane and H-plane gain patterns at 2.5GHz for both horizontal and vertical polarizations when Port 2 is excited and other ports terminated with 50 ohms are shown in Fig.4.19 (b). Again pole 1 and pole 2 represent horizontal and vertical polarization respectively while $\Phi=90^\circ$ and $\Phi=0^\circ$ correspond to antenna's E-plane and H-plane respectively. Fig.4.19 (b) clearly shows that antenna is linear horizontal polarized for receive mode operation.

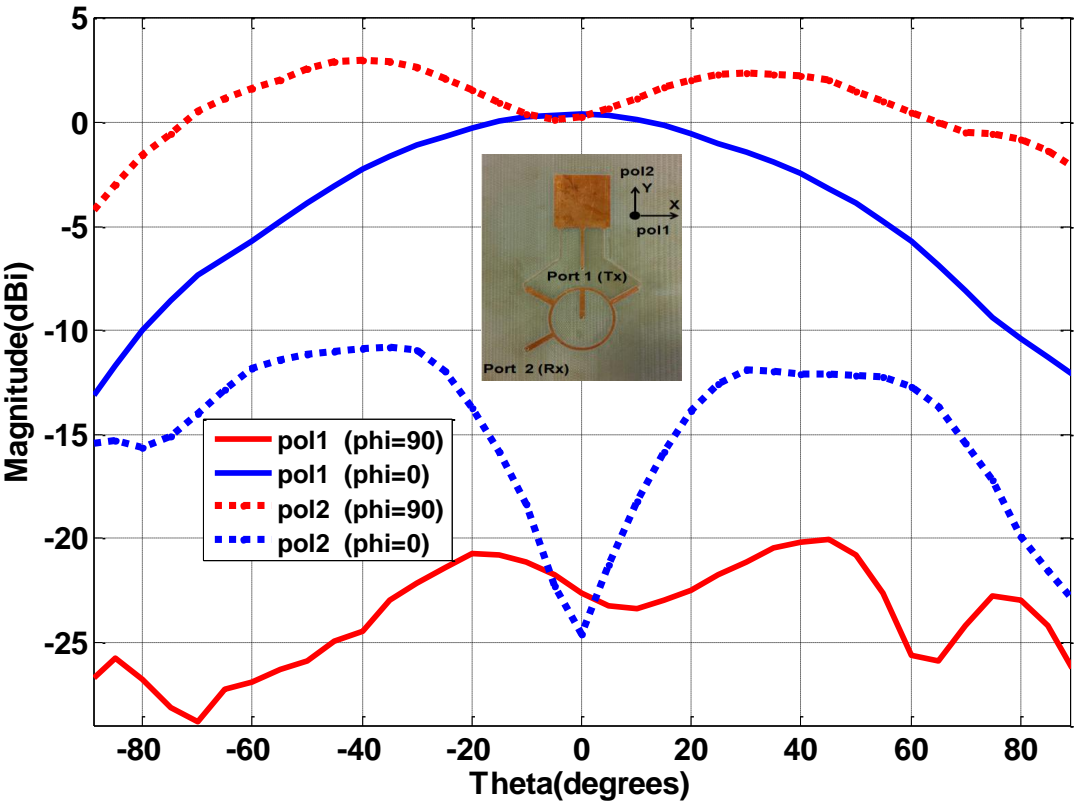


Figure 4.19: (a) 2D Gain Pattern of compact dual port Microstrip patch antenna at 2.5GHz for Port 1 excitation

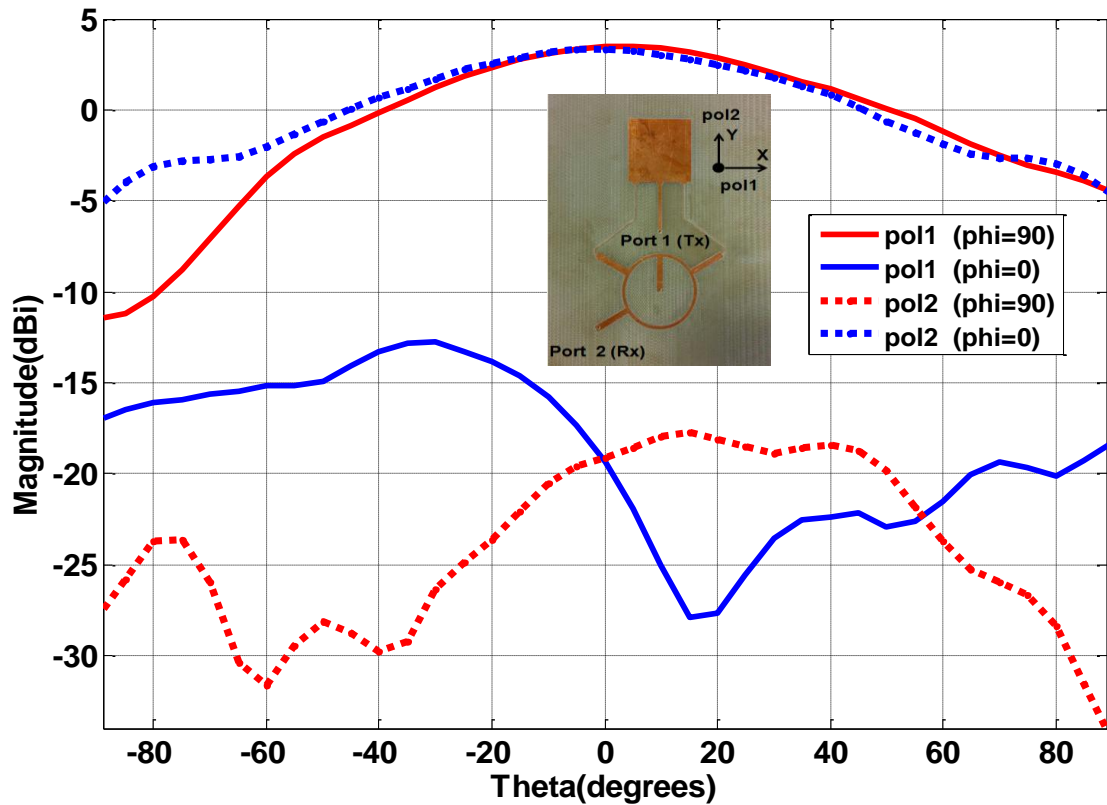
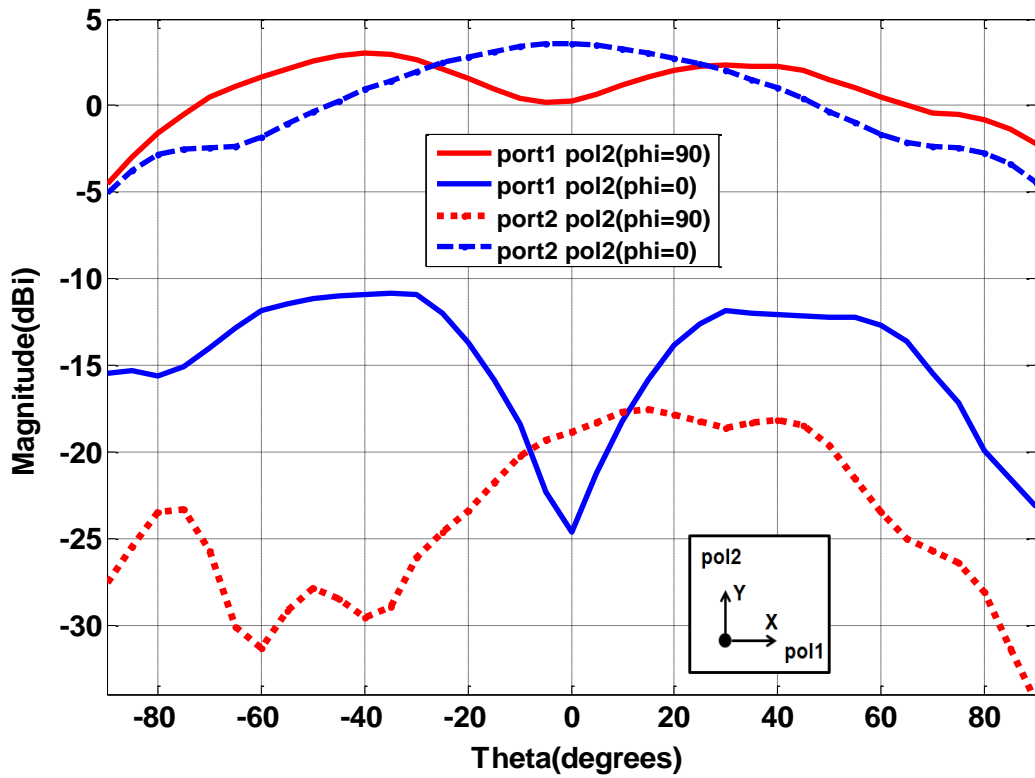
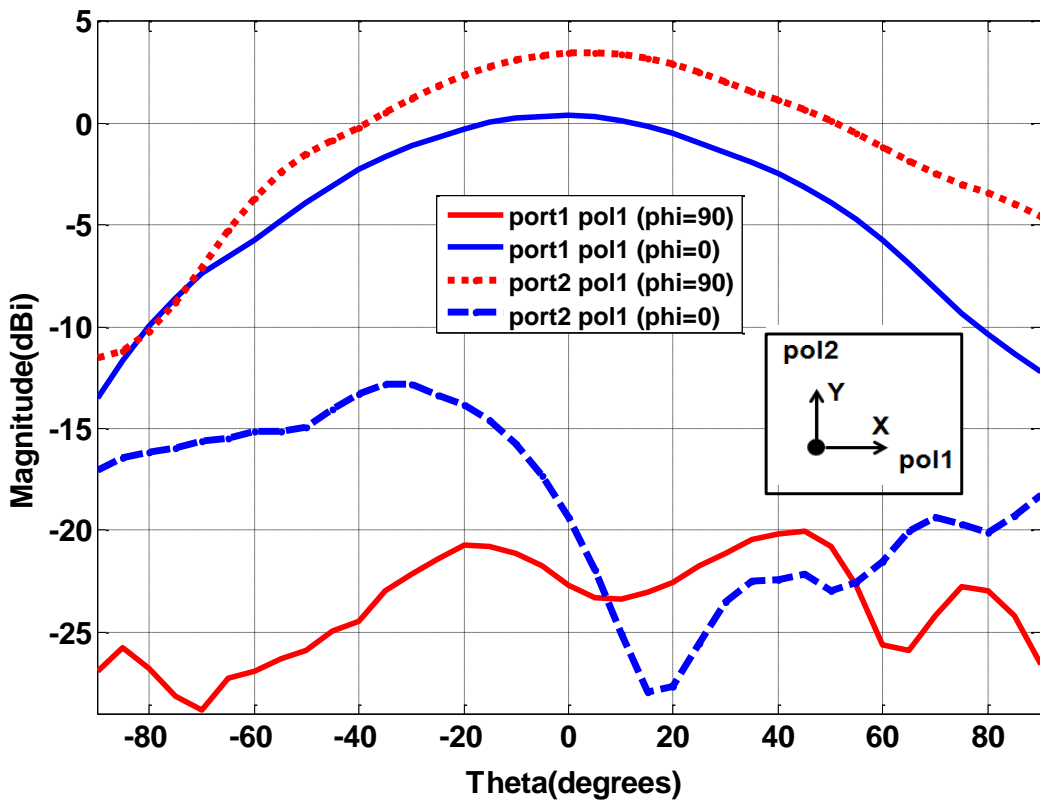


Figure 4.19 (b) 2D Gain Pattern of compact dual port Microstrip patch antenna at 2.5GHz for Port 2 excitation

The orthogonal polarization (dual polarization) nature of proposed compact antenna is also endorsed by measured 2D patterns of implemented antenna as shown in Fig.4.20 for vertical and horizontal polarization separately. Again pol1 and pol2 represent horizontal and vertical polarization respectively. In Fig.4.20 (a), measured 2D Gain Pattern of compact dual port microstrip patch antenna at 2.5GHz for vertical polarization has been sketched. As clear from Fig.4.20 (a), the proposed antenna is linear vertically polarized for Tx mode with port 1 excitation. Similarly measured 2D Gain Pattern of compact dual port microstrip patch antenna at 2.5GHz for horizontal polarization shown in Fig.4.20 (b) show that the antenna is horizontally polarized for port 2 feeding for Rx operation. The implemented antenna provides 3.1dBi and 3.7dBi maximum gain for port 1 and port2 excitations respectively for 2.5GHz operating frequency. For compact antenna structure, efficiency is around 65%. Antenna's efficiency will be higher if we use a lower loss substrate instead of FR-4.



(a)



(b)

Figure 4.20: (a) 2D Gain Pattern of compact dual port Microstrip patch antenna at 2.5GHz for vertical polarization (pol2) (b) for horizontal polarization (pol1)

For the presented antenna, polarization diversity provides around 40dB interport isolation and the additional 17dB isolation is achieved by 3-dB Ring Hybrid Coupler which performs as a simple SIC circuit. The implemented antenna circuit along with analog and digital SIC techniques can be used to implement a shared antenna based IBFD transceiver for 2.5GHz in band bidirectional communication link with 50MHz bandwidth.

4.5 Dual port ,dual Polarized Antenna with quarter wave microstrip (MS) feeds using single SIC Circuit for high Inter-Port isolation

The compact dual port dual polarized antenna with SIC has been designed and implemented by etching the antenna and Ring Hybrid coupler on single FR4 Epoxy substrate (with $\epsilon=4.4$, tangent loss $=.01$ and thickness (h)= 1.6 mm) as shown in Fig.4.21(a).

Measurement S-Parameters results for compact antenna are shown in Fig.4.21(b). Measured interport isolation between transmit and receive ports is greater 75dB at centre frequency .The antenna provides better than 55dB interport isolation for 50MHz antenna 10 dB input impedance bandwidth as shown in Fig.4.21(b).

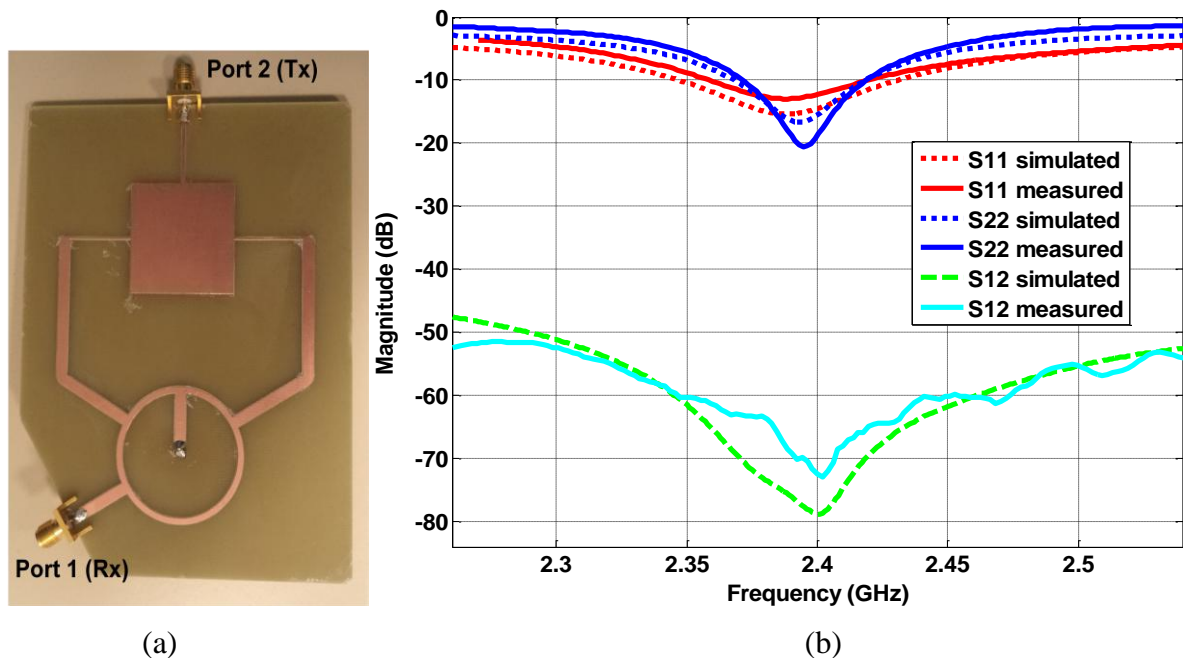


Figure 4.21: (a) Implemented compact dual polarized antenna with SIC (b) Simulated and measured S11, S22 and S12 for polarized dual polarized antenna with SIC

Measured co-polarization and cross polarization gain patterns for dual polarized differential fed microstrip patch antenna with $\lambda/4$ microstrip feeds are shown in Fig.4.22. The antenna has good polarization purity as it provides very low cross polarization level for each port excitation and especially for differential feeding configuration.

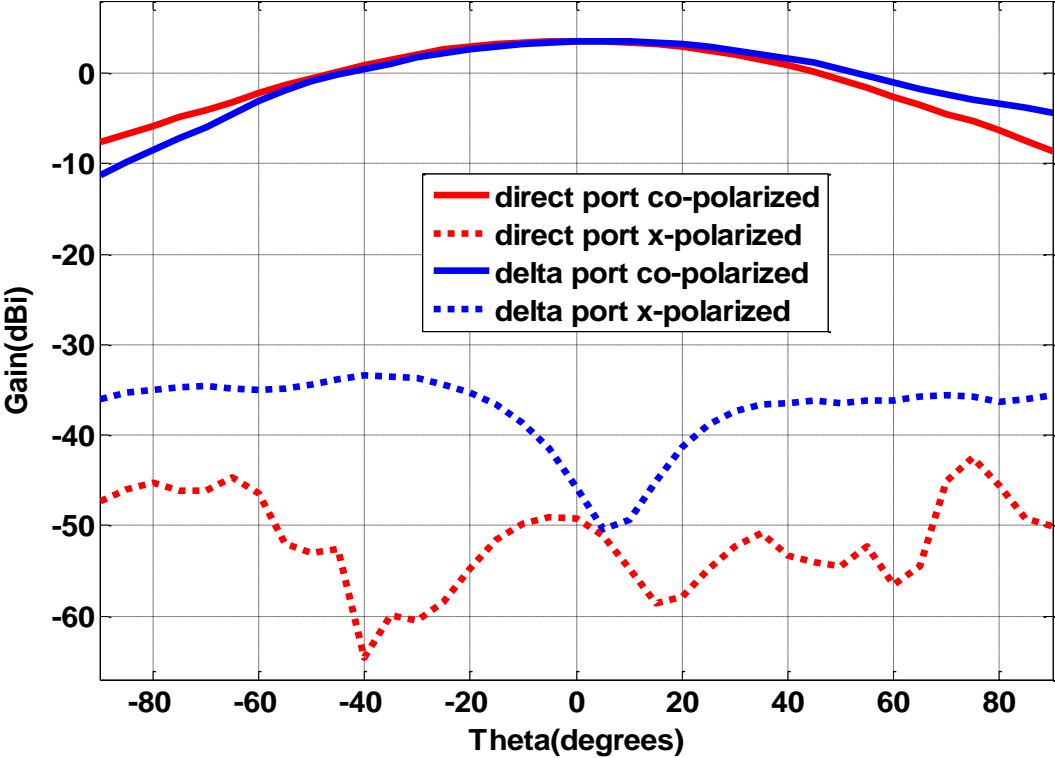
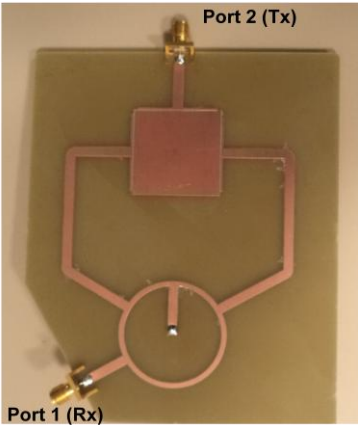


Figure 4.22: Measured co-polarization and cross polarization gain patterns for dual polarized differential fed antenna with $\lambda/4$ microstrip feeds

4.6 Dual port ,dual Polarized Antenna with microstrip-T (MS-T) feeds using single SIC Circuit for high Inter-Port isolation

For differential fed three ports antenna with $\lambda/4$ feeds, thin quarter wave microstrip lines have been used for antenna excitation from each port and these may cause power loss when antenna is excited through port 2. In order to solve this issue, T-shaped microstrip transmission lines can be used for antenna excitation from each port as already done for dual port antenna. T-shaped microstrip transmission lines excite the antenna through EM coupling and such antenna can be effectively used for active application because no additional capacitors at antenna ports are required for DC blocking.

The compact antenna using three ports antenna with T-shaped microstrip feeds along with ring hybrid coupler as SIC circuit has been designed and implemented on single FR4 (with $\epsilon=4.4$, tangent loss =.01 and thickness (h)= 1.6 mm) PCB as shown in Fig.4.23(a). As shown in Fig.4.23 (b) by measured S-parameters results for this compact the interport isolation between transmit and receive ports is around 70dB at centre frequency .The antenna provides around 60dB interport isolation for 50MHz antenna 10 dB input impedance bandwidth as shown in Fig.4.23 (b).Also this antenna structure has improved input matching for port 2 due to good input impedance matching for three ports antenna with microstrip-T feeds.



(a)

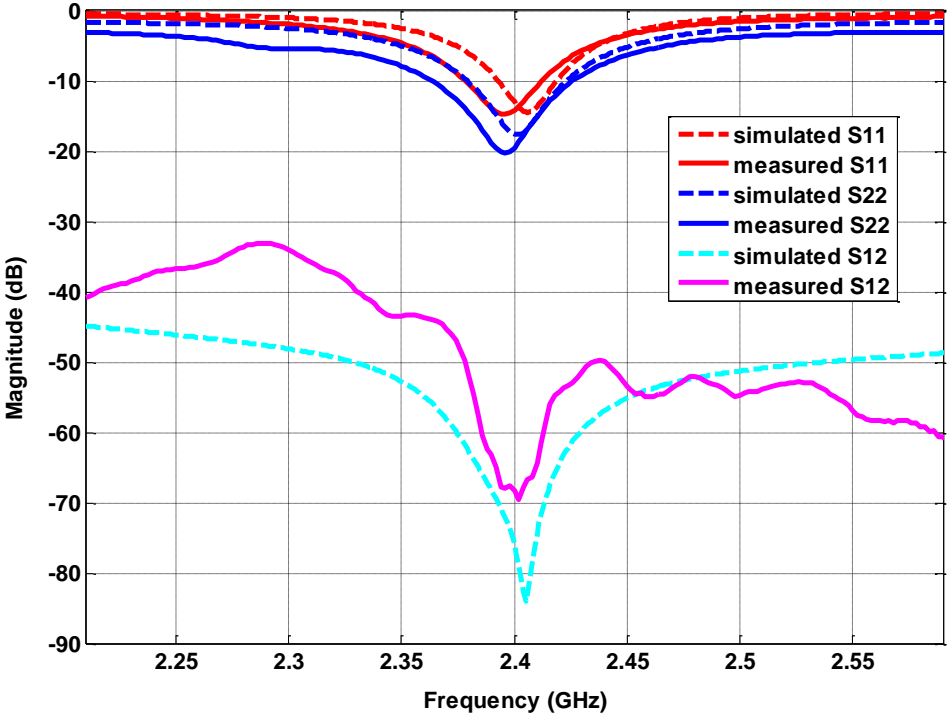


Figure 4.23: (a) Implemented compact dual S12 polarized antenna with SIC (b) Simulated and measured S11, S22 and S12 for dual polarized antenna with SIC

4.7 Dual port ,dual Polarized Antenna with quarter wave feeds (MS) using two SIC Circuits for high Inter-Port isolation

The proposed four ports antenna with two SIC Circuits can not be implemented in compact form on single PCB on single side due to cross over of microstrip interconnects for SICs interfacing with antenna. So the antenna and one SIC on same layer has been implemented in compact form as already done for three ports antenna with SIC and then second SIC through equal length RF cables has been connected to realize four ports antenna configuration with two SIC circuits as shown in Fig.4.24.

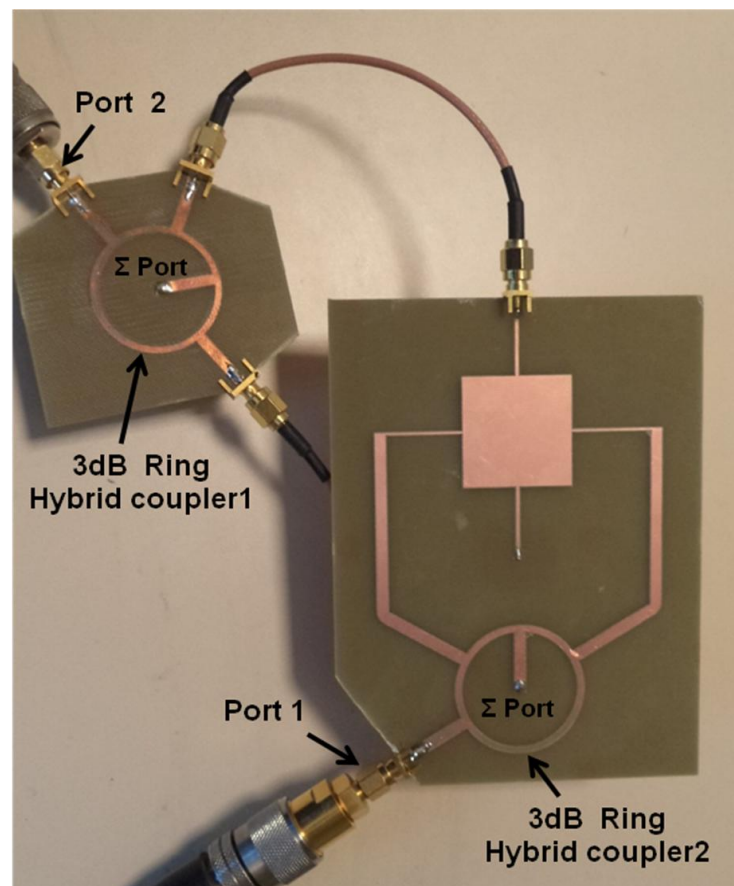


Figure 4.24: Implemented Dual polarized antenna with two Self Interference Circuits(SICs)

Measurement S-Parameters results for four ports antenna with two SICs are shown in Fig.4.25. Measured interport isolation between transmit and receive ports is greater 75dB at

centre frequency .The antenna provides better than 55dB interport isolation for 50MHz antenna 10 dB input impedance bandwidth .

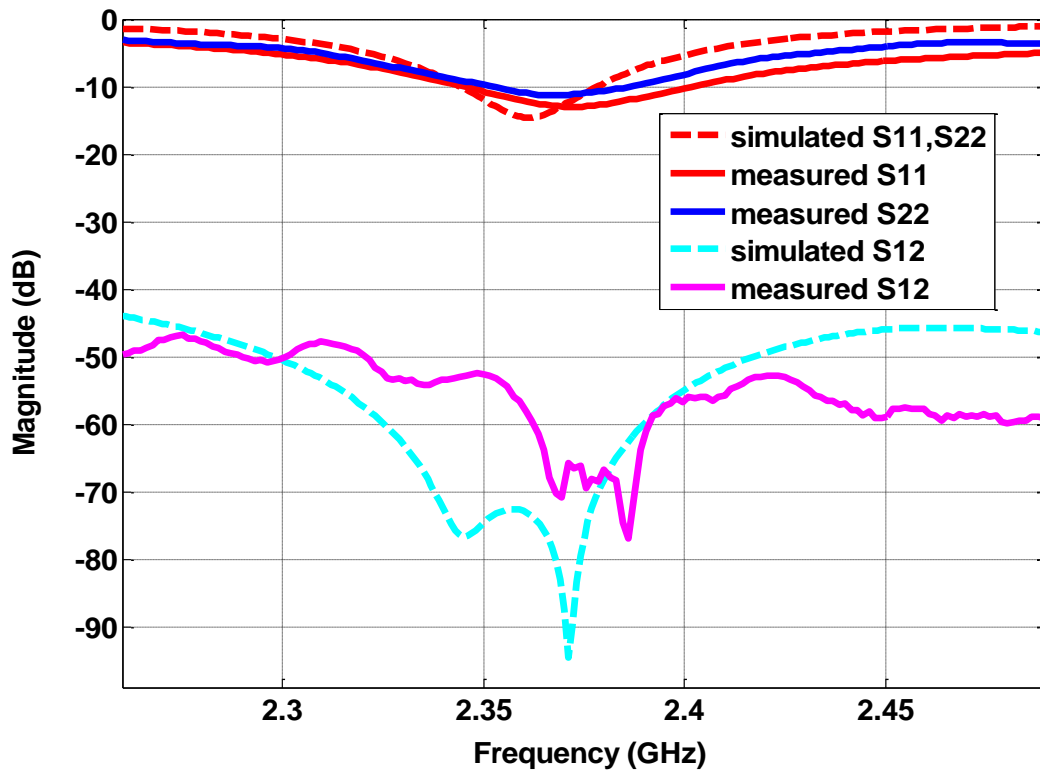


Figure 4.25: Simulated and measured S11, S22 and S12 parameters for four port Microstrip patch antenna two with SIC Circuits

4.8 Dual port ,dual Polarized Antenna array with quarter wave microstrip (MS) feeds using single SIC Circuit for high Inter-Port isolation

The proposed and implemented antenna array is based on same concept as already discussed for three ports microstrip patch antenna with $\lambda/4$ feeds and external ring hybrid coupler for differential feeding. The compact dual polarized antenna array implemented on single layer FR4 substrate (with $\epsilon=4.4$, tangent loss =.01 & thickness (h) = 1.6 mm) is shown in Fig.4.26.

Measured S-parameters results for compact dual polarized antenna array using differential feeding are shown in Fig.4.27. Measured interport isolation between transmit and receive ports is around 70dB at centre frequency. The antenna array provides around 60dB interport isolation for antenna's 10 dB input impedance bandwidth of 50MHz. The implemented array has comparable interport isolation performance as that of three ports microstrip patch antenna with $\lambda/4$ feeds and ring hybrid coupler as a SIC circuit. The

additional advantage of this design is high gain due to array setup. Thus, implemented compact dual polarized antenna array using differential feeding provides high interport isolation along with improved gain.

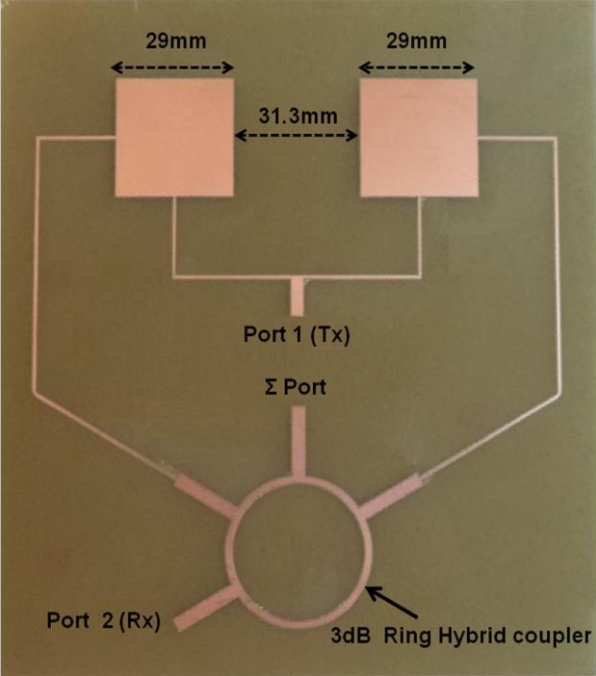


Figure 4.26: Implemented compact dual polarized antenna array using differential feeding

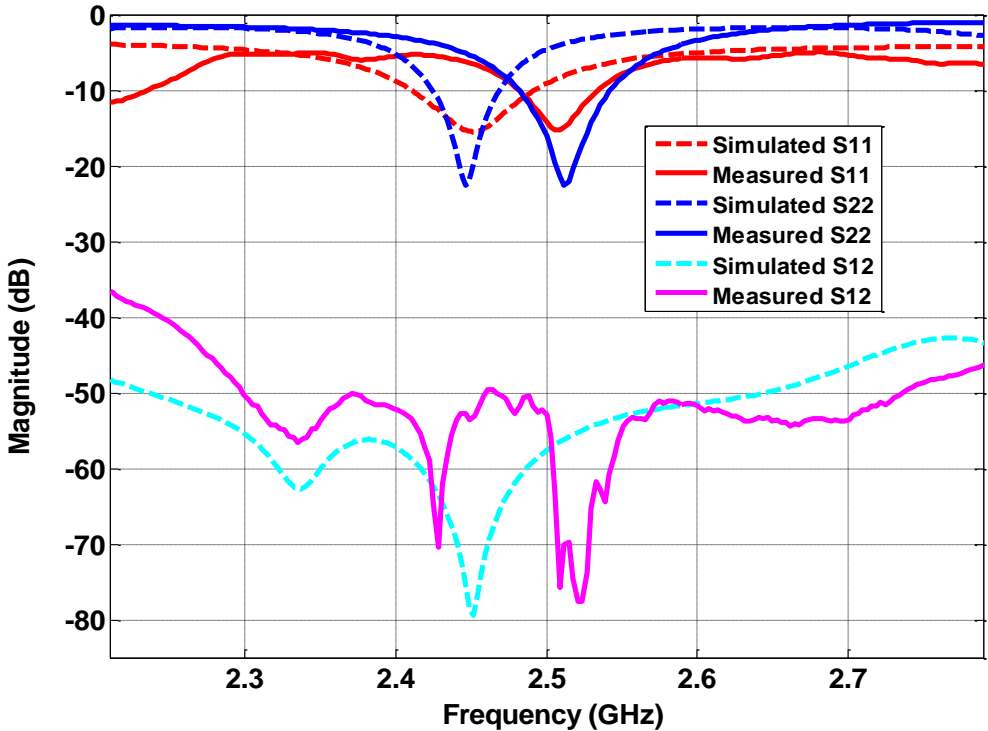


Figure 4.27: S-parameters measurement results for compact polarized antenna array with differential feeding

4.9 Dual port ,orthogonal polarized Slot Coupled Antenna

The implemented dual port, dual polarized antenna is shown in Fig.4.28 where the microstrip feed line under the ground plane is clearly shown in Fig.4.28 (b) to excite the radiating patch through small aperture in ground plane(slotted ground plane using port 2. The ground plane with rectangular aperture is sandwiched between two 1.6mm thick FR-4 substrate layers. The other port excites the radiating element through $\lambda/4$ feed line.

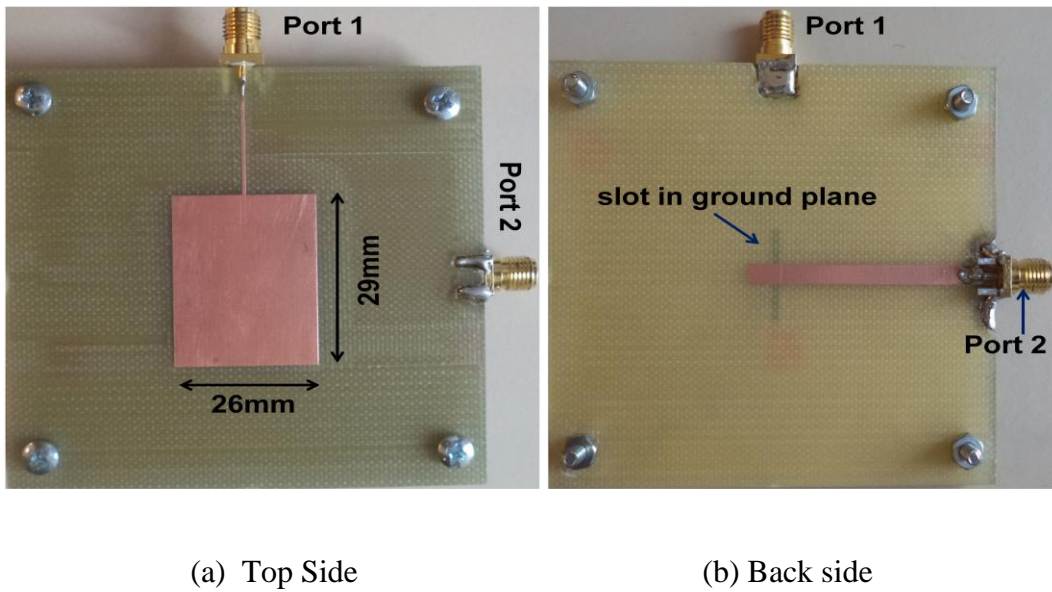


Figure 4.28: Constructed dual port, dual polarized slot coupled patch antenna

The simulated and measured S11, S22 and S12 results for proposed and implemented dual polarized slot coupled antenna are shown in Fig.4.29. The quarter wave microstrip fed (port 1) has 50MHz and slot coupled port (port2) has 100MHz input 10dB bandwidth. Thus, slot coupled port has better impedance bandwidth as compared to microstrip fed port. The implemented antenna structure provides better than 55dB interport isolation for 50MHz antenna's 10dB bandwidth. Thus, slot coupled microstrip patch antenna provides better interport isolation performance as compared to quarter wave microstrip fed patch antenna. There is a good agreement between simulated and measured results except the amount of interport isolation. The measured and simulated interport isolation results differ because the implemented antenna has finite slotted ground plane while the simulation results were obtained with infinite slotted ground plane.

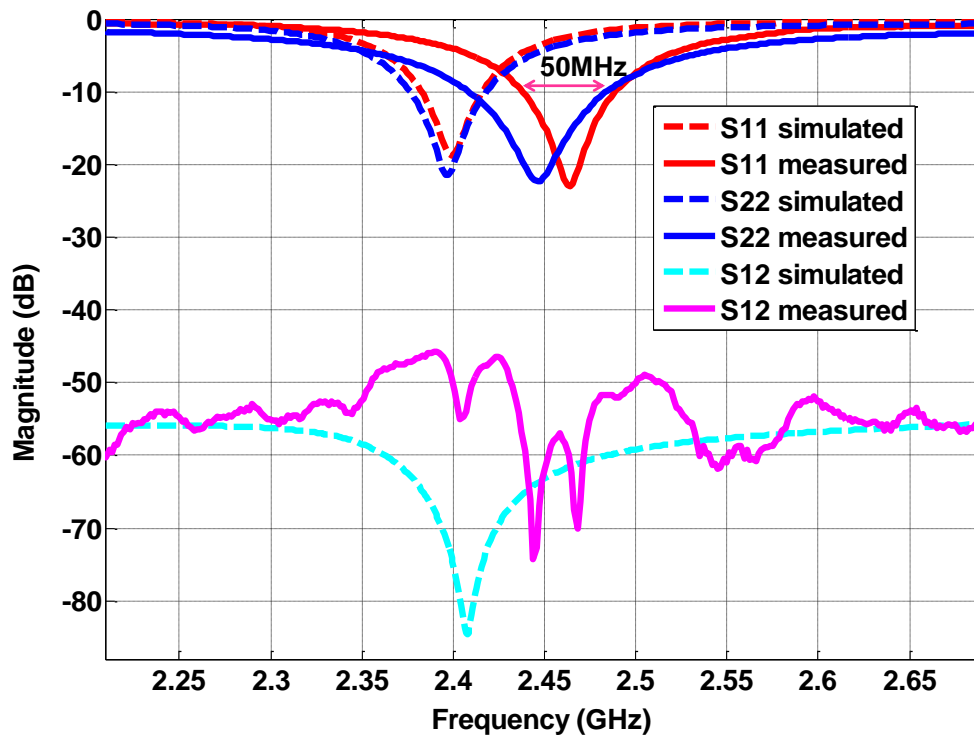


Figure 4.29: Simulated and measured S11, S22 and S12 parameters for dual polarized slot coupled antenna

4.10 Dual port ,orthogonal Polarized Slot Coupled Antenna with SIC Circuit

In this design, dual port orthogonal polarized three ports slot coupled antenna with external SIC circuit has been implemented which uses two quarter wave feeds for differential feeding and one slot coupled feed. The 3-dB Ring Hybrid coupler has been used as external SIC circuit to differentially feed radiating patch through quarter wave feeds as discussed earlier.

The compact dual port dual polarized antenna with SIC has been designed and implemented by etching the radiating patch and ring hybrid coupler on single FR4 Epoxy substrate (with $\epsilon=4.4$, tangent loss $=.01$ and thickness (h)= 1.6 mm) as shown in Fig.4.30. Measurement S-Parameters results for this compact antenna configuration are shown in Fig.5.31. Measured interport isolation between transmit and receive ports is greater 80dB at centre frequency. The antenna provides better than 73dB interport isolation for 50MHz antenna 10 dB input impedance bandwidth as shown in Fig.4.31.

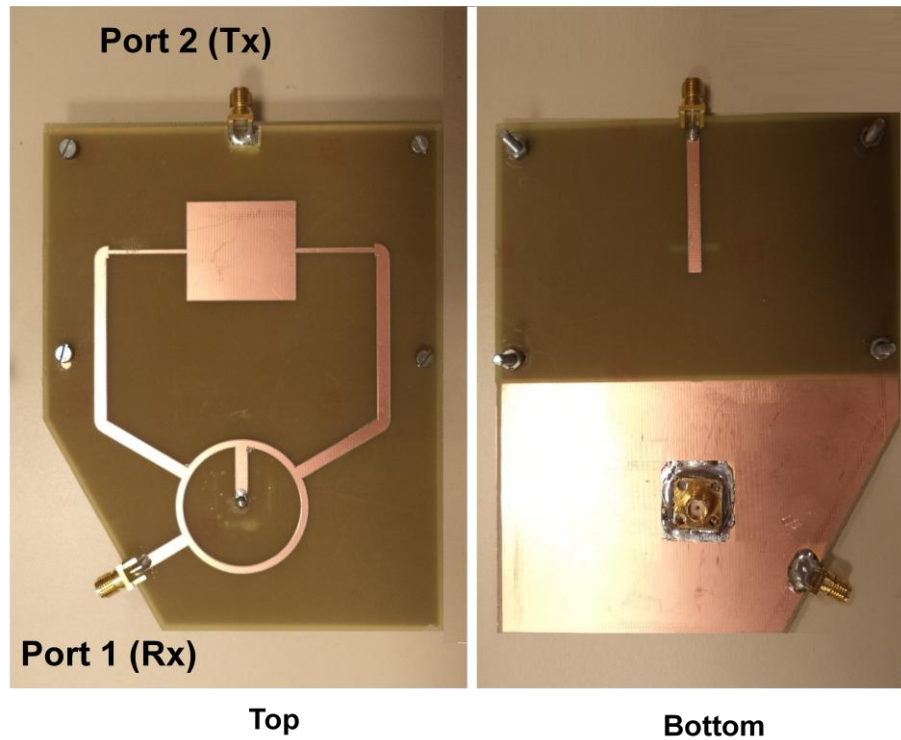


Figure 4.30: Constructed dual port, dual polarized differential fed slot coupled patch antenna

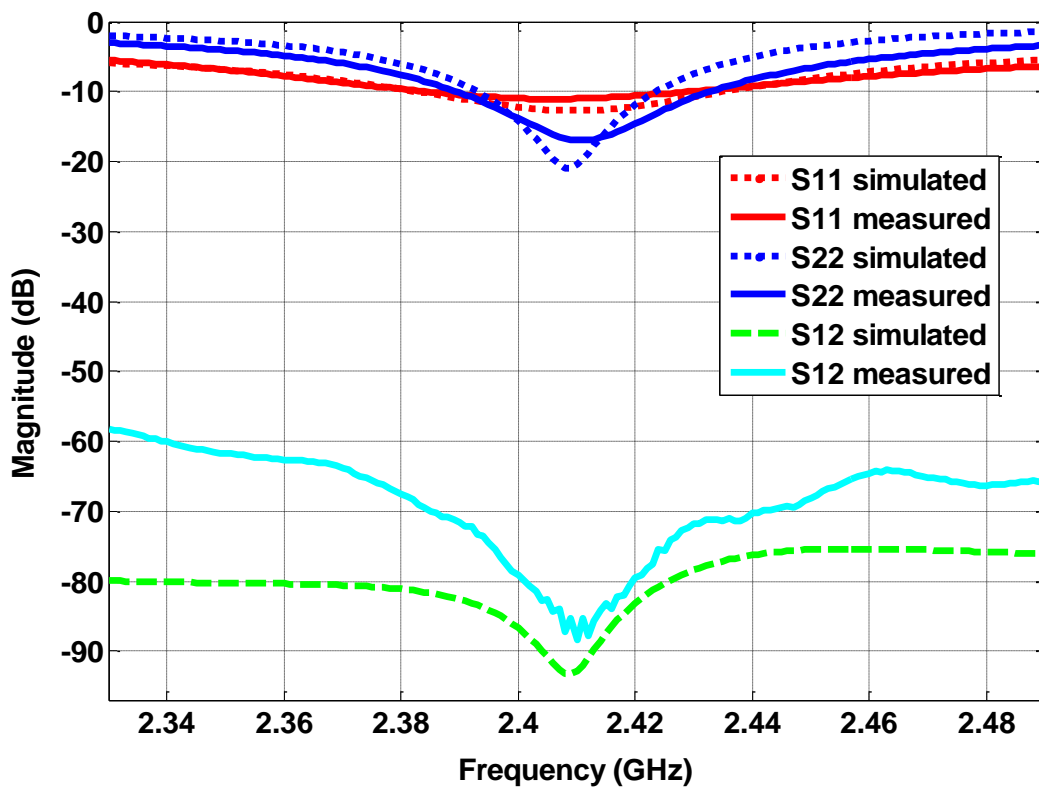


Figure 4.31: Simulated and measured S11, S22 and S12 parameters for dual polarized differential fed slot coupled antenna

Measured co-polarization and cross polarization gain patterns for dual polarized differential fed slot coupled microstrip patch antenna are shown in Fig.4.32. The antenna has excellent polarization purity as it provides very low cross polarization level for each port excitation.

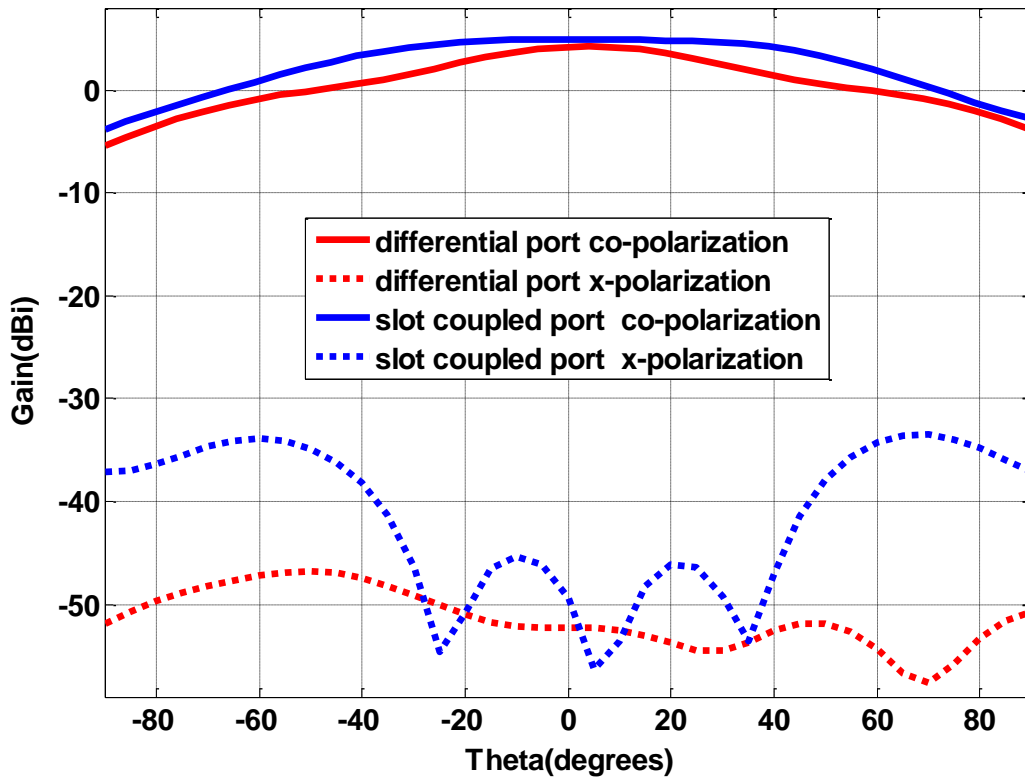


Figure 4.32: Measured co-polarization and cross polarization gain patterns for dual polarized differential fed slot coupled antenna

4.11 Three ports microstrip patch antenna with dual linear and linear co- polarization characteristics

Three ports proximity coupled microstrip antenna has been implemented which achieves improved port to port isolation with linear co-polarization and linear dual polarization radiation characteristics as compared to linear co-polarized antenna with two anti-parallel feeds and linear dual polarized antenna with two orthogonal feeds respectively. In both cases, patch is excited through EM coupling to have DC isolated ports in addition to RF isolation.

Implemented antenna on double layer (1.6mm+1.6mm) FR-4 substrate ($\epsilon = 4.4$, tangent loss =.02) is shown in Fig.4.33. Port 2 is linear co-polarized and port 3 is linear orthogonal polarized with respect to port 1 as discussed earlier.

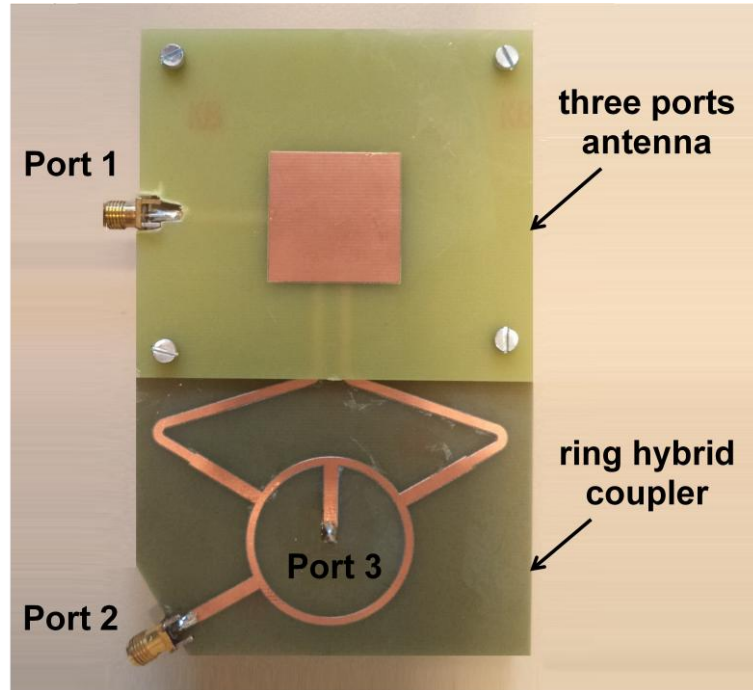


Figure 4.33: Implemented 2.4GHz compact proximity coupled patch antenna

For linear co-polarized configuration, measured input matching (S_{11} , S_{22}) and port to port RF isolation (S_{12}) results are shown in Fig.4.34. Implemented antenna's 10dB impedance bandwidth is more than 60MHz for both linear co-polarized ports. Measure RF isolation between port1 and port 2 is better than 10dB in 60MHz bandwidth as compared to 2.5dB interport isolation provided by two ports linear co-polarized proximity coupled patch antenna with dual anti-parallel feeds (shown as antenna A in Fig.4.34). Thus, interport isolation improvement of around 8dB is obtained for linear co-polarized configuration using differential feeding as discussed earlier. In addition to RF isolation, both linear co-polarized ports are DC isolated due to proximity feeding mechanism for each port.

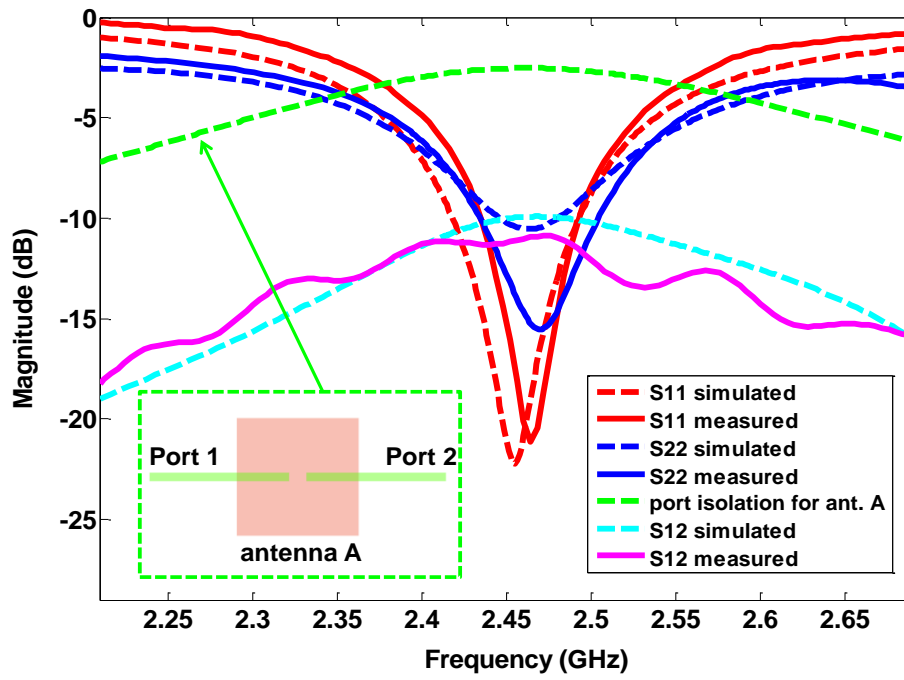


Figure 4.34: Measured input matching (S11, S22) and interport isolation (S12) results for implemented linear co-polarized patch antenna

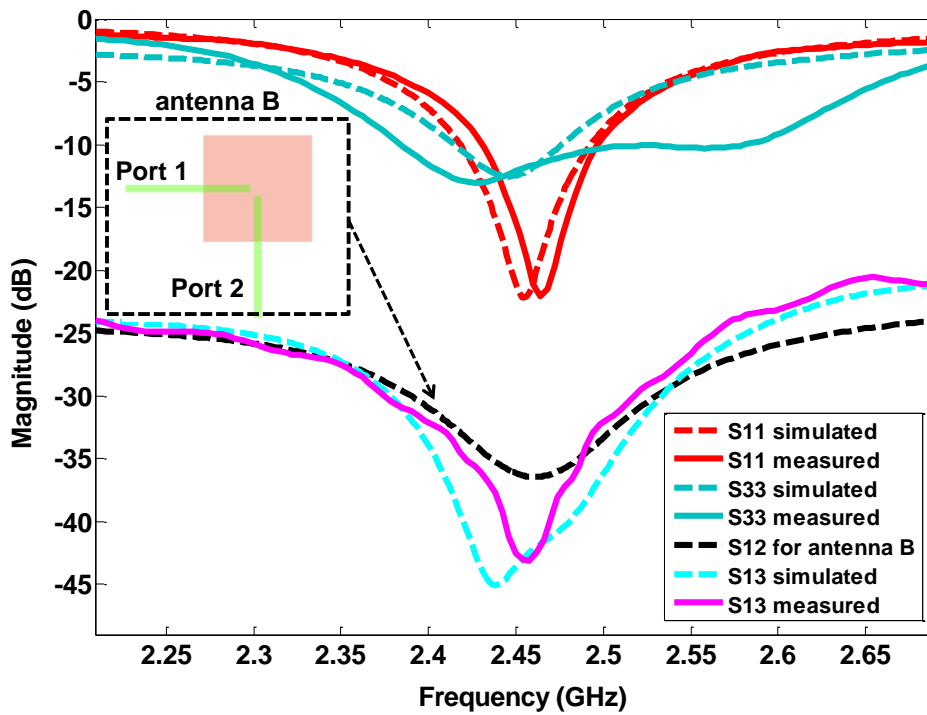


Figure 4.35: Measured input matching (S11, S33) and port isolation (S13) characteristics of implemented linear dual polarized patch antenna

Measured input matching (S_{11} , S_{33}) and interport RF isolation (S_{13}) characteristics for dual polarized case are shown in Fig.4.35. Measured 10dB impedance bandwidth is again more than 60MHz for both port 1 and port 3 while measured RF isolation between dual polarized ports is more than 43dB at centre frequency as compared to 36dB interport isolation provided by dual polarized proximity coupled antenna B which deploys two perpendicular feeds to excite two orthogonal TM_{01} and TM_{10} modes for dual polarization (shown as antenna B in Fig.4.35). Measured interport isolation for dual polarization case is better than 35dB for 60MHz band-width as was the case for antenna B. Again both ports are DC isolated due to EM excitation of radiating patch through proximity coupled port 1 and port 3.

4.12 Compact Dual Port, Single Element Planar Circular Disc Monopole Antenna for Wide-Band MIMO Based Wireless Applications

The proposed antenna uses a partial ground plane with two rectangular grooves which lie exactly below the respective 50Ω microstrip feeding lines in order to obtain enhanced antenna's impedance bandwidth of 2-6GHz. A circular cut with 14mm radius and centred at intersection of two partial rectangular ground planes is etched to reduce port to port RF coupling. The implemented dual port monopole antenna on 1.575mm thick RT/Duroid® 5880 substrate (with $\epsilon=2.2$, tangent loss =.001) provides more than 15dB RF interport isolation for antenna's 10dB impedance bandwidth of 2-6GHz with measured gain variations of 2-6dBi for each port excitation. In addition to interport isolation measurement for dual port antenna, the envelope correlation coefficient over the required frequency range has been calculated and plotted using S_{11} , S_{22} and S_{21} measurement results to endorse the performance of dual port implemented antenna for diversity applications.

Wideband mobile and wireless communication systems with high data rate capacity along with reliable communication link performance are in great demand for current fast growing wireless applications [67]. Multiple Input Multiple Output (MIMO) technology improves the data throughput of wireless and mobile communication systems by deploying radio transceivers with multiple antennas to transmit and receive RF signals in rich scattered wireless environments [68-69]. MIMO techniques accomplish the task of improvement in data throughput and system capacity through spatially separated multiple wireless channels working at same carrier frequency (uncorrelated signals) and without additional transmit

power requirements in Non Line of Sight (NLOS) communications [67],[70]. MIMO techniques are also very useful to improve the performance of wireless and mobile communication systems by minimizing the multi path propagation effect [71-72].

The MIMO antenna plays an important role to improve the overall performance of MIMO systems. Although, MIMO technology improves the capacity and reliability of wireless systems but the mutual coupling between multiple antennas degrades the obtainable MIMO performances due to increased signal correlation between multiple radio signals [73]. The coupling can be reduced by placing multiple antennas with large spatial displacements but it prevents the realization of compact transceiver [74]. The effect of mutual coupling can not be ignored in order to realize a compact MIMO transceiver where multiple antennas with minimum inter spacing are required to be fabricated on same substrate [67]. Realization of a compact MIMO antenna with required interport isolation is a challenging task [67].

The printed antennas are preferred for MIMO transceivers due to their ease of integration and low cost. For conventional compact MIMO transceivers, sufficiently separated multiple planar radiating elements are deployed and either isolation improvement techniques [75-85] or decoupling networks [86-87] are used to achieve required amount of interport isolation for MIMO applications. For example, the antenna using two folded monopoles presented in [75] operates in 2.30-2.39 GHz frequency range and uses additional ground wall with connecting line to decrease the mutual coupling between antennas. A printed diversity monopole antenna for 2.4 GHz WLAN operation band is presented in [76]. It deploys T-shaped ground plane between two orthogonal linear monopoles for ports decoupling. A negative group delay based correlation reduction technique for closely spaced antennas technique has been proposed in [77] which reduces mutual coupling between antennas and also un-correlates the radiation characteristic of antennas. A compact MIMO antenna using two planar-monopole antenna elements has been presented in [78] for portable UWB applications. In this design, microstrip feed lines have been used to excite the two orthogonally placed antenna elements. Two long protruding ground stubs etched in ground plane improve antenna's impedance bandwidth and reduce the mutual coupling. A 2.4GHz compact MIMO structure has been presented in [79], which uses two different types of radiating elements. It uses one proximity coupled square ring patch antenna co-located with probe fed PIFA. Both radiators are designed to work at 2.4GHz WLAN frequency and high inter-port isolation (below 25 dB) is obtained through orthogonal polarization. In [80], a dual port planar canonical antenna is presented which uses folded slots as radiating elements. Coupling parasitic elements between canonical antennas have been used for field cancellation

to improve the isolation. MIMO antennas with even number of ports can be designed by replicating this proposed dual port planar canonical antenna. A compact multiple-input multiple-output (MIMO) antenna with low correlation for UWB applications has been presented in [81]. The proposed structure is comprised of two identical radiating elements fed through 50 ohms microstrip lines and placed over half sized ground plane which is triangularly trimmed on two edges adjacent to radiating element to achieve better input impedance. The orthogonal placement of two antenna elements provides good interport isolation. The work in [82] presents a wideband isolation technique with neutralization lines for two crescent shaped printed monopole antennas placed very close to each other. The proposed antenna provides high isolation over 2.4-4.2GHz frequency band. Two antennas configuration, each comprised of two radiating elements has been presented in [83]. One configuration uses two parallel placed radiating elements while the other one utilizes reverse parallel placement of antenna elements. Inverted T-shaped stubs have been used to obtain low port to port coupling over UWB frequency range. A novel neutralization technique based on two defected ground structures (a line slot and T-shaped slot etched on the ground plane) has been used in [84] to reduce the coupling between two UWB slot antennas. An ultra wideband MIMO antenna array has been presented in [85] to achieve 21dB isolation over 2.5–12 GHz frequency range by exploiting polarization diversity of two straight edged monopole radiator fed with arced feeding mechanism and placed over partial ground planes. Some antennas deploy external decoupling networks to suppress mutual coupling between elements and such decoupling networks are either based on circuit approach [86] or use lumped elements [87] to obtain improved interport isolation. For example, a circuit based technique has been used in [86] to increase the isolation between two strongly coupled antennas while a lumped elements technique has been presented in [87] to reduce the coupling between two closely packed antennas. These techniques may also be deployed for MIMO antennas.

In contrast to above reviewed research works [75-87] where multiple antenna elements are incorporated in to one antenna design or etched on same substrate to realize a compact MIMO antenna, single antenna element with multiple RF isolated feeding ports can be used in more compact form for MIMO applications. Such configuration is termed as isolated mode antenna (iMAT) [88]. Such structures excite different propagating modes in antenna for feeding from each port to reduce mutual coupling between ports [89-93]. For example, a novel dual port, single element antenna for 4G MIMO terminals based on iMAT idea has been proposed and analysed in [89]. The concept of iMAT antenna has also been used in [90] for U-shaped single element antenna to obtain improved port to port isolation performance as

compared to compact two elements monopole antenna. A dual fed compact ultra-wideband microstrip monopole antenna with reconfigurable polarisation capability has been presented in [91] for cognitive radio systems where two orthogonal feeds using different transmission line technology have been used to improve RF isolation between two ports. One port uses 50Ω feed line using coplanar waveguide (CPW) structure while the other port excites the radiating patch using 50Ω Microstrip (MS) feed line. The proposed antenna provides more than 25dB port to port isolation for 3.1 GHz to 10.6 GHz bandwidth based on a reflection coefficient of less than -10 dB. A dual-polarized MIMO antenna proposed in [92] for indoor wireless access point applications uses two perpendicular coplanar waveguide fed ports in order to excite two orthogonally polarized modes. Implemented antenna structure utilizes stepped cut at four corners (SCFC) technique which obtains required bandwidth by modifying the shape of radiating patch. Implemented antenna on FR-4 substrate achieves around 15dB interport isolation for 10dB impedance bandwidth of 900MHz to 2.7GHz. A 2.4GHz dual port microstrip antenna which uses external loop in order to achieve around 75dB port to port peak isolation has been presented in [93] for in band full duplex applications. Implemented antenna achieves more than 40dB interport isolation in 50MHz bandwidth.

Most of reported antenna works in literature as reviewed above are either narrow band structures or focus on MIMO antennas for UWB applications with lower cut-off frequency of 3.1GHz. Such antenna structures are unable to support MIMO applications with operating frequencies around 2.4GHz including 802.11b, 802.11g, 2.4GHz 802.11n, 2.5GHz WiMax and LTE technology). In this work, dual port monopole antenna based on single circular disc radiator has been designed and its parametric study has been carried out to obtain required impedance bandwidth of 2-6GHz and more than 15dB interport RF isolation. The implemented antenna supports 2GHz- 6GHz MIMO applications including 2.4GHz operating frequency. As the obtainable bandwidth for single element based MIMO antennas depends upon many factors including feeding techniques and size of partial ground plane but the shape and size of single radiating element plays a critical role in this regard [94]. Thus, wideband planar single element should be selected as it could be potential wideband MIMO antenna when fed through multiple ports. In this work, we have selected circular planar radiating element as it provides better impedance bandwidth [95]. The optimized dual port antenna has been implemented on 1.575mm thick RT/Duroid® 5880 substrate to validate the simulation results. Measured transmission coefficient (S_{12} or S_{21}) and calculated correlation coefficient have been used as two metrics to evaluate the interport RF isolation performance for intended

impedance bandwidth of 2-6GHz for implemented dual port single element circular disc monopole antenna.

As our dual port monopole antenna is based on single radiating element so first of all a single port circular disc monopole antenna has been designed and its performance is evaluated in order to implement dual port antenna by adding second port to single port antenna and interport coupling has been suppressed by modifying the partial ground plane. The structure of single port circular disc monopole antenna is shown in Fig.4.36 where r and L_g represent the radius of circular disc and width of ground plane respectively. The optimized values of these two parameters are obtained through HFSS simulations in order to obtain required input impedance performance of antenna.

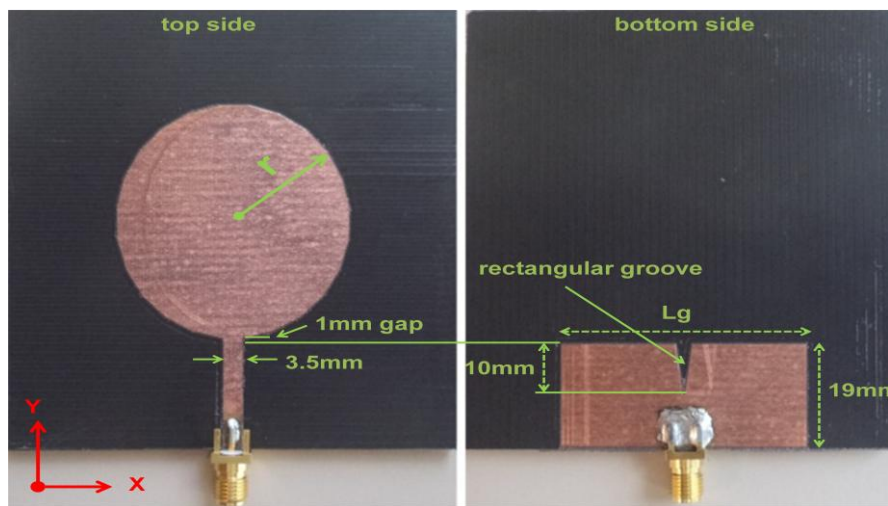


Figure 4.36: Single port circular disc monopole antenna with rectangular groove in partial ground plane

Circular disc is excited through 3.5mm wide and 20mm (50Ω) long microstrip line. The radius (r) of circular radiating element defines the lower cut-off frequency for antenna's 10dB impedance bandwidth [96] as endorsed by HFSS simulation results shown in Fig.4.37 for different value of radius (r) of circular disc radiating element. The lower cut-off frequency of antenna's 10dB bandwidth shifts from 1.766GHz to 2.258GHz when radius of circular disc is varied from 20mm to 14mm. The radius of circular radiating element is fixed to 20mm for our design in order to get lower frequency below 2GHz. A 3.5mm wide and 10mm deep rectangular groove has been placed exactly below the antenna feeding line to get extended 10dB input impedance bandwidth [97].

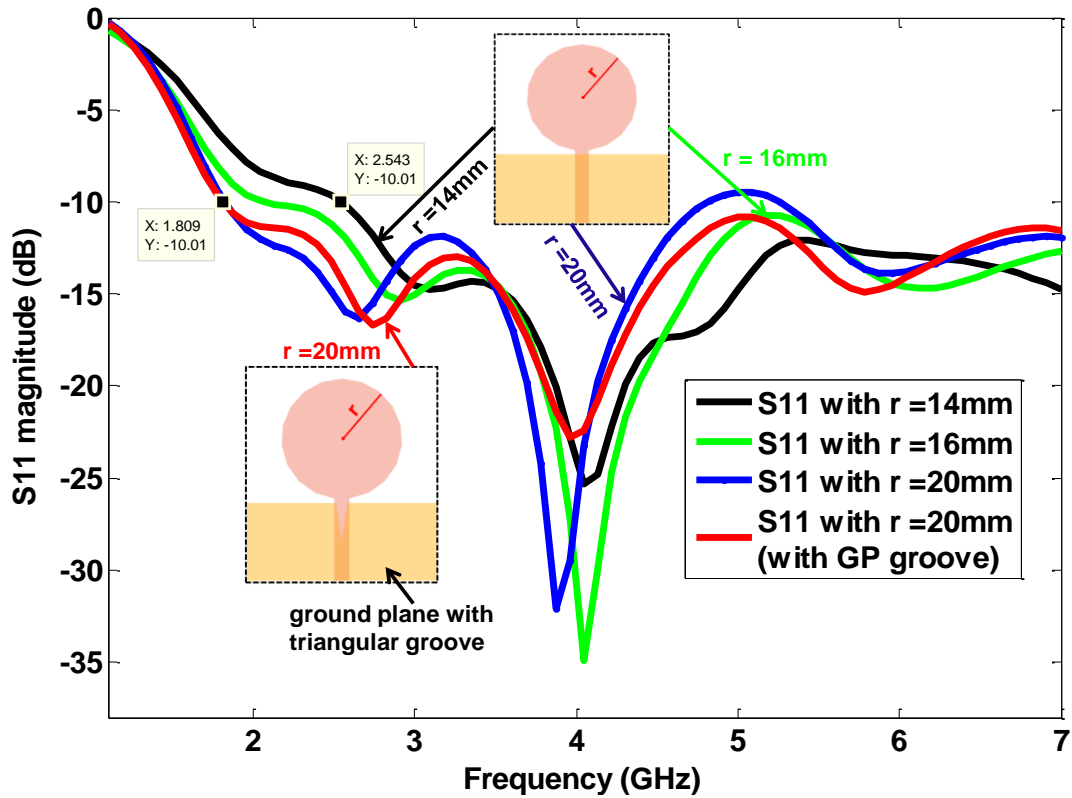


Figure 4.37: Simulated S11 variations with different values of circular disc radius (r)

The size of partial ground plane (L_g) also affects the impedance bandwidth of antenna in addition to spacing/gap between radiating element and ground plane. For our antenna, there is 1mm gap between ground plane and circular disc. Optimized ground plane dimensions are obtained by HFSS simulations for different values of ground plane's width (L_g) as shown in Fig.4.38. For smaller values of L_g , input matching of antenna deteriorates around 3GHz but it improves at higher frequencies starting from 4GHz as clearly visible from Fig.5.38 for $L_g=44$ mm. On the other hand, for larger values of L_g , antenna's matching degrades significantly in frequency range of 4-5GHz as clearly depicted for $L_g = 48$ mm. Thus, the optimized dimensions of partial ground plane are obtained as 19mmx44mm. The optimized antenna design has been implemented using 1.575mm thick RT/Duroid® 5880 substrate (with $\epsilon=2.2$, tangent loss =.001) as shown in Fig.4.36 with $r=20$ mm and $L_g=44$.

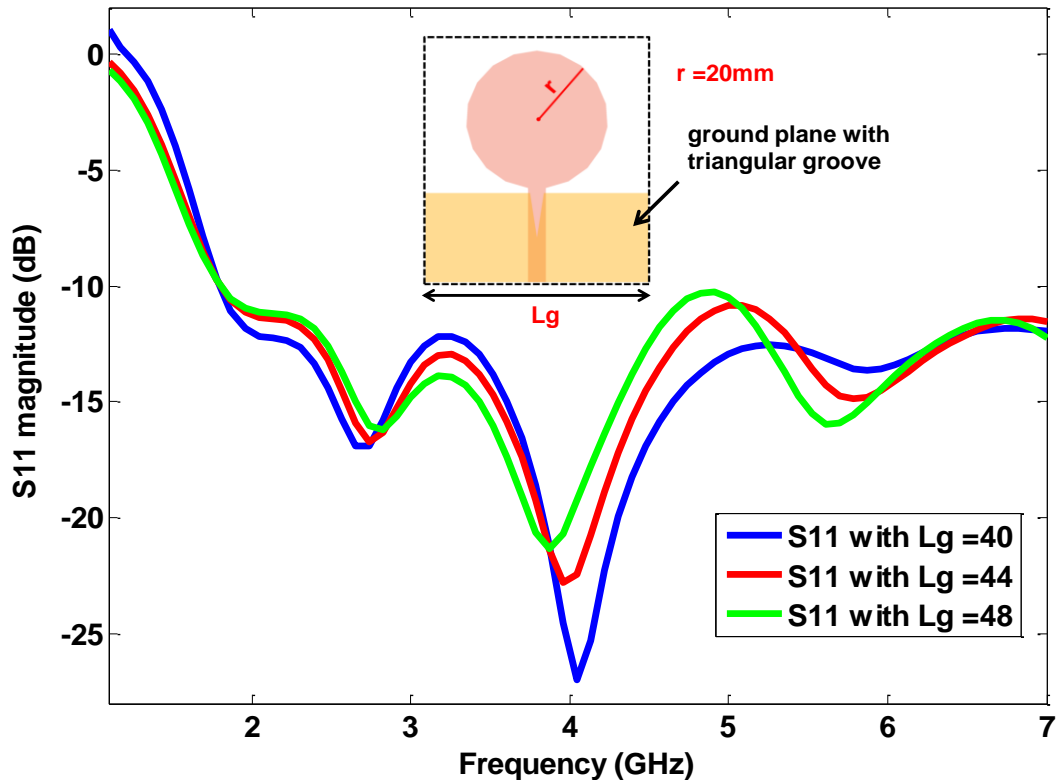


Figure 4.38: Simulated S11 for different values of ground plane width (L_g)

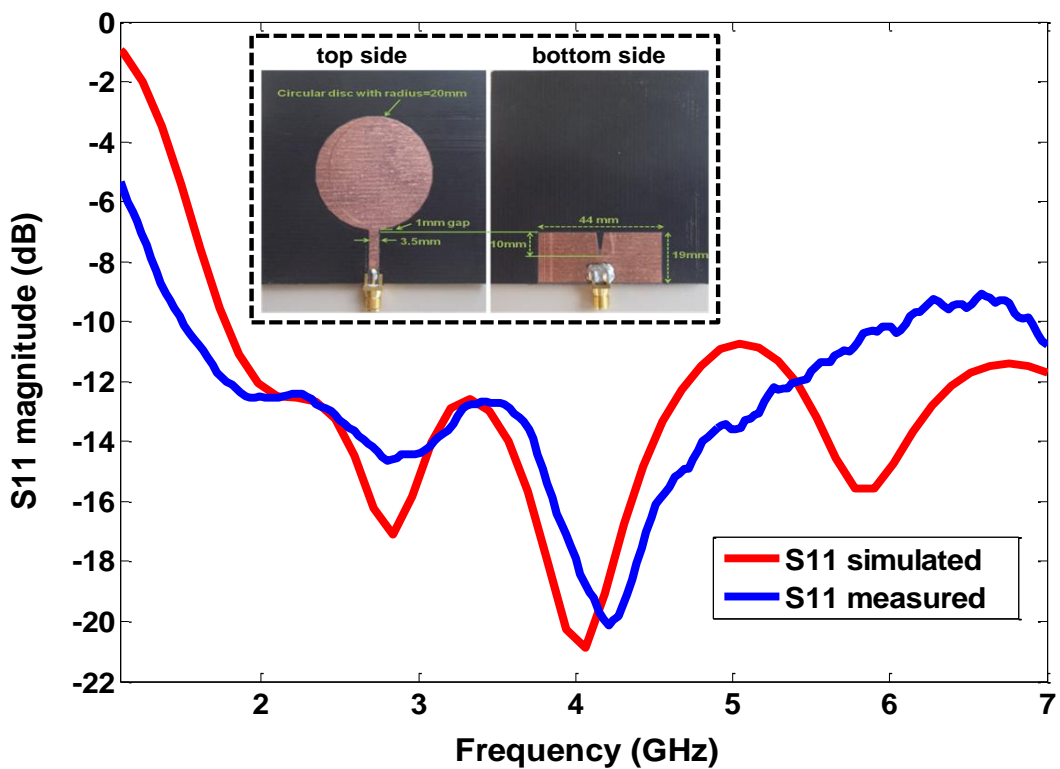


Figure 4.39: Simulated vs. measured S11 for implemented single port circular monopole antenna

HFSS simulation and measured input matching (S11) results for antenna implemented with optimized dimensions are shown in Fig.4.39. Measured 10dB impedance bandwidth for implemented single port circular disc antenna is 1.5GHz to 6GHz. HFSS simulated Peak Realized gain for Single port circular monopole antenna is also shown in Fig.4.40. The simulated gain varies between 3.5-6.6dBi in 2-6GHz frequency range.

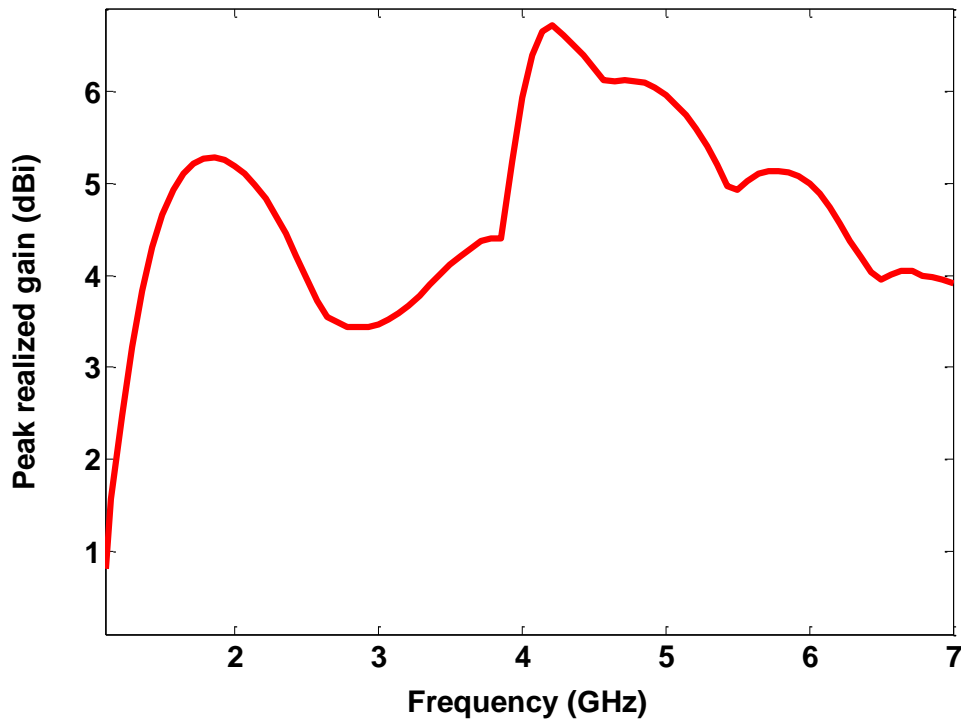


Figure 4.40: HFSS simulated peak realized gain for single port circular monopole antenna

The dual port circular monopole antenna design is based on single port circular monopole antenna prototype as stated earlier. As shown in Fig.4.41, the radius of circular radiating element is 20mm with 3.5mm wide and 20mm long feed line to excite the radiating element from each port. There is 1mm gap between ground plane and radiating element. A 3.5mm wide and 10mm deep rectangular groove is again placed exactly below the each feeding line of antenna to get extended 10dB input impedance bandwidth as is the case with single port monopole antenna prototype.

Additionally, a circular cut of radius R_c in ground plane has been etched to obstruct the currents path between the two ports to enhance the interport isolation. As shown in Fig.4.42

(b) by surface currents distributions, the mutual coupling is significantly reduced by circular cut etched in ground plane as compared to antenna structure without circular cut in ground plane shown in Fig.5.42 (a).

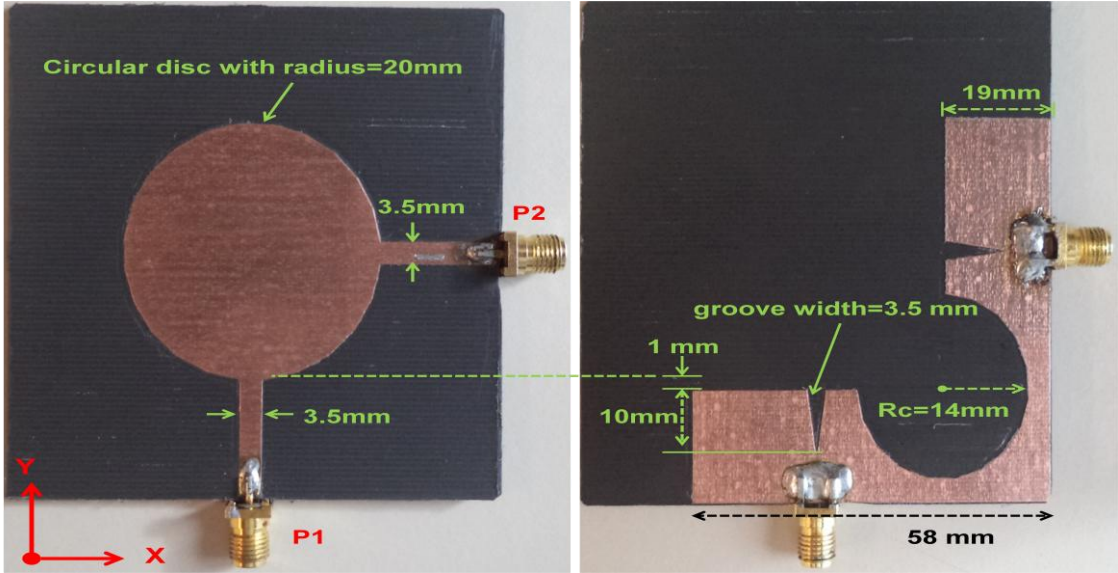


Figure 4.41: Dual port monopole antenna based on single circular disc element with circular cut of radius R_c in ground plane

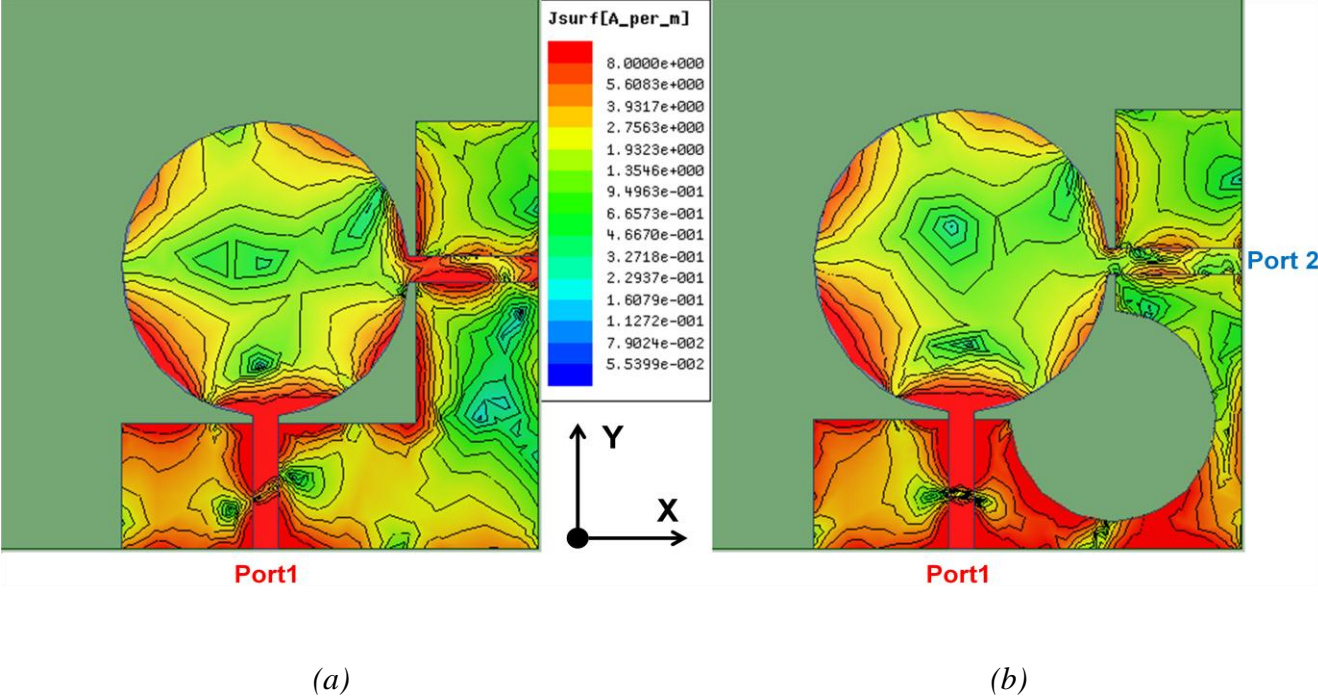
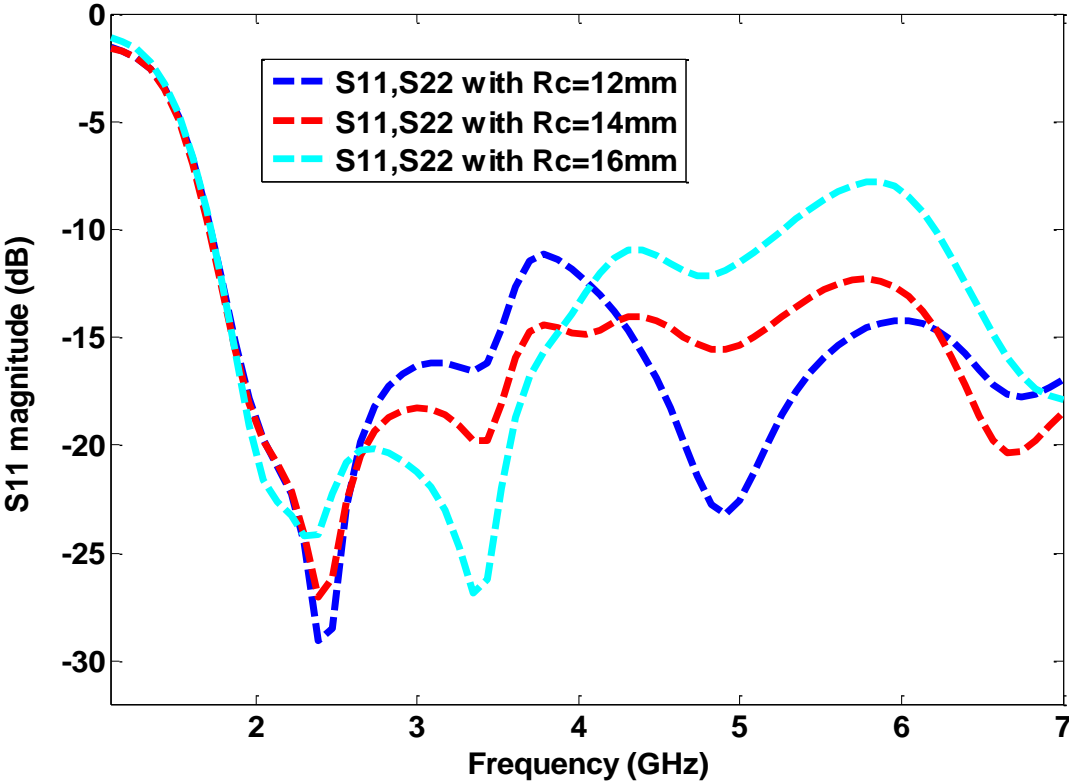
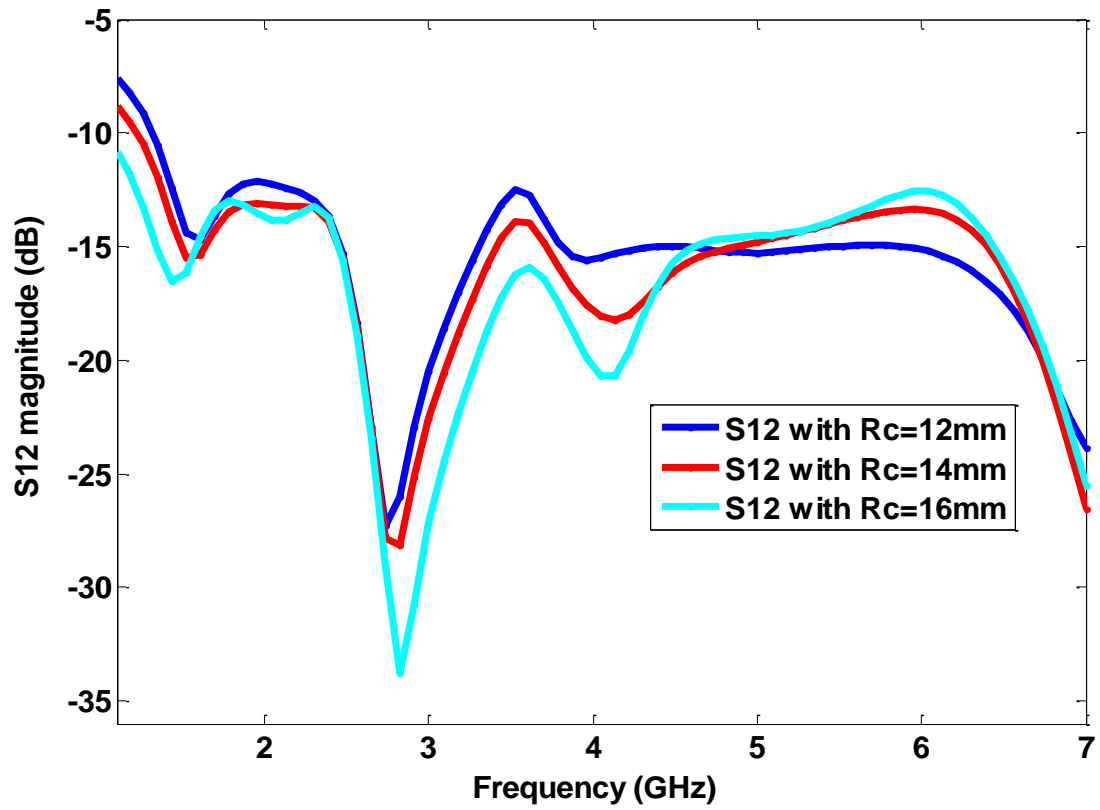


Figure 4.42: Current distributions for proposed dual port circular disc antenna at 6GHz with port 1 excitation (a) without circular cut (b)with $R_c=14\text{mm}$ circular cut in ground plane

The dimensions of ground plan slot (R_c) have been optimized by HFSS simulations to achieve improved port to port isolation (S_{12}) along with good antenna matching (S_{11}, S_{22}) for 2-6GHz operating frequency. HFSS S-Parameters simulation results for different values of R_c are shown in Fig.4.43. For smaller slot dimensions, both antenna matching and interport isolation is degraded near 3.5GHz as shown in Fig.4.43 for 12mm radius of circular slot. On the other hand for larger dimensions of slot in ground plane, the antenna matching and interport isolation degrades around 6GHz frequency as shown in Fig.4.43 for the case of $R_c=16$ mm. This is due to reduced ground plane size as already discussed for single port antenna. Although port to port isolation for this case is improved but the upper 10dB cut-off frequency is below 6GHz which is not acceptable for our required design. The circular slot with radius $R_c=14$ mm has been selected as optimized value for our implemented antenna as it achieves 2-6GHz 10dB antenna input impedance and interport isolation is better than 15dB for this case.



(a)



(b)

Figure 4.43: HFSS simulation results for (a) S11, S22 with different radius(Rc) of circular cut in ground plane (b) S12 with different Rc of circular cut in ground plane

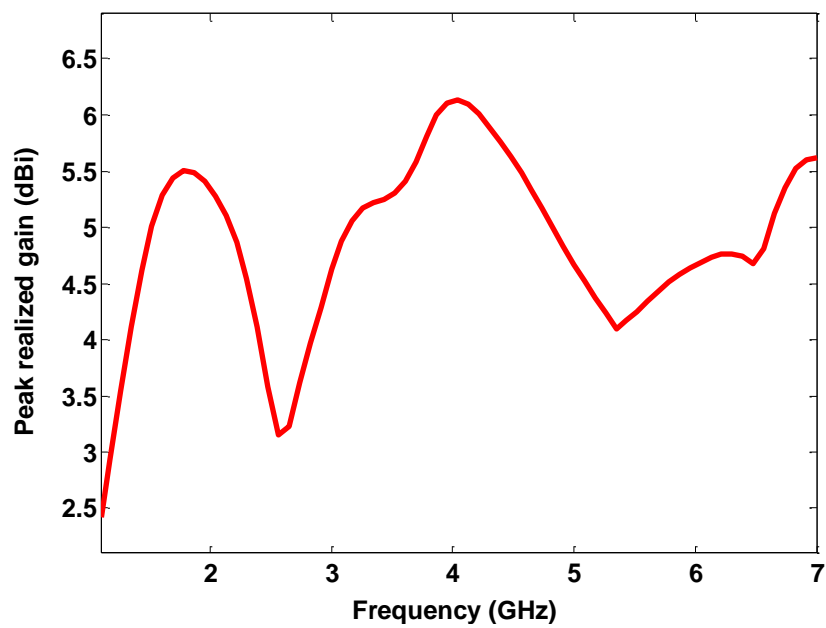


Figure 4.44: HFSS simulated peak realized gain for dual port single element circular monopole antenna

HFSS simulated peak realized gain for dual port circular disc monopole antenna is shown in Fig.5.44 for one port excitation and will be same for other port due to symmetrical feeding structure at both ports . The antenna gain varies between 3.2-6.1dBi in 2-6GHz operating frequency range.

Implemented dual port circular disc antenna with optimized antenna and ground plane dimensions is printed on 1.575mm thick RT5880 substrate (with $\epsilon=2.2$, tangent loss =.001) as shown in Fig.4.41 with $R_c=14$ mm. HFSS simulation and measured S_{11} , S_{22} and S_{12} results for implemented antenna are shown in Fig.4.45. The measured 10dB lower cut-off frequency of impedance bandwidth for each port starts from 1.7GHz and upper cut-off frequency extends to more than 7GHz upper cut-off frequency as clearly indicated in Fig.4.45 as 10dB impedance band width. Implemented dual port circular disc antenna provides around 15dB port to port isolation for 1.7-7GHz as marked by green dotted line on Fig.4.45. Thus, the compact implemented dual port antenna based on single circular disc radiator provides a good interport RF isolation over wide range of frequencies.

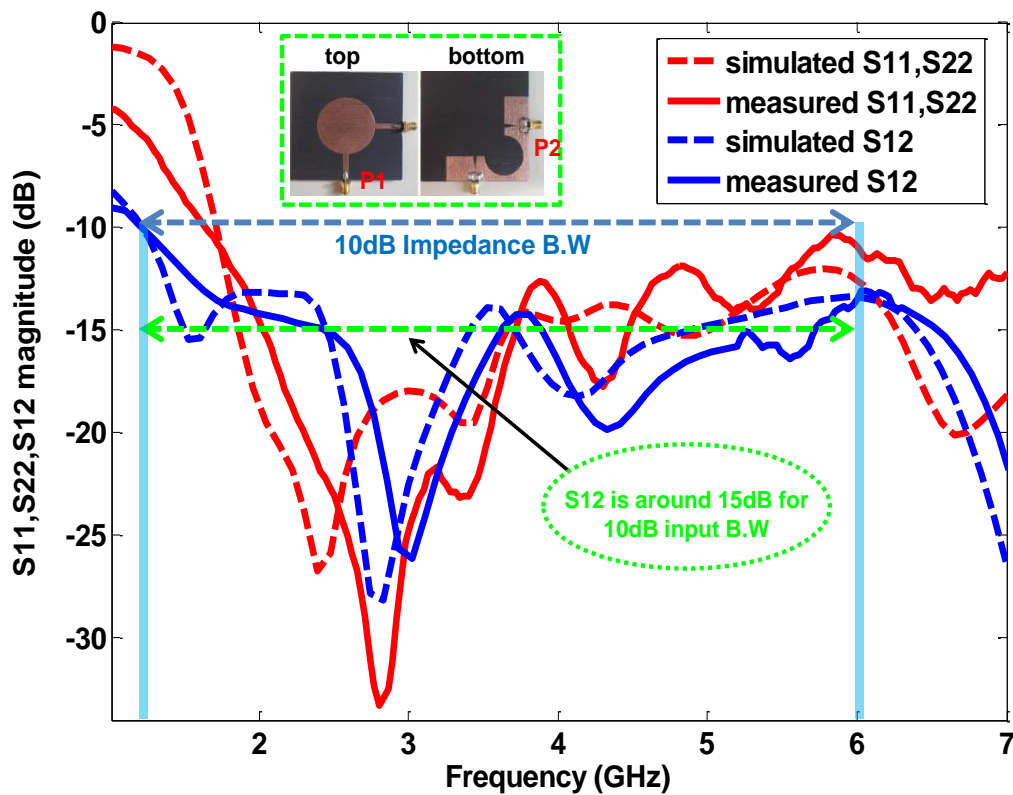


Figure 4.45: Simulated vs. measured S-Parameters for dual port monopole antenna printed on RT5880

Simulated and measured E-plane and H-plane gain patterns for implemented antenna at 3GHz, 4GHz, 5GHz and 6GHz frequencies are shown in Fig.4.46 for port 2 (P_2) excitation. Port 1 and Port 2 are along y-axis and x-axis respectively. Therefore for port 1 YZ and XZ represent E-plane and H-plane respectively while for port 2 XZ is E-Plane and YZ is H-plane respectively. The antenna deploys same feeding structure to excite the radiating element from other port and measured input matching for second port has also similar characteristics as clear from Fig.4.45 so excitation from other port will provide similar but orthogonal radiation patterns.

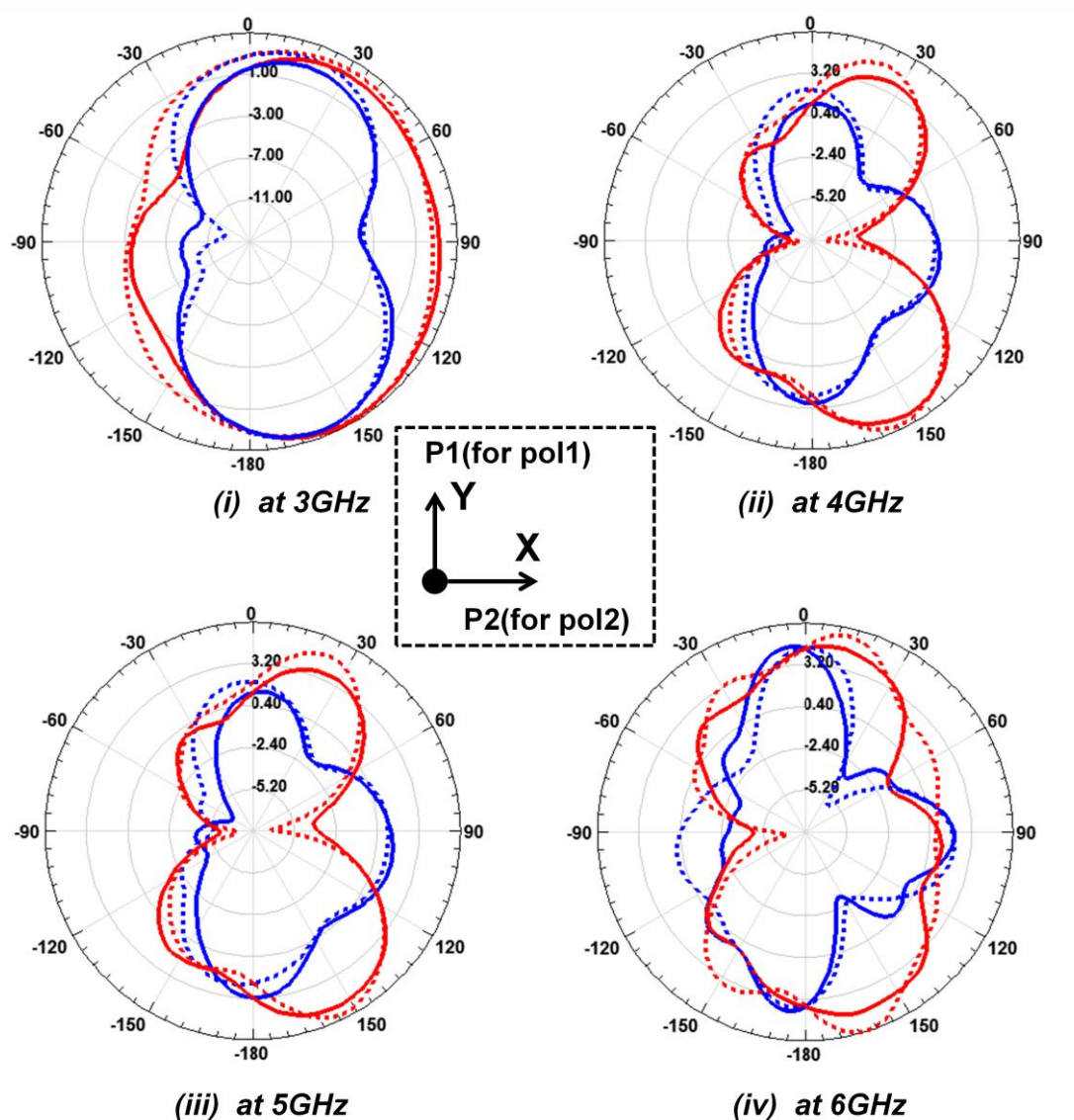


Figure 4.46: Simulated (dotted lines) vs. measured (solid lines) E-Plane (red lines) and H-plane (blue lines) gain patterns of dual port antenna at 3GHz, 4GHz, 5GHz and 6GHz for port 1 excitation

Envelope correlation coefficient is another metric or indicator for performance evaluation of multiport antennas used for MIMO applications. The value of envelope correlation coefficient for multiport antennas should be as low as possible to ensure minimum port to port mutual coupling for MIMO antenna operation. Envelope correlation coefficient can be directly determined from far-field patterns but it can be computed using S-parameters results using equation (4.1) as given in [98]:

$$|\rho_e| = \frac{|s_{11}^*s_{12} + s_{21}^*s_{22}|^2}{(1 - (|s_{11}|^2 + |s_{21}|^2))(1 - (|s_{22}|^2 + |s_{12}|^2))} \quad (4.1)$$

Acceptable antenna correlation for reliable MIMO performance is reported to be <0.5 [66].

Simulated and measured correlation coefficients computed by simulated and measured S-parameters respectively are shown in Fig. 4.47. The measured value of envelope correlation coefficient for our antenna is less than 0.02 over required impedance bandwidth which ensures that implemented dual port antenna can be effectively used for MIMO applications over 2-6GHz frequency range.

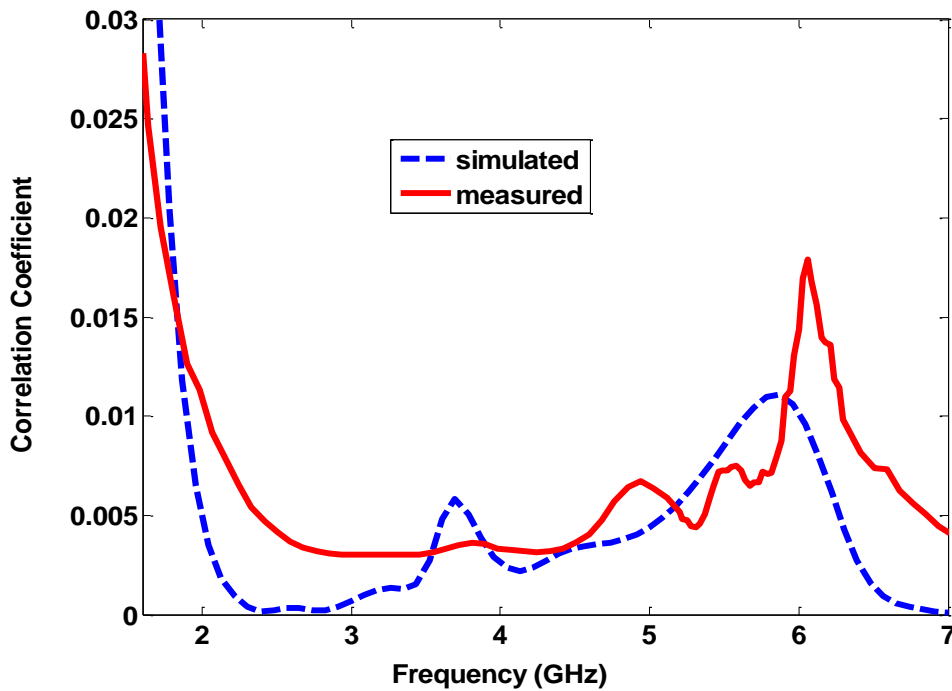


Figure 4.47: Simulated and measured correlation coefficient for dual port single element monopole antenna

A compact (64mmx64mm) dual port monopole antenna based on single circular disc radiating element has been proposed and implemented for 2-6GHz MIMO applications. Implemented antenna provides more than 15dB port to port RF isolation in target 10-dB impedance bandwidth of 2-6GHz along with good radiation characteristics. Measured and simulated S- parameter, gain patterns and correlation coefficients results are in good agreement for proposed and implemented antenna. The implemented dual port antenna can be effectively used for 2-6GHz MIMO applications based on its nice interport isolation which was also endorsed by correlation coefficients computed by measured S-parameters.

4.13 Interport RF isolation versus impedance bandwidth of dual port, dual polarized microstrip patch antennas

Dual port, dual linear polarized microstrip patch antennas with high interport isolation can be effectively used for In Band Full Duplex (IBFD) wireless operation in order to improve the spectral efficiency of communication systems [99-100]. For IBFD transceivers which use shared antenna for full duplex operation at same carrier frequency, single antenna with high interport isolation is normally implemented by using dual port, dual polarized microstrip patch antenna with some self interference (SI) suppression mechanism (to cancel RF leakage from transmit to receive port) [58] because more and more SI cancellation is at antenna stage to effectively suppress interference at analog and digital stages for realization of full duplex operation at same radio frequency [101].

The effect of antenna's impedance bandwidth on interport isolation has been investigated for dual port, dual linear polarized square microstrip antenna which deploys symmetrical feeding structure on two orthogonal ports on respective edges of patch. Three microstrip patch antennas with different operating frequencies (1GHz, 2.4GHz and 5.1GHz) and one 2.4GHz proximity coupled patch antenna have been investigated to show that peak interport isolation is reduced by additional surface currents generated in both cases. Input impedance matching (S_{11}, S_{22}) and interport isolation (S_{12}) measurement results for 1GHz and 2.4GHz patch antennas printed on 1.6mm thick FR-4 substrate along with 2.4GHz proximity coupled antenna fabricated using double layer FR-4 dielectric are presented to endorse simulation results.

Dual linear (horizontal and vertical) polarized microstrip patch antenna can be designed by exciting a square patch from two orthogonal ports as shown in Fig.5.48 for dual port single layer antenna which deploys quarter wave microstrip lines for impedance matching and patch excitation from respective ports. This configuration excites TM_{01} and TM_{10} orthogonal modes to produce horizontal and vertical polarized electric field [102] as clearly shown in Fig.4.48 for each port excitation.

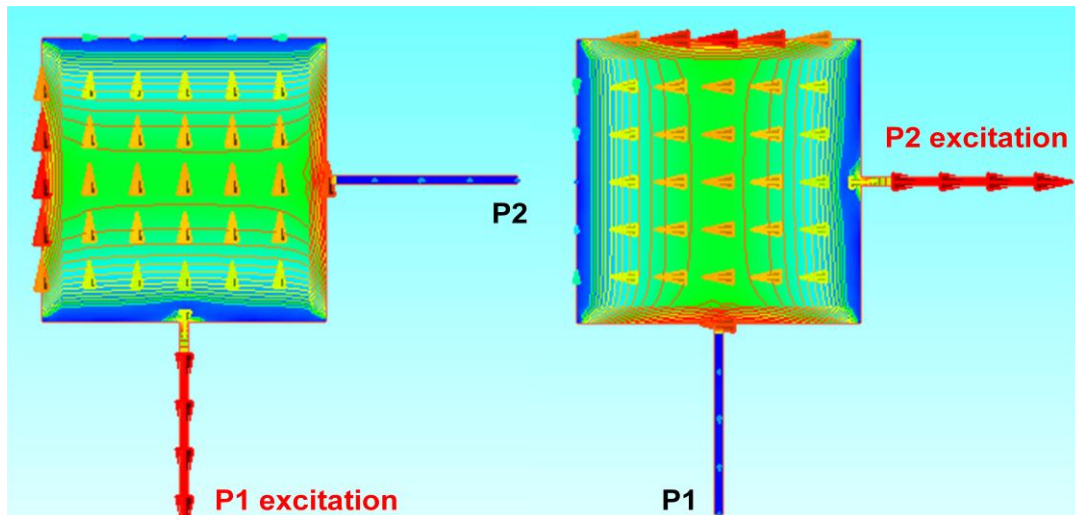


Figure 4.48: Single layer, dual polarized 2.4GHz microstrip patch antenna

The maximum interport isolation at required operating/resonant frequency is obtained when each port excites the patch from centre of respective edge [58],[102] as TM_{11} mode is not excited for this case although other higher order modes still exist [102].As shown in Fig.4.49 and recorded in Table 4.1 for 2.4GHz single layer dual port antenna, peak isolation shifts away from required operating frequency when feeding location of port2 is moved towards right (distance 's' as referred in Fig.5.49) due to unnecessary TM_{11} mode excitation in addition to required TM_{01} and TM_{10} exciting modes of radiating patch.

Microstrip patch antenna has very narrow impedance bandwidth and depends on my many factors including operating frequency, thickness of substrate and feeding structure for planar microstrip patch antennas [103]. For simple single layer dual port, dual polarized microstrip patch antenna with symmetrical feeding structure for each port, antenna's impedance bandwidth directly effects the maximum obtainable peak interport isolation

(S_{12}).Mathematical relation for inter-port isolation (S_{12}) for dual port microstrip patch antenna is given as[104]:

$$S_{12} = \frac{2Z_{12}Z_0}{(Z_{11}+Z_0)(Z_{22}+Z_0)-Z_{12}Z_{21}} \quad (4.2)$$

where Z_0 is the characteristic impedance of feeding microstrip line

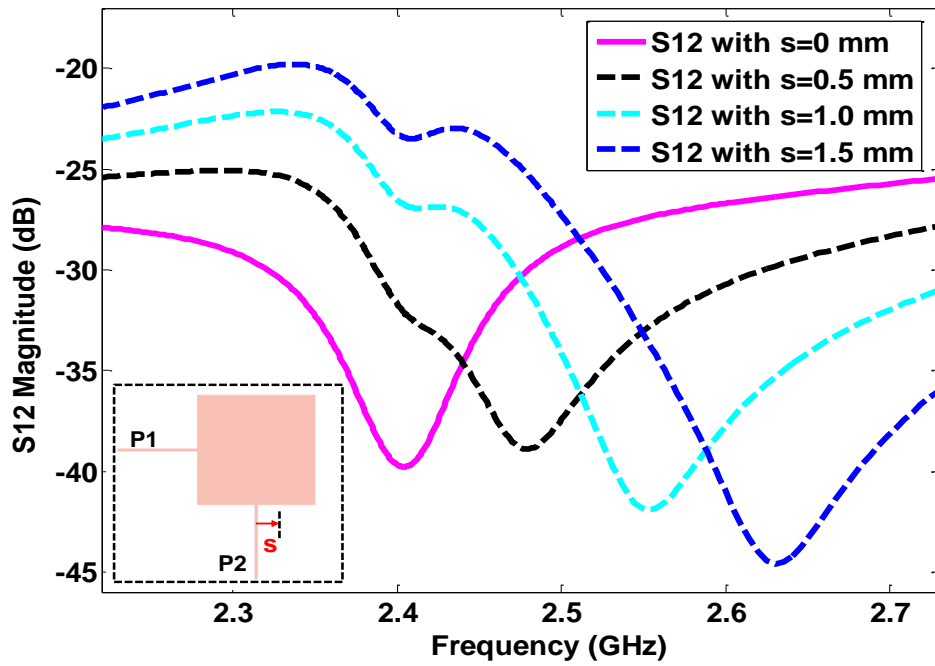


Figure 4.49: Peak isolation frequency variations vs. port 2 feeding location

Table 4.1: Peak isolation and frequency vs. port 2 feeding location

Offset distance (s)	0 mm	0.5 mm	1mm	1.5 mm
Peak isolation (dB)	39.8	38.9	41.9	44.5
Frequency (GHz)	2.406	2.48	2.55	2.63

For our investigation, impedance bandwidth of patch antenna has been increased by increasing operating frequency and using proximity coupling instead of single layer feeding to investigate the effect of impedance bandwidth on interport isolation of dual polarized patch antenna with two orthogonal feeds. It has been observed that peak isolation reduces in both cases due to additional surface currents when either operating frequency or substrate thickness is increased [105].

S12 vs. impedance bandwidth of single layer antennas: Input impedance bandwidth of microstrip patch antenna directly depends upon operating frequency as it is normally recorded as fraction/percentage of centre frequency. Patch antenna with higher working frequency provides more impedance bandwidth for given substrate's parameters. Three microstrip patch antennas working at 1GHz, 2.4GHz and 5.1GHz centre frequencies have designed and simulated for required analysis. Both 1GHz and 2.4GHz antennas have been implemented on 1.6mm thick FR-4 substrate ($\epsilon = 4.4$, tangent loss = .02) to verify simulation results.

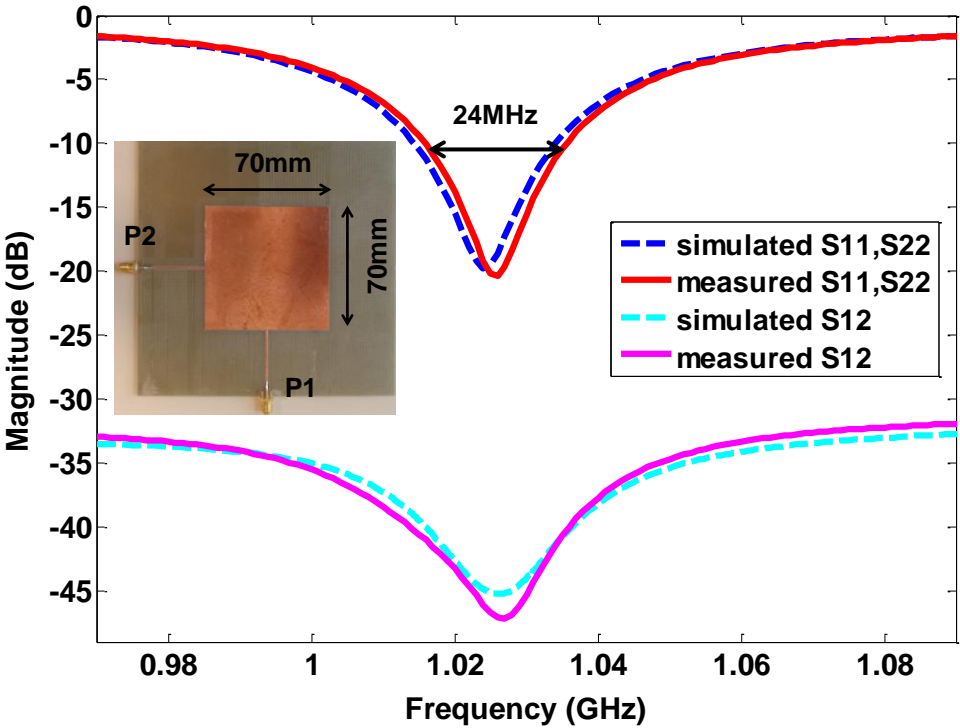


Figure 4.50: Simulated and measured S- parameters for dual polarized 1GHz microstrip patch antenna

Measured and simulated input matching and interport isolation results for 1GHz and 2.4GHz patch antennas printed on 1.6mm thick FR-4 substrate are shown in Fig.4.50 and Fig.4.51 respectively. Measured 10dB impedance band widths are 24MHz and 54MHz while peak interport isolations are around 47dB and 42dB for 1GHz and 2.4GHz microstrip patch antennas respectively. Thus, dual port, dual polarized patch antenna with narrow impedance bandwidth (24MHz for 1GHz antenna) has more peak interport as compared to that with more impedance bandwidth (54MHz for 2.4GHz antenna).ADS momentum simulation results for 5.1GHz antenna shown in Fig.4.52 also endorse this fact where 5.1GHz has more impedance bandwidth (126MHz) but peak interport isolation is reduced to less than 35dB as compared to 45dB peak interport isolation for 1GHz antenna.

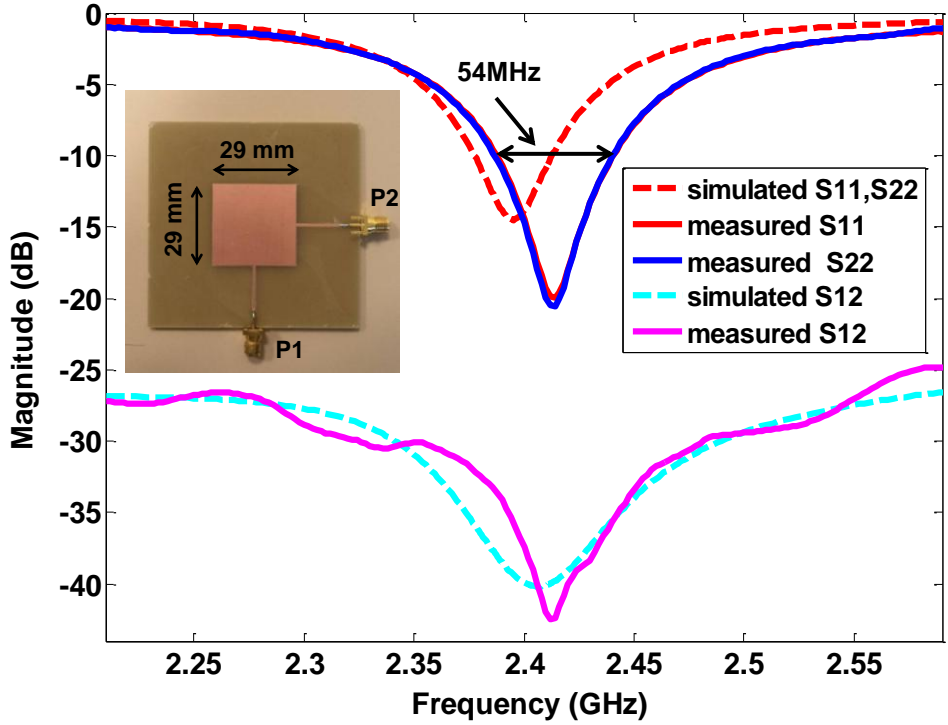


Figure 4.51: Simulated and measured S11, S22 and S12 parameters for dual polarized 2.4GHz microstrip patch antenna

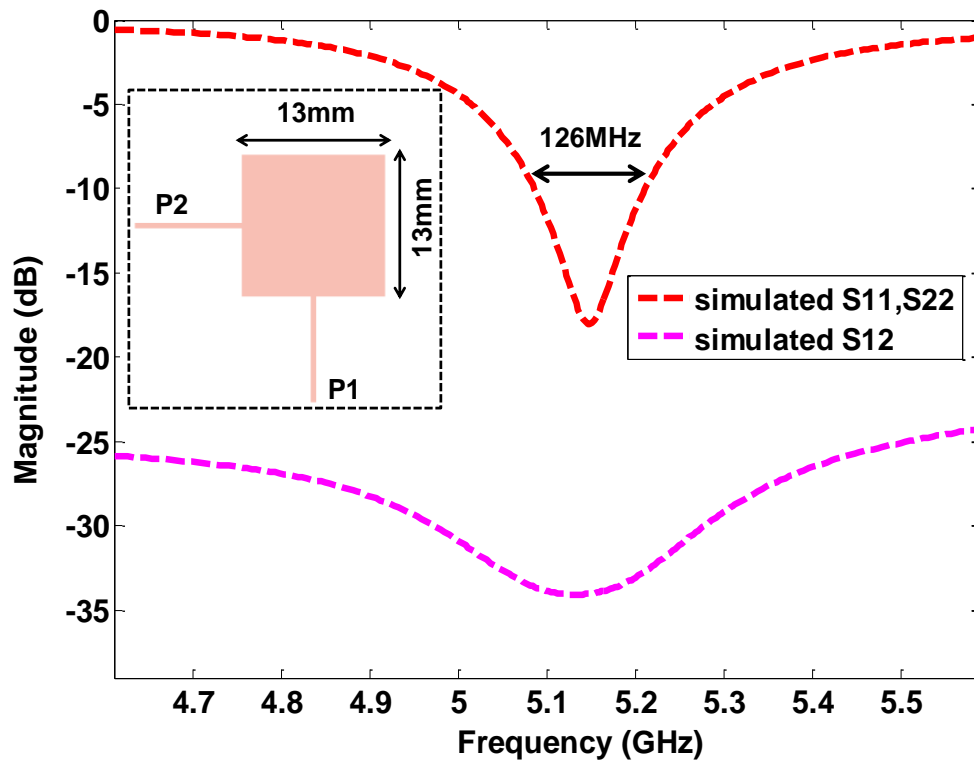


Figure 4.52: Simulated S11, S22 and S12 for dual polarized 5.1GHz antenna

2.4GHz dual polarized proximity coupled patch antenna: Proximity coupled patch antenna provides more impedance bandwidth as compared to single layer antenna [106]. Implemented dual polarized proximity-coupled patch deploys two orthogonal ports for dual polarization and each mode is excited by EM coupling through microstrip feed line printed on bottom substrate [106]. Measured input matching (S11, S22) and interport RF isolation (S12) characteristics for implemented 2.4GHz dual polarized proximity coupled antenna are shown in Fig.4.53. Measured 10dB impedance bandwidth is 87MHz for both ports while measured peak RF interport isolation is reduced to less than 35dB in this case as compared to 42dB peak isolation provided by 2.4GHz single layer antenna with 54MHz impedance bandwidth.

This analysis concludes that peak Interport RF isolation of dual port, patch antenna is reduced by unnecessary surface currents which are generated when high operating frequency or thick substrate is used to obtain improved impedance bandwidth.

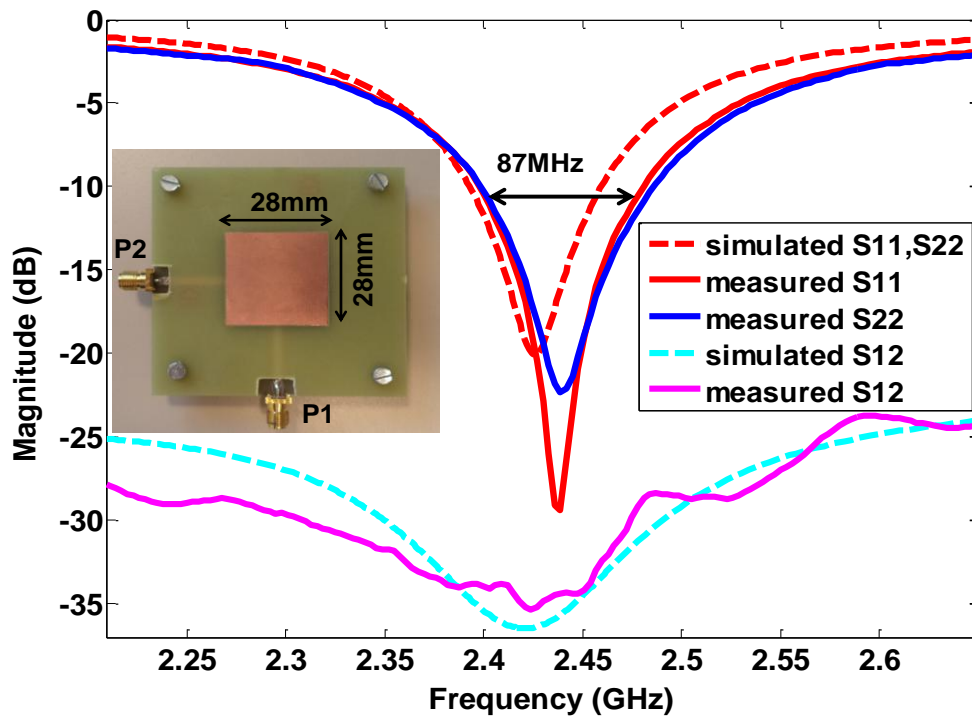


Figure 4.53: Measured input matching (S11, S22) and port isolation (S12) for implemented dual polarized 2.4GHz proximity coupled patch antenna

Conclusion and Future work

In this dissertation, the design simulation and hardware implementation details along with test and measurement results for proposed dual port, dual polarized microstrip antennas for single antenna based 2.4GHz wireless transceivers are presented. The design and simulations of proposed antennas have been carried out in following phases:

- (i) Study of various feeding techniques for microstrip patch antennas which can achieve high interport isolation without antenna performance degradation
- (ii) ADS Momentum simulations of proposed multi ports antennas with selected feeding techniques
- (iii) ADS Momentum simulations of optimized designed antennas with SIC circuits to get dual port antenna with additional high interport isolation.

Coplanar microstrip and aperture coupled feeding techniques have been mainly used along with simple 3-dB ring hybrid coupler as SIC circuit to design dual port antenna with high interport isolation for use in IBFD transceiver with single/shared antenna architecture.

Then, the implementation and performance evaluation details of fabricated In Band Full Duplex (IBFD) planar antennas are discussed. The design, simulation, implementation details and measurement results of several dual ports, dual polarized microstrip antennas are presented with their performance evaluation in terms of interport isolation measurements. Dual polarized microstrip patch antenna with different feeding mechanism along with SIC circuits have been implemented to achieve high interport isolation without antenna performance degradation. Around 70dB interport isolation for 50MHz bandwidth has been obtained for three ports antenna with external SIC circuit. Three ports slot coupled antenna with external SIC circuit provides more than 80dB isolation at centre frequency and around 75dB port to port isolation for antenna's 10dB impedance bandwidth of 50MHz. Dual port circular disc MIMO antenna has also been investigated and implemented for wide band applications. More than 15dB interport isolation has been measured over 2-6GHz frequency band for implemented dual port circular disc MIMO antenna.

As discussed earlier, peak Interport RF isolation of dual port, patch antenna is reduced by unnecessary surface currents which are generated when high operating frequency or thick substrate is used to obtain improved impedance bandwidth. As a future work, dual port single antenna with improved impedance bandwidth along with high port to port isolation can be investigated. For such antennas, use of electromagnetic band-gap (EBG) materials is one way to improve port to port RF isolation even with improved impedance bandwidth as is the case with proximity coupled antennas. Microstrip patch antenna design with such materials can reduce these additional surface currents generated by high operating frequency and antenna printed on thick substrate and increase port to port RF coupling for dual port patch antenna.

In future, we will investigate the real time performance of our implemented antennas by interfacing them with WARP (Wireless Open Access Research Platform) board to realize an In-Band Full Duplex (IBFD) wireless transceiver for 2.4GHz wireless communication operation. WARP (Wireless Open Access Research Platform) is a programmable wireless platform to prototype advanced custom wireless designs using two flexible RF interfaces and multiple peripherals [107]. For this realization, digital domain self interference cancellation techniques are also being investigated by other group members of our Lab. Our goal is to implement a real time 2.4GHz In-Band Full Duplex (IBFD) system using our implemented antenna in conjunction with digital self interference cancellation techniques.

REFERENCES

- [1] Yun Liao, Lingyang Song and Zhu Han, "Full-Duplex Wireless Communication and Networks: Key Technologies and Applications," IEEE International Conference on Communications in China (ICCC 2014), Shanghai, China, Oct. 2014.
- [2] Ashutosh Sabharwal, Philip Schniter, Dongning Guo, Daniel W. Bliss, Sampath Rangarajan, and Risto Wichman, "In-band Full-duplex Wireless: Challenges and Opportunities" IEEE Journal on Selected Areas in Communications, Special Issue on In-Band Full-Duplex Wireless Communications and Networks, vol. 31, no. 9, pp. 1637-1652, Sep. 2014.
- [3] A. Goldsmith. Wireless Communications. Cambridge University Press, New York, NY, USA, 2005.
- [4] A. Otyakmaz, R. Schoenen, S. Dreier, B.H. Walke, "Parallel operation of half- and full-duplex FDD in future multi-hop mobile radio networks," 14th European Wireless Conference, June 2008. pp. 1 - 7.
- [5] B. Debaillie et al., "Analog/RF solutions enabling compact full-duplex radios," IEEE J. Sel. Areas Commun., vol. 32, pp. 1662-1673, 2014.
- [6] D. W. Bliss, P. A. Parker, and A. R. Margetts. Simultaneous transmission and reception for improved wireless network performance. In Proceedings of the 2007 IEEE Workshop on Statistical Signal Processing, 2007.
- [7] M. Duarte and A. Sabharwal. Full-duplex wireless communications using off-the-shelf radios: Feasibility and first results. In Forty-Fourth Asilomar Conference on Signals, Systems, and Components, 2010.
- [8] E. Everett, M. Duarte, C. Dick, and A. Sabharwal. Empowering full-duplex wireless communication by exploiting directional diversity. In Signals, Systems and Computers (ASILOMAR), 2011 Conference Record of the Forty Fifth Asilomar Conference on, pages 2002–2006, Nov. 2011.
- [9] M. Jain, J. I. Choi, T. Kim, D. Bharadia, S. Seth, K. Srinivasan, P. Levis, S. Katti, and P. Sinha. Practical, real-time, full duplex wireless. MobiCom '11, pages 301–312, New York, NY, USA, 2011. ACM.
- [10] B. Radunovic, D. Gunawardena, P. Key, A. Proutiere, N. Singh, V. Balan, and G. Dejean. Rethinking indoor wireless mesh design: Low power, low frequency, full-duplex. In Wireless Mesh Networks (WIMESH 2010), 2010 Fifth IEEE Workshop on, pages 1–6, 2010.
- [11] J. I. Choi, M. Jain, K. Srinivasan, P. Levis, and S. Katti. "Achieving single channel, full duplex wireless communication,". In Proceedings of the sixteenth annual international conference on Mobile computing and networking, MobiCom '10, pages 1–12, New York, NY, USA, 2010.

- [12] D. Bharadia, E. McMillin, and S. Katti, "Full Duplex Radios," ACM SIGCOMM 2013, Hong Kong, 2013.
- [13] T. Lee. The Design of CMOS Radio-Frequency Integrated Circuits. Cambridge University Press, 2004.
- [14] Rohde & Schwarz. Rohde & Schwarz FSW Signal and Spectrum Analyzer User Manual, 2012.
- [15] Ahmed, E.; Eltawil, A.M.; Sabharwal, A., "Rate Gain Region and Design Tradeoffs for Full-Duplex Wireless Communications," in *Wireless Communications*, IEEE Transactions on , vol.12, no.7, pp.3556-3565, July 2013
- [16] A. Sahai, G. Patel, C. Dick, and A. Sabharwal, "Understanding the impact of phase noise on active cancellation in wireless full-duplex," in *Proceedings of Asilomar Conference on Signals, Systems and Computers*, 2012.
- [17] A.Sahai, G. Patel, and A. Sabharwal, "Pushing the limits of full-duplex: Design and real-time implementation, <http://arxiv.org/abs/1107.0607>," in *Rice University Technical Report TREE1104*, June 2011.
- [18] M. A. Khojastepour, K. Sundaresan, S. Rangarajan, X. Zhang, and S. Barghi, "The case for antenna cancellation for scalable full-duplex wireless communications," in *Proceedings of the 10th ACM Workshop on HotNets*, 2011
- [19] E. Everett, "Full-duplex infrastructure nodes: Achieving long range with half-duplex mobiles," Master's thesis, Rice University, 2012.
- [20] A. Sendonaris, E. Erkip, and B. Aazhang, "User cooperation diversity part I: System description," *IEEE Trans. Comm.*, vol. 51, no. 11, pp. 1927–1938, Nov. 2003.
- [21] J. N. Laneman, D. N. C. Tse, and G. W. Wornell, "Cooperative diversity in wireless networks: Efficient protocols and outage behavior," *IEEE Trans. Inform. Theory*, vol. 50, no. 12, pp. 3062–3080, Dec. 2004.
- [22] H. Kang and S. Lim, "High Isolation Transmitter and Receiver Antennas Using High-Impedance Surfaces for Repeater Applications," *J. Electromagnetic Waves and Applications*, vol. 27, no. 18, 2013, pp. 2281–87.
- [23] D. Korpi et al., "Advanced Self-Interference Cancellation and Multi-antenna Techniques for Full-Duplex Radios," 2013 Asilomar Conf. Signals, Systems and Computers, 3–6, Nov. 2013, pp. 2281–87.
- [24] P. Lindberg and E. Ojefors, "A Bandwidth Enhancement Technique for Mobile Handset Antennas Using Wave traps," *IEEE Trans. Antennas and Propagation*, vol. 54, no. 8, Aug. 2006, pp. 2226–33.
- [25] M. Karaboikis et al., "Compact Dual-Printed Inverted-F Antenna Diversity Systems for Portable Wireless Devices," *IEEE Antennas and Wireless Propagation Letters*, vol. 3, no. 1, pp. 9–14, 2004.2

- [26] S. Venkatasubramanian et al., "Impact of Neutralization on Isolation in Co-Planar and Back-to-Back Antennas," Proc. 9th Euro. Conf. Antennas and Propagation, Lisbon, Portugal, Apr.2015.
- [27] S. Venkatasubramanian et al., "On the Constraints to Isolation Improvement in Multi-Antenna Systems," Proc. 9th Euro. Conf. Antennas and Propagation, Lisbon, Portugal, Apr. 2015.
- [28] W.-K. Kim, M.-Q. Lee, J.-H. Kim, H.-s. Lim, J.-W. Yu, B.-J. Jang, and J.-S. Park, "A passive circulator for RFID application with high isolation using a directional coupler," in 36th European Microwave Conference, pp. 196–199, IEEE, 2006.
- [29] M. E. Knox, "Single antenna full duplex communications using a common carrier," in IEEE 13th Annual Wireless and Microwave Technology Conference, pp.1–6, 2012.
- [30] Xie, J.J., Yin, Y.Z., Wang, J.H., Liu, X.L.: 'Wideband dual-polarized electromagnetic fed patch antenna with high isolation and low cross-polarization', Electron. Lett., 2013, 49, (3), pp. 171–173
- [31] Luo, K., Ding, W., Hu, Y., Cao, W.: 'Design of dual-feed dual-polarized microstrip antenna with high isolation and low cross polarization', Prog. Electromagn. Res.Lett., 2013, 36, pp. 31–40
- [32] Everett, E.; Sahai, A.; Sabharwal, A., "Passive Self-Interference Suppression for Full-Duplex Infrastructure Nodes," in Wireless Communications, IEEE Transactions on , vol.13, no.2, pp.680-694, February 2014
- [33] A. K. Khandani, "Shaping the future of wireless: Two-way connectivity." <http://www.nortel-institute.uwaterloo.ca/content/Shaping> Future of Wireless Two-way Connectivity 18ne2012.pdf, June 2012.
- [34] E. Aryafar, M. Khojastepour, K. Sundaresan, S. Rangarajan, and M. Chiang, "MIDU: Enabling MIMO full duplex," in Proceedings of ACM MobiCom, 2012.
- [35] M. Duarte and A. Sabharwal, "Full-duplex wireless communications using off-the-shelf radios: Feasibility and first results," in Proc. 44th Asilomar Conference on Signals, Systems, and Computers, Nov. 2010.
- [36] M. Jain, J. I. Choi, T. Kim, D. Bharadia, S. Seth, K. Srinivasan, P. Levis, S. Katti, and P. Sinha, "Practical, real-time, full duplex wireless," in Proc. 17th Annual International Conference on Mobile computing and Networking, 2011, pp. 301–312.
- [37] D. W. Bliss, P. A. Parker, and A. R. Margetts, "Simultaneous transmission and reception for improved wireless network performance," in Proceedings of the 2007 IEEE/SP 14th Workshop on Statistical Signal Processing. Washington, DC, USA: IEEE Computer Society, 2007, pp.478–482.
- [38] Knox, Michael E. "Single antenna full duplex communications using a common carrier." Wireless and Microwave Technology Conference (WAMICON), 2012 IEEE 13th Annual. IEEE, 2012.
- [39] Y. Rikuta ,H.Arai. "A Self-Diplexing Antenna Using Slitted Patch Antenna" in Proceedings of the International Symposium on Antennas and Propagation Japan; 2002.

- [40] Ruina Lian; Shufeng Zheng; Ying-Zeng Yin; Jianjun Wu; Shaoshuai Zhang; Guan-Xi Zhang “A Single-Layer Wideband Dual-Polarized Antenna with High Isolation” Progress in Electromagnetic Research C;2014, Vol. 49, p115, May 2014
- [41] M. Steer, Microwave and RF engineering: A systems approach. Scitech Publishing Inc., 2010.
- [42] A. G. Stove, “Linear FMCW radar techniques,” IEE Proceedings F (Radar and Signal Processing), vol. 139, no. 5, pp. 343–350,1992.
- [43] J. G. Kim, S. Ko, S. Jeon, J. W. Park, and S. Hong, “Balanced topology to cancel Tx leakage in CW radar,” IEEE Microwave and Wireless Components Letters, vol. 14, Sept. 2004.
- [44] C.-Y. Kim, J.-G. Kim, and S. Hong, “A quadrature radar topology with TX leakage canceller for 24-GHz radar applications,” IEEE Transactions on Microwave Theory and Techniques, vol. 55, no. 7, pp. 1438 1444, 2007.
- [45] K. Lin, R. Messerian, and Y. Wang, “A digital leakage cancellation scheme for monostatic FMCW radar,” in Microwave Symposium Digest, 2004 IEEE MTT-S International, vol. 2, pp. 747–750 Vol.2, 2004.
- [46] Sharp E. D. and Diab M. A., “Van Atta reflector array”, IRE trans. on Antenna and Propagation”, vol.AP-8, pp, 436-438.
- [47] Karode, S.L.; Fusco, V.F., "Self-tracking duplex communication link using integrated retrodirective antennas," in Microwave Symposium Digest, 1998 IEEE MTT-S International , vol.2, no., pp.977-980 vol.2, 7-12 June 1998
- [48] Buchanan, N.B.; Fusco, V., "Angle of arrival detection using Retrodirective RADAR," in Radar Conference (EuRAD), 2010 European , vol., no., pp.133-136, Sept. 30 2010-Oct. 1 2010
- [49] C. Anderson, S. Krishnamoorthy, C. Ranson, T. Lemon, W. Newhall, T. Kummetz, and J. Reed, “Antenna isolation, wideband multipath propagation measurements, and interference mitigation for on-frequency repeaters,” in Proceedings of IEEE SoutheastCon, pp. 110 –114, Mar 2004.
- [50] W. Slingsby and J. McGeehan, “Antenna isolation measurements for on-frequency radio repeaters,” in Ninth International Conference on (Conf. Publ. No. 407) Antennas and Propagation, pp. 239 –243 vol.1, Apr 1995.
- [51] T. Riihonen, S. Werner, and R. Wichman, “Mitigation of loopback self-interference in full-duplex MIMO relays,” IEEE Transactions on Signal Processing, vol. 59, pp. 5983 –5993, Dec. 2011.
- [52] H. Hamazumi, K. Imamura, N. Iai, K. Shibuya, and M. Sasaki, “A study of a loop interference canceller for the relay stations in an SFN for digital terrestrial broadcasting,” in IEEE Global Telecommunications Conference, vol. 1, pp. 167–171, 2000.
- [53] P. Larsson and M. Prytz, “MIMO on-frequency repeater with self-interference cancellation and mitigation,” in IEEE 69th Vehicular Technology Conference, VTC Spring 2009, pp. 1–5, 2009.

- [54] B. Chun and Y. H. Lee, "A spatial self-interference nullification method for full duplex amplify-and-forward MIMO relays," in *Wireless Communications and Networking Conference (WCNC)*, 2010 IEEE, pp. 1–6, Apr. 2010.
- [55] Yun Liao, Tianyu Wang, Lingyang Song, and Zhu Han, "Cooperative Spectrum Sensing for Full-Duplex Cognitive Radio Networks," *14th IEEE International Conference on Communication Systems (ICCS)*, Macau, Nov. 2014.
- [56] Kannan Srinivasan, Steven Hong, Mayank Jain, Jung Il Choi, Jeff Mehlman, Sachin Katti, and Philip Levis "Beyond Full Duplex Wireless" in *Asilomar Conference on Signals, Systems and Computers*, 2012.
- [57] M .J. Cryan and P. S . Hall, "Integrated Active Antennas with simultaneous transmit-receive operation.," *Electronics Letters*, Vol. 32, No. 4, February 1996, pp 286-287.
- [58] H. Nawaz and I. Tekin, "Dual polarized patch antenna with high inter-port isolation for 1GHz in-band full Duplex applications," *2016 IEEE International Symposium on Antennas and Propagation (APSURSI)*, Fajardo, PR, USA, 2016, pp. 2153-2154.
- [59] Kurup, D.G., Rydberg, A., and Himdii, M.: 'Compact microstrip T-coupled patch antenna for dual polarization and active antenna application' , *Electron. Lett.*, 2009, 38, pp. 1240-1241
- [60] G. Kurup and A. Rydberg, "Amplifying active reflect-antenna using a microstrip-T coupled patch design and measurement," in *IEEE Transactions on Microwave Theory and Techniques*, vol. 51, no. 8, pp. 1960-1965, Aug. 2003.
- [61] D. M. Pozar, "A Microstrip Antenna Aperture Coupled to a Microstrip Line", *Electronics Letters*, Vol. 21, pp. 49-50, January 17, 1985.
- [62] M. Pozar, "A Review of Aperture Coupled Microstrip Antennas: History, Operation, Development, and Application", *Microwave Online System Company world wide web site*, July 1996
- [63] J.-F. Zurcher, "The SSFIP: A global concept for high performance broadband planar antennas", *Electronics Letters*, vol. 24, pp. 1433-1435, November 1988.
- [64] S. Targonski and D. M. Pozar, "Design of wideband circularly polarized aperture coupled microstrip antennas", *IEEE Trans. Antennas and Propagation*, vol. 41, pp. 214-220, February 1993.
- [65] L. Inclan-Sanchez, J. L. Vazquez-Roy and E. Rajo-Iglesias, "Diplexed dual-polarization proximity coupled patch antenna," *2007 IEEE Antennas and Propagation Society International Symposium*, Honolulu, HI, 2007, pp. 2061-2064
- [66] M. Khan and K. F. Warnick, "Noise figure reduction by port decoupling for dual circular polarized microstrip antenna," in *Electronics Letters*, vol. 50, no. 23, pp. 1662-1664, 2014.

- [67] L. Malviya, R. K. Panigrahi, and M. V. Kartikeyan, "A 2×2 dual-band MIMO antenna with polarization diversity for wireless applications," *Progress In Electromagnetics Research C*, Vol. 61, 91-103, 2016.
- [68] G. J. Foschini and J. Gans, "On Limits of Wireless Communications in a Fading Environment when Using Multiple Antennas", *Bell Labs Technical Journal*, vol. 1, no. 2, Lucent Technologies, pp 41- 59, 1996.
- [69] H. Sampath, S. Talwar, J. Tellado, V. Erceg, and A. Paulraj, "A fourth- generation MIMO-OFDM broadband wireless system: Design, performance, and field trial results," *IEEE Commun. Mag.*, vol. 40, no. 9, pp. 143-149, 2002.
- [70] Jayasooriya, C.K.K., Kwon, H.M., Bae, S., et al.: 'Miniaturized circular antennas for MIMO communication systems- pattern diversity'. *Int. ITG Workshop on Smart Antennas*, 2010, pp. 331–334.
- [71] S. B. Sahay, K. C. Bhagwat and P. R. J. Mohan, "Exploitation of MIMO techniques for reliable HF communication," *2012 International Conference on Signal Processing and Communications (SPCOM)*, Bangalore, 2012, pp. 1-4.
- [72] K. Pachori and A. Mishra, "Performance analysis of MIMO systems under multipath fading channels using linear equalization techniques," *International Conference on Advances in Computing, Communications and Informatics (ICACCI)*, 2015, Kochi, 2015, pp. 190-193.
- [73] Minz, L., Garg, R.: 'Reduction of mutual coupling between closely spaced PIFAs', *Electron. Letters*, 2010, 46, (6), pp. 392–394
- [74] Park, J., Choi, J., Park, J.-Y., et al.: 'Study of a T-shaped slot with a capacitor for high isolation between MIMO antennas', *IEEE Antennas Wirel. Propagation Letters*, 2012, 11, pp. 1541–1544
- [75] K. Chung, J. H. Yoon,"Integrated MIMO Antenna with High Isolation Characteristic" *Electron. Letters*, vol. 43, pp. 199-201, 2007.
- [76] T.Y. Wu, S.T. Fang and K.L. Wong, "Printed diversity monopole antenna for WLAN operation," *Electron. Letters*, 38, (25), pp. 1625–1626, 2002.
- [77] C. Jae-Young, et al., "Low correlation MIMO antenna for LTE 700MHz band," in *Antennas and Propagation (APSURSI)*, 2011 IEEE International Symposium on 2011, pp. 2202-2204.
- [78] L. Liu, S. W. Cheung and T. I. Yuk, "Compact MIMO Antenna for Portable Devices in UWB Applications," in *IEEE Transactions on Antennas and Propagation*, vol. 61, no. 8, pp. 4257-4264, Aug. 2013.
- [79] Li, H., Xiong, J., Ying, Z., et al.: 'Compact and low profile co-located MIMO antenna structure with polarization diversity and high port isolation', *Electron. Letters*, 2010, 46, (2), pp. 108–110
- [80] S. Soltani and R. D. Murch, "A Compact Planar Printed MIMO Antenna Design," in *IEEE Transactions on Antennas and Propagation*, vol. 63, no. 3, pp. 1140-1149, March 2015.

- [81] A. Toktas and A. Akdagli, "Compact multiple-input multiple-output antenna with low correlation for ultra-wide-band applications," in *IET Microwaves, Antennas & Propagation*, vol. 9, no. 8, pp. 822-829, 2015.
- [82] C. H. See, R. A. Abd-Alhameed, Z. Z. Abidin, N. J. McEwan and P. S. Excell, "Wideband Printed MIMO/Diversity Monopole Antenna for WiFi/WiMAX Applications," in *IEEE Transactions on Antennas and Propagation*, vol. 60, no. 4, pp. 2028-2035, April 2012.
- [83] X. S. Yang, L. Zhang, L. L. Zhou, R. Q. Wang and X. J. Li, "Planar two-element UWB MIMO antennas with high isolations," *IEEE International Conference on Computational Electromagnetics (ICCEM)*, Hong Kong, 2015, pp. 363-365
- [84] C. M. Luo, J. S. Hong and L. L. Zhong, "Isolation Enhancement of a Very Compact UWB-MIMO Slot Antenna With Two Defected Ground Structures," in *IEEE Antennas and Wireless Propagation Letters*, vol. 14, no. , pp. 1766-1769, 2015
- [85] M. S. Khan, A. D. Capobianco, A. Naqvi, B. Ijaz, S. Asif and B. D. Braaten, "Planar, compact ultra-wideband polarization diversity antenna array," in *IET Microwaves, Antennas & Propagation*, vol. 9, no. 15, pp. 1761-1768, 12 10 2015
- [86] Chen, S.C., and Wang, Y.S.: 'A decoupling technique for increasing the port isolation between two strongly coupled antennas', *IEEE Transactions on Antennas Propagation* , 2008, 56, pp. 3650–3658
- [87] Xian, Q., Hui, L.W., and Sailing, H.: 'A decoupling technique for increasing the port isolation between two closely packed antennas'. *Antennas and Propagation Society Int. Symp.*, Chicago, IL, USA, July2012, pp. 1–2
- [88] Skycross, Inc, iMAT Antenna Whitepaper, January 2008, <http://www.skycross.com/>.
- [89] N.K. Kiem, D.N. Dinh, H.T. Viet, & D.N. Chien, "A novel design of dual-feed single-element antenna for 4G MIMO terminals", *Progress in Electromagnetics Research Symposium*, pp. 1827, 2012.
- [90] F. M. Caimi, and M. Montgomery, "Dual feed, single element antenna for WiMAX MIMO application," *International Journal of Antennas and Propagation*, Vol. 2008, Article ID 219838, 5 pages, 2008.
- [91] T. Aboufoul, A. Alomainy and C. Parini, "A planar dual fed UWB monopole antenna with polarization diversity for cognitive radio sensing," *Antennas and Propagation Conference (LAPC)*, 2012 Loughborough, Loughborough, 2012, pp. 1-4.
- [92] Moradikordalivand, Alishir, et al. "Dual polarized MIMO antenna system for WiFi and LTE wireless access point applications." *International Journal of Communication Systems* (2014)
- [93] Nawaz, H. and Tekin, I., "Dual port single patch antenna with high interport isolation for 2.4 GHz in-band full duplex wireless applications". *Microw. Opt. Technol. Lett.*, 58: 1756–1759. doi: 10.1002/mop.29899, 2016

- [94] K. P. Ray, "Design Aspects of Printed Monopole Antennas for Ultra-Wide Band Applications," *International Journal of Antennas and Propagation*, vol. 2008, Article ID 713858, 8 pages, 2008. doi:10.1155/2008/713858
- [95] N. P. Agrawall, G. Kumar and K. P. Ray, "Wide-band planar monopole antennas," in *IEEE Transactions on Antennas and Propagation*, vol. 46, no. 2, pp. 294-295, Feb 1998.
- [96] Jianxin Liang, C. C. Chiau, Xiaodong Chen and C. G. Parini, "Study of a printed circular disc monopole antenna for UWB systems," in *IEEE Transactions on Antennas and Propagation*, vol. 53, no. 11, pp. 3500-3504, Nov. 2005.
- [97] Gilliard N. Malheiros-Silveira, Ricardo T. Yoshioka, Jose E. Bertuzzo, and Hugo E. Hernandez-Figueroa, "Printed monopole antenna with triangular-shape groove at ground plane for blue-tooth and UWB applications," *Microwave and Optical Technology Letters*, vol. 57, no. 1, pp. 28–31, 2014.
- [98] S. Blanch, J. Romeu, and I. Corbella, "Exact representation of antenna system diversity performance from input parameter description," *Electronics Letters*, vol. 39, no. 9, pp. 705–707, 2003.
- [99] A. Batgerel and S. Y. Eom, "High-isolation microstrip patch array antenna for single channel full duplex communications," in *IET Microwaves, Antennas & Propagation*, vol. 9, no. 11, pp. 1113-1119, 2015, doi: 10.1049/iet-map.2014.0624
- [100] M. E. Knox, "Single antenna full duplex communications using a common carrier," *Wireless and Microwave Technology Conference (WAMICON), 2012 IEEE 13th Annual*, Cocoa Beach, FL, 2012, pp. 1-6.
- [101] B. Debaillie et al., "Analog/RF solutions enabling compact full-duplex radios," *IEEE J. Sel. Areas Communication*, vol. 32, pp. 1662-1673, 2014.
- [102] X. L. Liang, S. S. Zhong, and W. Wang, "Design of a Dual-Polarized Microstrip Patch Antenna with Excellent Polarization Purity," *Microwave Optical Technology Letters*, 44, 4, February 2005, pp. 329-331. doi:10.1002/mop.20625
- [103] Liton Chandra Paul et al., "The Effect of Changing Substrate Material and Thickness on the Performance of Inset Feed Microstrip Patch Antenna, *American Journal of Networks and Communications*. Vol. 4, No. 3, 2015, pp. 54-58.
- [104] ShiChang Gao and ShunShi Zhong, "A dual-polarized microstrip antenna array with high isolation fed by coplanar network," *Radio and Wireless Conference, 1998. RAWCON 98. 1998 IEEE*, Colorado Springs, CO, 1998, pp. 213-216.
- [105] Ramesh Garg, Prakash Bhartia, Inder Bahl, A pisak Ittiboon," *Microstrip Antenna Design Handbook*," Artech House 2001.
- [106] D. M. Pozar and B. Kaufman, "Increasing the bandwidth of a microstrip antenna by proximity coupling," in *Electronics Letters*, vol. 23, no. 8, pp. 368-369, April 9 1987.
- [107] WARP Project, <http://warpproject.org>"